doi.org/10.26434/chemrxiv.13606556.v1

Ab Initio Prediction of High-Temperature Magnetic Relaxation Rates in Single-Molecule Magnets

Daniel Reta, Jon G. C. Kragskow, Nicholas Chilton

Submitted date: 19/01/2021 • Posted date: 20/01/2021

Citation information: Reta, Daniel; Kragskow, Jon G. C.; Chilton, Nicholas (2021): Ab Initio Prediction of High-Temperature Magnetic Relaxation Rates in Single-Molecule Magnets. ChemRxiv. Preprint. https://doi.org/10.26434/chemrxiv.13606556.v1

Organometallic molecules based on $[Dy(Cp^R)_2]^+$ cations have emerged as clear front-runners in the search for high-temperature single-molecule magnets. However, despite a growing family of structurally-similar molecules, these molecules show significant variations in their magnetic properties, demonstrating the importance of understanding magneto-structural relationships towards developing more efficient design strategies. Here we refine our ab initio spin dynamics methodology and show that it is capable of quantitative prediction of relative relaxation rates in the Orbach region. Applying it to all reported $[Dy(Cp^R)_2]^+$ cations allows us to tease out differences in their relaxation dynamics, highlighting that the main discriminant is the magnitude of the crystal field splitting. We subsequently employ the method to predict relaxation rates for a series of hypothetical organometallic sandwich compounds, revealing an upper limit to the effective barrier to magnetic relaxation of around 2200 K, which has been reached. However, we show that further improvements to single-molecule magnets can be made by moving vibrational modes off-resonance with electronic excitations.

Ab initio prediction of high-temperature magnetic relaxation rates in single-molecule magnets

Daniel Reta, Jon G. C. Kragskow and Nicholas F. Chilton*

Department of Chemistry, School of Natural Sciences, The University of Manchester, Oxford Road, Manchester, M13 9PL, UK.

Abstract

Organometallic molecules based on $[Dy(Cp^R)_2]^+$ cations have emerged as clear front-runners in the search for high-temperature single-molecule magnets. However, despite a growing family of structurally-similar molecules, these molecules show significant variations in their magnetic properties, demonstrating the importance of understanding magneto-structural relationships towards developing more efficient design strategies. Here we refine our *ab initio* spin dynamics methodology and show that it is capable of quantitative prediction of relative relaxation rates in the Orbach region. Applying it to all reported $[Dy(Cp^R)_2]^+$ cations allows us to tease out differences in their relaxation dynamics, highlighting that the main discriminant is the magnitude of the crystal field splitting. We subsequently employ the method to predict relaxation rates for a series of hypothetical organometallic sandwich compounds, revealing an upper limit to the effective barrier to magnetic relaxation of around 2200 K, which has been reached. However, we show that further improvements to single-molecule magnets can be made by moving vibrational modes off-resonance with electronic excitations.

Introduction

The ultimate miniaturisation of classical memory devices lies in the use of atoms or molecules to store binary data.[1] Single-molecule magnets (SMMs), molecules that exhibit slow magnetic relaxation and memory effects, provide a flexible platform for realising high-density data storage. The first single-molecule magnet $\{Mn_{12}\}$ was shown to display magnetic hysteresis and a magnetic reversal (or magnetic relaxation) rate that is exponentially dependent on temperature above 2.5 K,[2] which is the hallmark of thermally-activated relaxation over an intrinsic energy barrier (U_{eff}).[3] The relaxation process was theoretically elaborated and confirmed as a concatenated series of single spin-phonon transitions known as the Orbach process (often called a multi-phonon process) allowing the SMM to traverse its

excited spin states and reverse its magnetization.[4-6] The operation of SMMs is thus inextricably linked to their electronic structure, highlighting the crucial role of magnetic anisotropy in producing an energy barrier for magnetic relaxation. With the discovery that monometallic lanthanide complexes could also show SMM behaviour,[7,8] a conceptual shift in SMM design took place. Owing to the radially-contracted 4f orbitals and nearly unquenched orbital momentum of the trivalent lanthanides, simple electrostatic considerations gave design criteria to achieve large anisotropy;[9-12] for instance linear coordination geometry for Dy(III), or equatorial coordination geometries for Er(III). This has driven a huge increase in U_{eff} barriers[13] and pushed the single-phonon-driven Orbach process to higher temperatures, often replaced by a two-phonon Raman process dominating below *ca.* 50 K.[14] An important component of larger U_{eff} barriers is the presence of larger energy gaps between electronic excited states (*i.e.* stronger crystal field splitting), making it is far from obvious that the same low-energy phonons (lattice acoustic modes) should be responsible for effecting magnetic relaxation as was proposed for $\{Mn_{12}\}$.[2] Fortunately, recent theoretical efforts have begun to establish robust and systematic methodologies to treat these problems,[15-21] targeting a new approach of engineering spin-phonon coupling.

The most successful class of SMMs thus far have converged to a series of Dy(III)-based metallocenium cations[19,22,23] (Figure 1, left): $[Dy(Cp^{iPr4})_2][B(C_6F_5)_4]$ (**1**),[22] $[Dy(Cp^{ttt})_2][B(C_6F_5)_4]$ (**2**),[19] $[Dy(Cp^{iPr5})_2][B(C_6F_5)_4]$ (**3**),[22] $[Dy(Cp^{iPr4Et})_2][B(C_6F_5)_4]$ (**4**),[22] $[Dy(Cp^{iPr4Me})_2][B(C_6F_5)_4]$ (**5**)[22] and $[Dy(Cp^{iPr5})(Cp^{*})][B(C_6F_5)_4]$ (**6**).[23] These complexes are chemically very similar to one-another as they only differ in the cyclopentadienyl (Cp) substituents and even share the same $[B(C_6F_5)_4]^-$ counterion, though they do crystallise in different space groups: P_{2_1}, $P_{\acute{1}}$, $P_{2_1/n}$, $P_{2_1/n}$, $P_{2_1/c}$ and $P_{2_1/c}$, for **1-6** respectively. Despite their similarity, these compounds display a significant variation in their magnetic relaxation rates (Figure 1, right). Our numbering scheme is chosen to reflect the ordering of their 100 s blocking temperatures (the temperature at which the relaxation time is 100 s, herein $T_{B,100s}$), and while there are some crossovers in different temperature regimes, overall **1** is the fastest, **6** is the slowest, and **2-5** are very similar. Indeed, considering estimated standard deviations (ESDs) for the experimental relaxation rates shows that, within error, the relaxation rates in the Orbach region for **3-5** cannot be distinguished (Figure S1).[24] Due to their differing relaxation rates, their $T_{B,100s}$ values span almost 50 K; $T_{B,100s}$ lies well within the Raman regime for **1**, while it falls at the intersection between the Raman and Orbach regimes for **2-5**, and is at the start of the Orbach regime for **6**. Thus, **1-6** are an ideal set of compounds to unpick how subtle

chemical differences result in such different magnetic relaxation rates, and, ideally, to establish the route forward to even better performing SMMs.

In this paper we refine our *ab initio* method for spin-dynamics[19,21,25] and calculate the relaxation dynamics of **1**-**6** to determine what causes the differences in their dynamic magnetic properties. We show that our methodology is capable of quantitative prediction of relative rates of magnetic relaxation, subject to a *ca.* ten-fold overestimation with respect to experiment, giving us confidence in using the approach to compare the underlying spin-phonon coupling in the Orbach region. Using a vibrational-mode-weighted-decomposition of the relaxation rate matrices, we find that the largest discriminant in the magnetic relaxation rates between **1** and **6** is their static electronic structures; that is, the energy gaps are largest for **6** and smallest for **1**. This confirms initial suggestions that the shorter Dy-Cp distances in **6** are responsible for its record-breaking properties. However, there is a limit to how large the CF splitting can be, and hence, we perform spin-dynamics calculations on theoretical *bis*-Cp^R/Cb^R-Dy(III) SMMs (where Cb is cyclobutadienyl) to show that *i)* energy barriers are unlikely to be increased much beyond U_{eff} = 2217(16) K for **6**, and *ii)* yet slower relaxation rates can be achieved by reducing the resonance between vibrational modes and electronic states; for instance, an isolated $[Dy(C_5Me_5)_2]^+$ cation is predicted to have relaxation rates four orders of magnitude slower than **6**, despite having a smaller U_{eff} barrier.

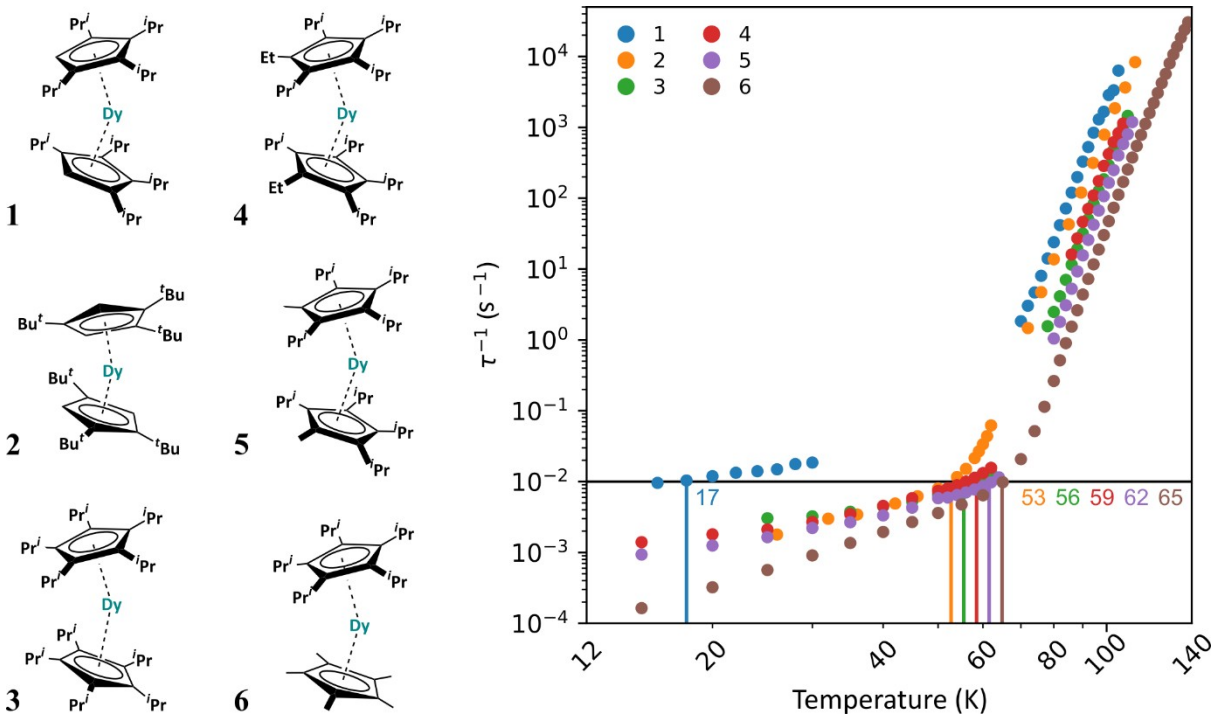

Figure 1. (Left) Schematic representation of the cations in **1-6**. (Right) Magnetic relaxation rates for **1-6** ordered by $T_{B,100s}$.

Methods

Our approach for modelling the spin dynamics of Dy(III)-based SMMs has been given in detail in our recent works,[19,21,25] and is explained in the Supporting Information Section S4. Generally, it consists of three steps: *i)* calculation of the molecular vibrational modes in the gas-phase using density-functional theory (DFT); *ii)* calculation of spin–phonon coupling (note: our calculations are in the gas phase and hence are not truly phonons, but nonetheless we use the common terminology to reflect the experimental situation) using complete active space self-consistent field spin-orbit (CASSCF-SO) calculations; and *iii)* simulation of spin-dynamics. Unlike the first iteration of our method[19] we no longer calibrate atomic displacements (as this effect is largely due to acoustic modes which are not currently included in our model), we now use a resolution of the identity method for approximation of two electron integrals in CASSCF-SO,[25] and have revised our definition of zero-point displacement (Eq. S1). We also herein explore three different definitions of the spin-phonon coupling, including temperature-dependent spin-phonon coupling *via* temperature-dependent displacements (Eq. S2)[21] and a first order Taylor expansion, and compare the choice of Boltzmann or Bose-Einstein phonon statistics; see Supporting Information Section S4. Calculating the relaxation rates for compound **2** to assess these options, we find that the rates show no dependence on the choice of spin-phonon coupling or phonon statistics (Figures S19 and S20), and henceforth we employ Bose-Einstein statistics and a first-order Taylor expansion to calculate the spin-phonon coupling.

The gas-phase normal modes of the cations in **1-6** are calculated with PBE[26,27] and PBE0[28] density-functionals in conjunction with Grimme's empirical dispersion correction[29] within the Gaussian09d[30] suite of programs (Section S2 in the SI). We determine the maximal displacement along each normal mode using Boltzmann statistics of each harmonic oscillator at 100 K, and subsequently calculate the spin-phonon couplings using CASSCF-SO within the OpenMolcas[31] package (Section S4 in the SI). At the crystalline and optimised geometries, we determine the electronic structure with a state-average CASSCF calculation for the 21 S = 5/2 states of Dy(III) followed by non-perturbative SO coupling, and the lowest 16 states ($^6H_{15/2}$ multiplet) of the molecule are projected onto a crystal field (CF) Hamiltonian acting in the $2J + 1$ $\left|m_J\right\rangle$ basis.[32] Improving the quality of the CASSCF method to include

more spin states (see Table S5) makes a negligible difference to the results (Tables S6-S9 and Figures S13-S14), and indeed there is also negligible difference using the PBE0-optimised geometries (Figure S17-18).

The spin-phonon coupling for each vibrational mode is determined from the CF decomposition of a CASSCF-SO calculation for distorted structures in the positive and negative directions along normal mode coordinates, with reference to the CF decomposition at the equilibrium geometry. The dependence of the CF parameters (CFPs) with distortion is fitted to a third-order polynomial (Eqn. S18), which can be used to interpolate the CFPs at a given temperature according to a temperature-dependent displacement (Eqns. S11, S16), or to determine the first derivative of the CFPs in a Taylor expansion (Eqn. S12). With this information, the perturbing CF matrices for each mode are determined in the equilibrium electronic eigenbasis and used to calculate the transition rates between all CF states. It is here that the only free parameter in our model is introduced, as a single fixed Gaussian linewidth parameter for each normal mode. In the final step, the master equation is constructed and solved to obtain the relaxation rates.[19]

Results

The DFT-optimised structures obtained for **1**-**6** are very similar to the experimentally determined crystal geometries (Table S3), where the largest RMSD (Dy atom, Cp rings, and Cp-bound C atoms) is 0.358 Å for **4**. Comparing the electronic structures between optimised and crystalline geometries, we find that the optimised geometries always show smaller energy gaps between the electronic states than the crystal geometries (Figure S15) and that the optimised geometries show overall CF splittings that correlate well with the ordering of T_B (Figure 2 and S15), but that this does not hold for all compounds when considering the crystal geometries (Figure S16). We find that the main anisotropy axis of the ground Kramers doublet is well-approximated by the average Dy-$Cp_{centroid}$ vector, and that the ground doublet is $|\pm 15/2\rangle$, followed sequentially by $|\pm 13/2\rangle$, $|\pm 11/2\rangle$, $|\pm 9/2\rangle$, $|\pm 7/2\rangle$ and $|\pm 5/2\rangle$ excited doublets, while the two most energetic doublets are mixed m_J functions (Table S6), in agreement with previous works.[19,23] The energy gaps between the ground and first excited doublets (optimised geometries) are 414, 461, 478, 479, 476 and 530 cm^{-1} for **1**-**6**, respectively, in good correlation with the ordering of the experimental relaxation rates; **1** is the smallest, **6** is the largest, and **2**-**5** are very similar. Our results for **6** are in good agreement

with the original XMS-CASPT2 calculations performed for a similar optimized structure (Table S10).[23]

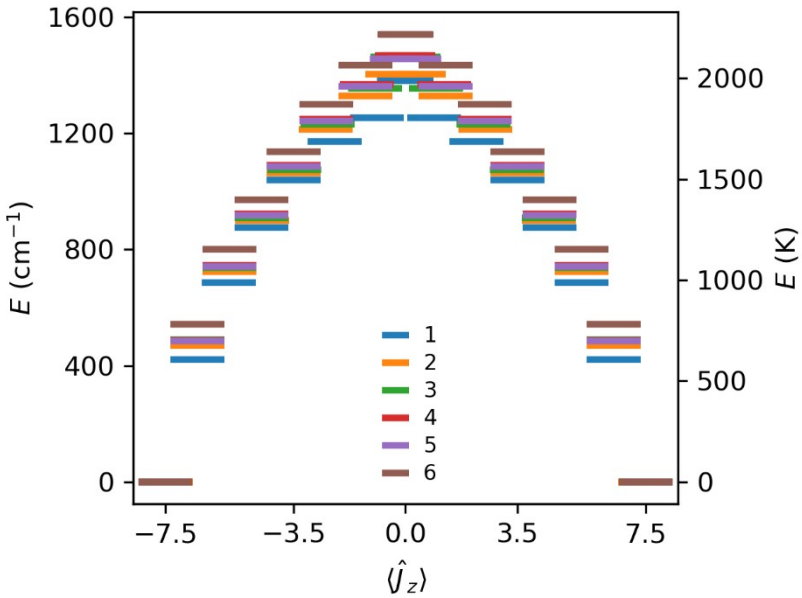

Figure 2. Comparison of the electronic structure of compounds **1-6** calculated with the crystal field parameters obtained from CASSCF-SO calculations at the PBE-optimised gas-phase geometries.

Employing our *ab initio* spin-dynamics approach (see Methods and Supporting Information), we calculate the magnetic relaxation rates for **1-6,** where the only free parameter is a constant vibrational linewidth for all modes. Here we compare full-width-half-maximum (FWHM) linewidths of 6, 10 and 20 cm^{-1} for all compounds, which are consistent with the IR spectra (FWHM *ca.* 6 – 26 cm^{-1}, Figures S8-S12). Calculation of the spin-dynamics for **1-6** using the PBE vibrational modes (Figure 3; results using PBE0 are nearly identical, Figure S21, hence we will only consider the PBE results further) show that calibration of the normal mode energies to IR spectra (linear calibration: slopes of 0.94 – 1.04 and intercepts of -9 – +70 cm^{-1}, Figures S8-S12, Table S4 and reference 19) is not crucial: we see the largest influences in **2**, however overall the changes are modest. For larger FWHM values, more modes come into resonance for more transitions and thus relaxation rates generally increase with linewidth (Figures 3 and S21). Crucially, however, for FWHM = 6, 10 or 20 cm^{-1}, our method predicts the correct ordering of the calculated rates: **1** is always fastest, **6** is always slowest, and **2-5** are very similar (Figure 4). Interestingly, in all cases we overestimate the relaxation rates by about a factor of *ca.* 10 ($\tau_{\text{¿}}/\tau_{\text{exp}}$ at 100 K with FWHM =

10 cm^{-1} ranges from 5 – 40 for **1**-**6**). It is tempting to decrease the linewidth in order to match the experimental rates as closely as possible, and this would require FWHM values of *ca.* 1 – 4 cm^{-1} for **1-6** (Figures S22). However, for FWHM < 6 cm^{-1} the calculated rates no longer show the experimental ordering (*e.g.* for FWHM = 2 cm^{-1} Figure 4) and the profiles start to deviate significantly from those obtained with larger linewidths; thus, we suggest that results with FWHM < 6 cm^{-1} are not reliable (indeed such narrow linewidths are not consistent with the experimental IR spectra). While mode-energy- and temperature-dependent linewidths based on finite phonon lifetimes have been proposed by Lunghi et al.,[15] we have found that this is not appropriate for modelling the magnetic relaxation in bis-alkoxide Dy(III) SMMs,[33] and this conclusion remains unchanged for the present $[Dy(Cp^{R})_2]^+$ cations (see Figure S23 and S24). Hence, we identify that our method using the PBE density-functional without calibration and a single linewidth parameter of *ca.* 10 cm^{-1} is capable of quantitative prediction of the relative Orbach relaxation rates, subject to an overestimation of approximately one order of magnitude in comparison to experiment.

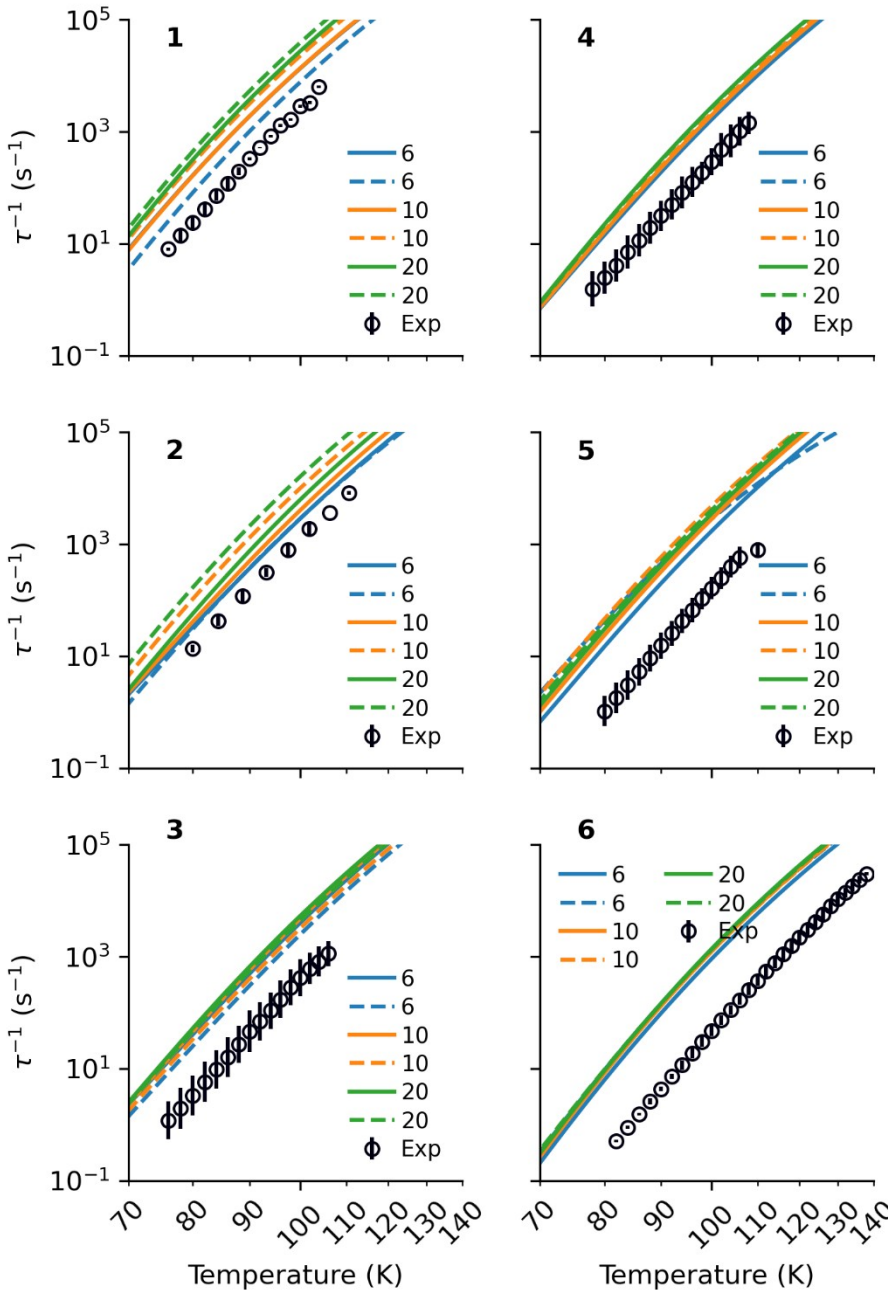

Figure 3. Comparison of experimental (circles) and *ab initio* calculated (lines, PBE density-functional) relaxation rates for **1-6**. Solid and dashed lines are obtained without and with IR calibration, respectively. Fixed FWHM linewidths of 6 (blue), 10 (orange) and 20 cm^{-1} (green) are employed. Experimental error bars are estimated standard deviations derived from the generalised Debye model.[24] Note: solid blue line for compound **1** is obscured by the solid orange line.

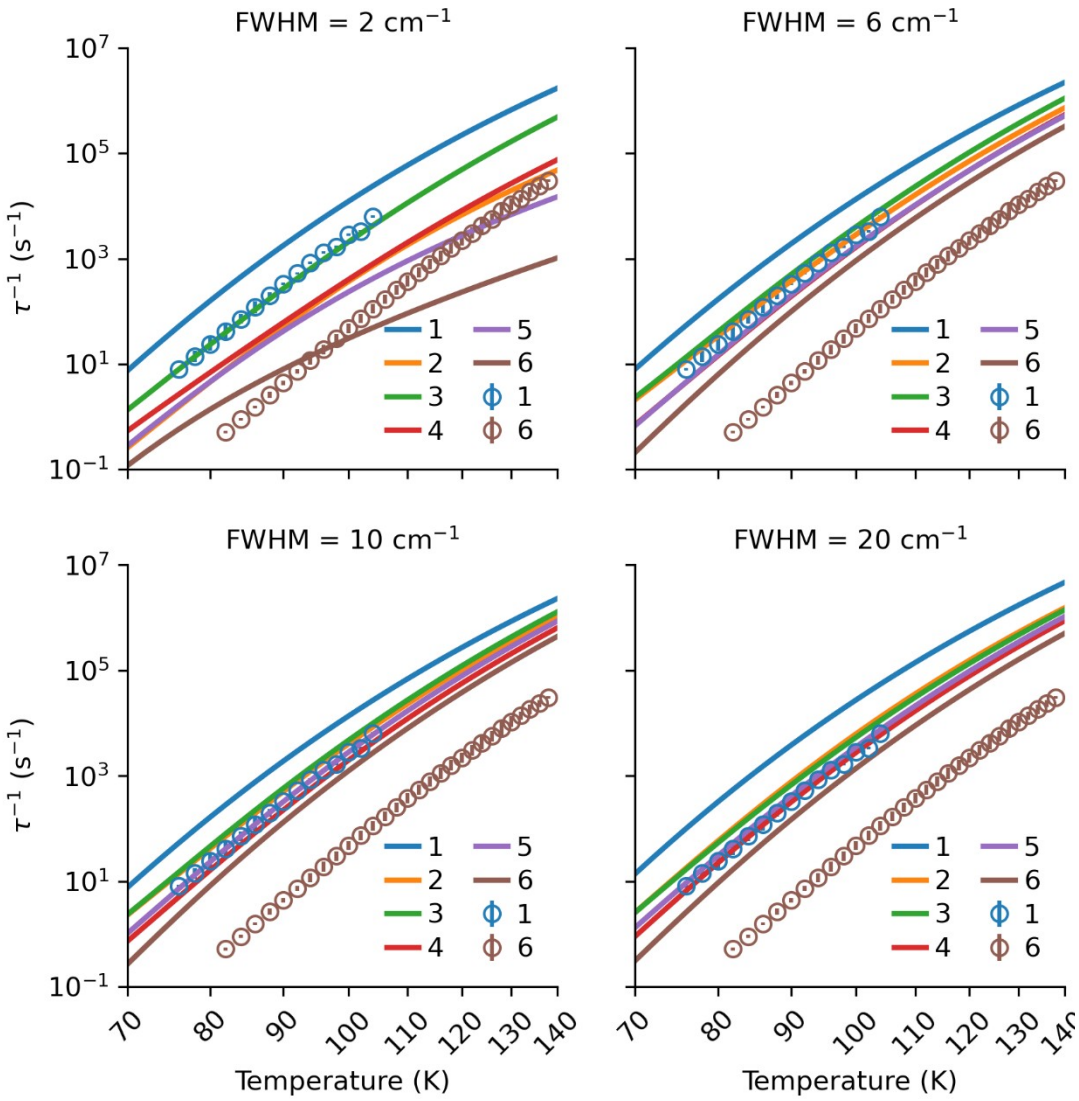

Figure 4. Comparison of calculated rates for **1-6**, obtained without IR calibration using the PBE density-functional. Experimental data for **1** and **6** is shown in circles. Experimental error bars are estimated standard deviations derived from the generalised Debye model.[24]

Discussion

With the results from our *ab initio* spin-dynamics calculations in hand, and confidence that the relative relaxation rates of **1-6** are well described, we are now in a position to investigate the differences in magnetic relaxation between these compounds, and specifically why it is so slow for **6**. This is challenging because the calculated magnetic relaxation rate at a given temperature is the smallest magnitude non-zero eigenvalue of the 16×16 rate matrix, $\acute{\gamma}$, and there is no analytical solution that maps the matrix elements of $\acute{\gamma}$ onto its eigenvalues. In our first publication on this topic, we simply considered that the "first step in magnetic relaxation" (the $|\pm 15/2\rangle \rightarrow |\pm 13/2\rangle$ elements of $\acute{\gamma}$) would be most important,[19] but later found

that this is not always the most probable first step in relaxation across different Dy(III) SMMs.[25,21] Our second approach was to employ a "knockout" procedure, where the various $|\pm 15/2\rangle \rightarrow |\pm x\rangle$ elements of $\acute{\gamma}$ are set to zero one-by-one, and the transition responsible for the largest reduction to the overall relaxation rate when removed is determined.[21] While this gave useful information for bis-alkoxide complexes,[21] performing this analysis here (extending to all elements of $\acute{\gamma}$, not just those starting in $|\pm 15/2\rangle$) shows that no single element of $\acute{\gamma}$ has a decisive effect on the overall relaxation rates for any of **1-6** (Figure S25 – S31). Furthermore, analysing the spin phonon coupling strength[34] for all available modes and comparing them to the electronic energy gaps of **1-6** does not provide a clear answer either (Figure S32-S37).

Therefore, we have devised a new method for unpicking the differences in the relaxation dynamics between these molecules, and herein we focus on the differences between **1** and **6** which show the greatest disparity in their properties. Firstly, we compare the $\acute{\gamma}$ matrices between the two compounds to assess which transitions are different. The difference map of $\log_{10}[\acute{\gamma}_6] - \log_{10}[\acute{\gamma}_1]$ (Figure S38) shows that the average difference between the lower-triangular elements is $10^{0.7} \approx 5$ times slower for **6** than **1**, in reasonable correlation with the overall magnetic relaxation rates (calculated to be 11 times slower). However, there is a significant spread of differences, and indeed some intriguing features such as elements in $\acute{\gamma}_6$ that are 10^{10} times faster than in $\acute{\gamma}_1$ (dark purple square). Whilst comparing individual elements of $\acute{\gamma}$ provides some insight, there is no clear answer as to the root-cause of these differences. This is because each element in $\acute{\gamma}$ is the sum over all vibrational modes (273 and 237 modes for **1** and **6**, respectively) of the product (Eqn. 1) of the spin-phonon coupling $\left|\langle f|\widehat{H}_{SP\,j}|i\rangle\right|^2$, which reports on how strongly vibrational mode j couples electronic states i and f), the vibrational occupation $\left|\langle n_j - 1|Q_j|n_j\rangle\right|^2$ or $\left|\langle n_j + 1|Q_j|n_j\rangle\right|^2$, which is the probability of absorption or emission of a vibrational quantum, respectively), and the vibrational density of states (DOS, $\rho_j(|E_f - E_i|)$, which reports the proximity of the vibrational mode energy $\hbar\omega_j$ to the electronic transition).

$$\gamma_{fi}=\sum_{j}^{3N-6}\gamma_{fi,j}=\begin{cases}\sum_{j}^{3N-6}\frac{2\pi}{\hbar}\left|\langle f|\hat{H}_{SPj}|i\rangle\right|^2\left|\langle n_j-1|Q_j|n_j\rangle\right|^2\rho_j\left(\left|E_f-E_i\right|\right)E_f>E_i\\ \sum_{j}^{3N-6}\frac{2\pi}{\hbar}\left|\langle f|\hat{H}_{SPj}|i\rangle\right|^2\left|\langle n_j+1|Q_j|n_j\rangle\right|^2\rho_j\left(\left|E_f-E_i\right|\right)E_f<E_i\end{cases} \tag{1}$$

Although every transition is the sum over all modes, due to the conservation of energy and relatively sharp vibrational DOS (ρ_j is a Gaussian function centered at $\hbar\omega_j$ with FWHM discussed above), between one and four vibrational modes tend to dominate any given element of $\acute{\gamma}$. Thus, we calculate the mode-weighted spin-phonon coupling ($\langle\hat{H}_{SP}\rangle_{fi}$), vibrational occupation ($\langle Q_j\rangle_{fi}$), and vibrational DOS ($\langle\rho\rangle_{fi}$) for each element of $\acute{\gamma}$ (Eqns. 2 – 4); the effective number of modes associated with each transition ($\langle n\rangle_{fi}$) can then be determined simply (Eqn. 5). Hence, the total rate matrix $\acute{\gamma}$ can be exactly decomposed into matrix representations of each component (Eqn. 6), where $\circ$ indicates the element-wise (Hadamard) product. This decomposition allows us to pick-and-mix the individual components of the relaxation rate matrix from any compound in order to generate a fictional relaxation rate matrix $\acute{\gamma}_{fict}$, and hence assess the contributing factors to the overall magnetic relaxation rates after diagonalization.

$$\langle\hat{H}_{SP}\rangle_{fi}=\sum_{j}^{3N-6}\frac{\gamma_{fi,j}}{\gamma_{fi}}\left|\langle f|\hat{H}_{SPj}|i\rangle\right|^2 \tag{2}$$

$$\langle Q\rangle_{fi}=\begin{cases}\sum_{j}^{3N-6}\frac{\gamma_{fi,j}}{\gamma_{fi}}\left|\langle n_j-1|Q_j|n_j\rangle\right|^2 E_f>E_i\\ \sum_{j}^{3N-6}\frac{\gamma_{fi,j}}{\gamma_{fi}}\left|\langle n_j+1|Q_j|n_j\rangle\right|^2 E_i>E_f\end{cases} \tag{3}$$

$$\langle\rho\rangle_{fi}=\sum_{j}^{3N-6}\frac{\gamma_{fi,j}}{\gamma_{fi}}\rho_j\left(\left|E_f-E_i\right|\right) \tag{4}$$

$$\langle n\rangle_{fi}=\frac{\gamma_{fi}}{\frac{2\pi}{\hbar}\langle\hat{H}_{SP}\rangle_{fi}\langle Q\rangle_{fi}\langle\rho\rangle_{fi}} \tag{5}$$

$$\acute{\gamma}=\frac{2\pi}{\hbar}\langle\acute{H}_{SP}\rangle\circ\langle\acute{Q}\rangle\circ\langle\acute{\rho}\rangle\circ\langle\acute{n}\rangle \tag{6}$$

Starting from a base $\acute{\gamma}$ matrix of either **1** or **6**, the simplest test is to swap out the individual components one-by-one and determine the relaxation rates of $\acute{\gamma}_{fict}$ (Table 1). We find that by swapping either the spin-phonon coupling, the vibrational DOS or the effective number of modes, the relaxation rates are only altered by a factor of 1 – 3 times faster or slower (but note some of these shifts are counterintuitive, owing to the non-trivial

relationship between matrix elements and eigenvalues). However, when we swap the vibrational occupation between the two molecules, relaxation in **6** becomes 12 times faster, and relaxation in **1** becomes 10 times slower. Because magnetic relaxation in the Orbach regime depends on absorption of vibrational quanta, which must be near-resonant with the CF energy gaps (Eqn. 4), the dominance of vibrational occupation found here is direct evidence that the main discriminant in relaxation dynamics between best-in-class **6** versus worst-in-class **1** is the size the CF splitting, as previously suggested.[23]

Table 1. Breakdown of relaxation rates between **1** and **6** *via* a mode-averaging procedure. Relaxation rates are calculated using the PBE density-functional, without IR calibration, at 100 K with FWHM = 10 cm^{-1}. Top portion corresponds to a base $\acute{\gamma}$ matrix of **1**, while bottom portion corresponds to a base matrix of **6**. Rows are ordered by increasing rate.

$\langle \acute{H}_{SP} \rangle$	$\langle \acute{Q} \rangle$	$\langle \acute{\rho} \rangle$	$\langle \acute{n} \rangle$	τ^{-1}	τ^{-1}/τ^{-1}_{1}
1	**6**	**1**	**1**	1.32×10^{3}	0.10
1	**1**	**1**	**1**	1.37×10^{4}	1
6	**1**	**1**	**1**	142×10^{4}	1.04
1	**1**	**1**	**6**	1.80×10^{4}	1.31
1	**1**	**6**	**1**	3.27×10^{4}	2.39
$\langle \acute{H}_{SP} \rangle$	$\langle \acute{Q} \rangle$	$\langle \acute{\rho} \rangle$	$\langle \acute{n} \rangle$	τ^{-1}	τ^{-1}/τ^{-1}_{6}
6	**6**	**6**	**1**	9.71×10^{2}	0.78
6	**6**	**6**	**6**	1.25×10^{3}	1
6	**6**	**1**	**6**	1.43×10^{3}	1.14
1	**6**	**6**	**6**	4.52×10^{3}	3.62
6	**1**	**6**	**6**	1.52×10^{4}	12.16

In order to assess whether the original proposal for removal of the C-H groups in **2** in order to improve magnetic memory (*i.e.* engineering the spin-phonon coupling) is indeed behind the increased performance of the **6** (calculated to be 1.4 times slower than **2** at 100 K), or if the changes are simply due to an increased CF splitting as it is for **1**, we have performed the mode-weighted analysis comparing **2** with **6** (Table S11). Starting from the base $\acute{\gamma}$ matrix of **2** and swapping the vibrational occupation component for that found in **6** decreases the rate by a factor of 5.3, and swapping out the spin-phonon coupling decreases the rate by a factor of 1.3, while swapping out the vibrational DOS or the effective number of modes from **6** actually increase the rate by factors of 1.1 and 1.5, respectively (and vice versa, the inverse is true). Hence, it seems that both an increased CF splitting in **6** (*via* the vibrational occupation terms) and a reduced spin-phonon coupling are responsible for slowing down relaxation in **6**

compared to **2**, but that the former effect is dominant. Hence, this analysis suggests that the enhancements achieved in slowing magnetic relaxation in $[Dy(Cp^R)_2]^+$ cations has not come about *via* engineering the spin-phonon coupling, but rather by enlarging the CF splitting.

To explore how far performance of Dy(III) SMMs can be enhanced, we have made a selection of homoleptic *bis*-persubstituted-aromatic sandwich complexes of the $[Dy(C_5R_5)_2]^+$ (R = H, Me) and $[Dy(C_4R_4)_2]^-$ (C_4R_4 is a persubstituted cyclobutadienyl dianion, R = H, Me, ^{i}Pr, ^{t}Bu) varieties, in addition to three proposed SMM candidates from the literature (*viz.* $[Dy(C_5I_5)_2]^+$,[20] {DyFlourene^{i}Pr} = [Dy(3,6,9-tri-*iso*-propyl-flourenide)$_2$]$^+$,[20] and $[Dy(N_5)_2]^+$ [35]), and used our *ab initio* spin-dynamics methodology to predict their magnetic relaxation rates (Figure 5a). Compared to references 20 and 35, here we have performed a full spin-dynamics calculation to arrive at predicted magnetic relaxation rates, rather than assessing the spin-phonon coupling and/or electronic states alone. This allows us to predict that $[Dy(C_5I_5)_2]^+$ would have relaxation rates 1-2 orders of magnitude faster than **6**, and {DyFlourene^{i}Pr} would be 3-6 orders of magnitude faster than **6**. Hence, these results broadly confirm the analysis of Ullah *et al.*, who concluded that $[Dy(C_5I_5)_2]^+$ would be a good SMM and that {DyFlourene^{i}Pr} would not be a good SMM, however we doubt whether $[Dy(C_5I_5)_2]^+$ would surpass the performance of **6** based on our results. Following a different strategy, Kotrle and Herchel proposed a series of inorganic sandwich complexes, predicting $[Dy(N_5)_2]^+$ to be a good SMM candidate with U_{eff} = 1475 K.[35] Using our methodology, we find that $[Dy(N_5)_2]^+$ would indeed have a significant energy barrier to relaxation, U_{eff} = 1292 K with $\tau_0 = 6.43\times10^{-12}$ s (the difference in predicted energy barrier is likely due to our use of CASSCF-SO *vs.* the inclusion of dynamic correlation in ref. 35), but that its relaxation dynamics are 2-4 orders of magnitude faster than for **6**.

Examining the cyclobutadienyl and cyclopendadienyl compounds, we find that all dianionic cyclobutadienyl ligand sets generate a total splitting of the $J = \pm15/2$ multiplet that is equal to or larger than compound **6** with two monoanionic Cp^R ligands, but interestingly, only $[Dy(C_4{}^tBu_4)_2]^-$ shows a comparable gap between the ground and first excited doublets (Figures 5b and 5c); thus, it seems that while dianionic ligands do generally increase the CF splitting, the effect is non-trivial when considering individual m_J components. Indeed, we find that $[Dy(C_4{}^tBu_4)_2]^-$ has a very similar relaxation rate to **6**, but that both $[Dy(C_4H_4)_2]^-$ and $[Dy(C_5Me_5)_2]^+$, which have smaller energy gaps between the ground and first excited doublets, show relaxation rates orders of magnitude smaller than **6**; all other compounds examined here are predicted to have faster relaxation than **6**. Fitting the calculated relaxation

rates above 100 K to an Arrhenius law for the Orbach mechanism shows that the predicted U_{eff} barriers are a maximum of around 2100 K for this class of compound (Table S12): specifically for the two compounds predicted to have slower relaxation than **6**, we find U_{eff} = 2093 K and τ_0 = 2.48×10^{-11} s for $[Dy(C_4H_4)_2]^-$ and U_{eff} = 1549 K and τ_0 = 8.90×10^{-8} s for $[Dy(C_5Me_5)_2]^+$, compared to U_{eff} = 2048 K and τ_0 = 1.03×10^{-12} s for **6** (*cf.* U_{eff} = 2217(16) K and τ_0 = 4.2(6)×10^{-12} s found experimentally[23]). While $[Dy(C_4H_4)_2]^-$ has a similar U_{eff} barrier to **6**, the τ_0 pre-factor is an order of magnitude larger and hence its relaxation is an order of magnitude slower. Analysis using a mode-weighted decomposition (Table S13) shows that the phonon DOS is the dominant term leading to a slower relaxation rate in $[Dy(C_4H_4)_2]^-$ as compared to **6**. For $[Dy(C_5Me_5)_2]^+$, the U_{eff} barrier is significantly lower than **6** due to a considerably smaller $Cp_{centroid}$-Dy-$Cp_{centroid}$ angle of 144° vs. 160° (and despite shorter Dy-$Cp_{centroid}$ distances, Table S12), however, the τ_0 pre-factor is four orders of magnitude larger than for **6**: this is clearly the decisive difference in the relaxation dynamics. Using a mode-weighted decomposition, we again find that the phonon DOS is the origin of the far larger τ_0 in $[Dy(C_5Me_5)_2]^+$ than for **6** (Table 2). For both $[Dy(C_4H_4)_2]^-$ and $[Dy(C_5Me_5)_2]^+$ this is confirmed by comparing the vibrational mode distributions with the electronic energy levels (Figures S39 and S40 *cf.* S37), showing that in addition to there being far fewer vibrational modes than in **6**, they are also less frequently on-resonance with electronic transitions. Hence, it seems that while U_{eff} barriers may have reached their limit in such sandwich compounds, engineering molecular vibrational modes can play a significant role in increasing the relaxation times of SMMs.

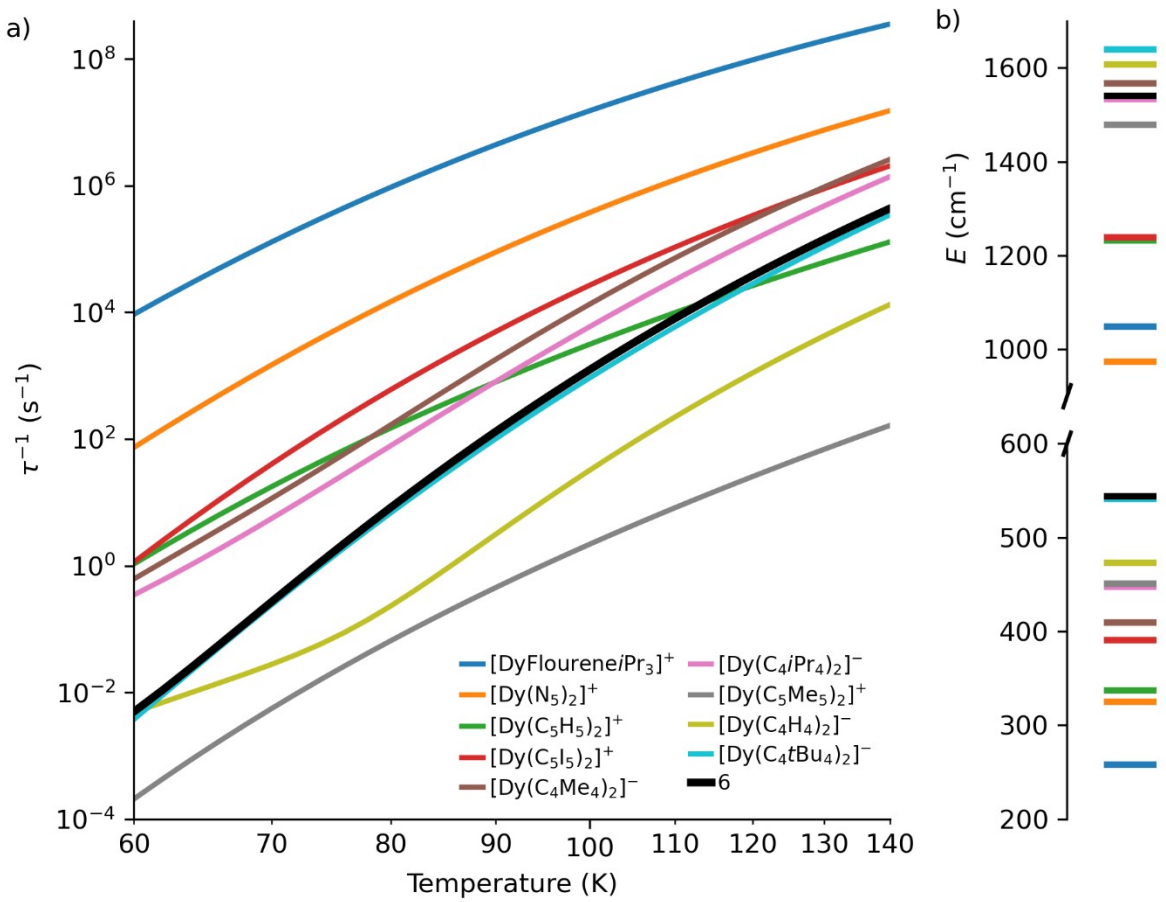

Figure 5. (a) Comparison of calculated rates for theoretical SMMs compared to **6**, obtained using the PBE density-functional. (b) Energy of highest (top) and first excited (bottom) doublet in the $^6H_{15/2}$ multiplet.

Table 2. Breakdown of relaxation rates between $[Dy(C_5Me_5)_2]^+$ and **6** *via* a mode-weighting procedure. Relaxation rates are calculated using the PBE density-functional, without calibration, at 100 K with FWHM = 10 cm^{-1}. Top portion corresponds to a base $\acute{\gamma}$ matrix of $[Dy(C_5Me_5)_2]^+$, while bottom portion corresponds to a base matrix of **6**. Rows are ordered by increasing rate.

$\langle \acute{H}_{SP} \rangle$	$\langle \acute{Q} \rangle$	$\langle \acute{\rho} \rangle$	$\langle \acute{n} \rangle$	τ^{-1}	$\tau^{-1}/\tau^{-1}_{[Dy(C_5Me_5)_2]^+}$ ¿
$[Dy(C_5Me_5)_2]^+$	**6**	$[Dy(C_5Me_5)_2]^+$	$[Dy(C_5Me_5)_2]^+$	1.48×10^0	0.01
$[Dy(C_5Me_5)_2]^+$	$[Dy(C_5Me_5)_2]^+$	$[Dy(C_5Me_5)_2]^+$	**6**	2.37×10^0	0.01
6	$[Dy(C_5Me_5)_2]^+$	$[Dy(C_5Me_5)_2]^+$	$[Dy(C_5Me_5)_2]^+$	5.02×10^0	0.02
$[Dy(C_5Me_5)_2]^+$	$[Dy(C_5Me_5)_2]^+$	$[Dy(C_5Me_5)_2]^+$	$[Dy(C_5Me_5)_2]^+$	2.19×10^2	1
$[Dy(C_5Me_5)_2]^+$	$[Dy(C_5Me_5)_2]^+$	**6**	$[Dy(C_5Me_5)_2]^+$	1.83×10^3	8.36
$\langle \acute{H}_{SP} \rangle$	$\langle \acute{Q} \rangle$	$\langle \acute{\rho} \rangle$	$\langle \acute{n} \rangle$	τ^{-1}	τ^{-1}/τ^{-1}_{6}
6	**6**	$[Dy(C_5Me_5)_2]^+$	**6**	3.35×10^0	0.003
6	**6**	**6**	$[Dy(C_5Me_5)_2]^+$	9.24×10^2	0.74

$[Dy(C_5Me_5)_2]^+$	**6**	**6**	**6**	9.57×10^2	0.77
6	**6**	**6**	**6**	1.25×10^3	1
6	$[Dy(C_5Me_5)_2]^+$	**6**	**6**	3.00×10^3	2.40

Conclusion

Design criteria for increasing magnetic anisotropy in Dy(III)-based SMMs have been produced and verified, leading to dramatic increases in effective energy barriers to magnetic relaxation and vast improvements in SMM performance. However, the route towards further improvements is unclear. By developing an *ab initio* methodology for calculating spin-dynamics with relative quantitative accuracy, along with a new analysis technique, we are now able to probe the origins of differing SMM performance directly. This has allowed us to prove that the current best-performing SMM $[Dy(Cp^{iPr5})(Cp^*)][B(C_6F_5)_4]$ (**6**) is better than both the worst in its class $[Dy(Cp^{iPr4})_2][B(C_6F_5)_4]$ (**1**) and the original dysprosocenium SMM $[Dy(Cp^{ttt})_2][B(C_6F_5)_4]$ (**2**) because it has a larger CF splitting. Subsequently, we have predicted that further enhancements to U_{eff} seem minimal and that progress in slowing magnetic relaxation in the Orbach regime could be obtained by moving vibrational modes off-resonance with electronic transitions, even if U_{eff} barriers are adversely affected.

Acknowledgements

We thank the European Research Council (ERC-2019-STG-851504), EPSRC (PhD scholarship to J.G.C.K.), The Royal Society (University Research Fellowship to N.F.C.) and The University of Manchester (Presidential Fellowship to N.F.C.) for support. We thank Daniel Corbett and the Computational Shared Facility at The University of Manchester for assistance.

References

[1] Sessoli, R. *Nature*, **548**, 400–401 (2017).
[2] Sessoli, R., Gatteschi D., Caneschi, A., & Novak, M., *Nature*, **365** (6442), 141–143, (1993).
[3] Orbach, R., *Proc. Roy. Soc. A.*, **264**, 458–484, (1961).
[4] Gatteschi, D., Sessoli, R. & Villain, J., *Molecular Nanomagnets.* (Oxford University Press, 2006).
[6] Bartolomé, J., Luis, F. & Fernández, J. F., *Molecular Magnets. Physics and Applications*. (NanoScience and Technology; Springer Berlin Heidelberg: Berlin, Heidelberg, 2014).
[7] Naoto, I., Miki, S., Tadahiko, I., Shin-ya, K. & Kaizu, Y., *J. Am. Chem. Soc.*, **125** (29), 8694–8695 (2003).
[8] Ishikawa, N., Miki, S., Tomoko, O., Naohiro, T., Tomochika, I. & Kaizu, Y., *Inorg. Chem.*, **42** (7), 2440–2446 (2003).
[9] Sievers, J., *Zeitschrift für Phys. B Condens. Matter*, **45** (4), 289–296 (1982).
[12] Aravena, D. & Ruiz, E., *Inorg. Chem.*, **52** (23), 13770–13778 (2013).
[13] Giansiracusa, M. J., Kostopoulos, A. K., Collison, D., Winpenny, R. E. P. & Chilton, N. F., *Chem. Commun.*, **55**, 7025 (2019).
[14] Shrivastava, K. N., *Phys. status solidi*, **117** (2), 437–458 (1983).
[15] Lunghi, A., Totti, F., Sessoli, R. & Sanvito, S., *Nat. Commun.*, **8**, 14620, (2017).
[21] Yu, K.-X., Kragskow, J. G. C., Ding, Y.-S., Zhai, Y.-Q., Reta, D., Chilton, N. F. & Zheng, Y.-Z. *Chem*, **6**, 1777-1793 (2020).
[22] McClain, K. R.; Gould, C. A.; Chakarawet, K.; Teat, S. J.; Groshens, T. J.; Long, J. R.; Harvey, B. G. *Chem. Sci.*, **9**, 8492-8503 (2018).
[23] Guo, F.-S.; Day, B. M.; Chen, Y.-C.; Tong, M.-L.; Mansikkamäki, A. & Layfield, R. A. *Science*, **362**, 1400, (2018).
[24] Reta, D. & Chilton, N. F., *Phys. Chem. Chem. Phys.*, **21**, 23567-23575 (2019).
[25] Evans, P., Reta, D., Whitehead, G. F.S., Chilton, N. F. & Mills, D. P. *J. Am. Chem. Soc.*, **141**, 19935−19940 (2019).
[26] Perdew, J. P., Burke, K. & Ernzerhof, M. *Phys. Rev. Lett.*, **77** (18), 3865–3868, (1996).
[27] Perdew, J. P., Burke, K. & Ernzerhof, M. *Phys. Rev. Lett.*, **78** (7), 1396–1396 (1997).
[28] Adamo, C. & Varone, V., *J. Chem. Phys.*, **110**, 6158-69 (1999).
[29] Grimme, S. *Wiley Interdiscip. Rev. Comput. Mol. Sci.*, **1** (2), 211–228 (2011).
[30] Frisch, M. J. et al. Gaussian 09, Revision D.01, Gaussian, Inc., Wallingford CT, 2016
[31] Aquilante, F. *et al. J. Comput. Chem.*, **37,** 506–541 (2016).
[32] Ungur, L. & Chibotaru, L. F., *Chemistry - A European Journal*, **23**, 3708–3718 (2017).
[33] Ding, Y-S., Han, T., Zhai, Y. Q., Reta, D., Chilton, N. F., Winpenny, R. E. P. & Zheng, Y. Z., *Chem. Eur. J.*, 26, 5893–5902 (2020).
[34] Chang, N. C., Gruber, J. B., Leavitt, R. P. & Morrison, C. A., *J. Chem. Phys.*, **76**, 3877–3889, (1982).
[35] Kotrle, K. & Herchel, R. *Inorg. Chem.*, 58, 20, 14046–14057 (2019).

SUPPLEMENTARY INFORMATION

Ab initio prediction of high-temperature magnetic relaxation rates in single-molecule magnets

Daniel Reta, Jon G. C. Kragskow and Nicholas F. Chilton*

Department of Chemistry, School of Natural Sciences, The University of Manchester, Oxford Road, Manchester, M13 9PL, UK.

Contents

S1. Experimental relaxation rates

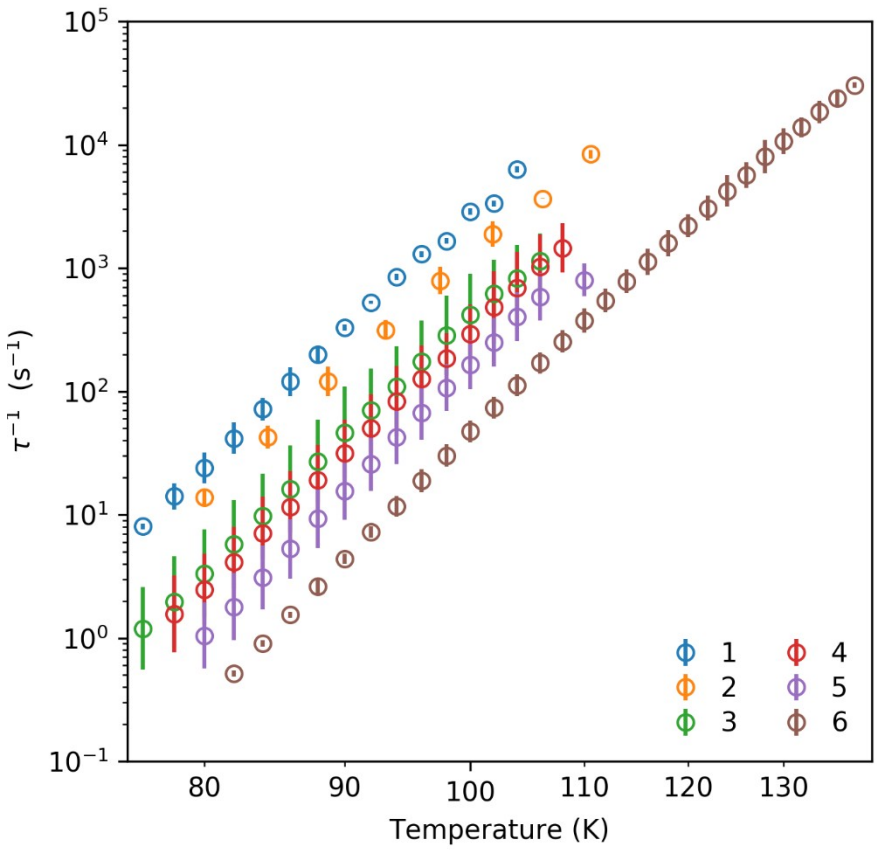

Figure S1. Comparison of relaxation rates in the Orbach region for **1-6**. Experimental error bars are estimated standard deviations derived from the generalised Debye model.[1]

S2. Density Functional Theory calculations: Geometry optimization and normal modes

Gas-phase molecular geometry optimizations on the **1-6** cations were performed with Gaussian09d[2] suite of programs using PBE[3,4] exchange-correlation and PBE0[5] hybrid functionals with cc-pVTZ[6] basis set for all coordinating atoms, cc-pVDZ[6] for the rest of non-metal atoms, the Stuttgart RSC 1997[7] effective core potential (ECP) for the 28 core electrons of yttrium and the corresponding valence basis set for the remaining valence electrons, and Grimme's dispersion corrections.[8-10] To facilitate convergence, dysprosium is substituted by yttrium (where the isotopic mass is set to 162.5, that of the naturally abundant dysprosium), which is justified by their similar ionic radii and the fact that these derivatives are widely found to be structural analogues. Calculation of normal modes was performed by explicit calculation of the Hessian at the optimized

geometry, making sure that the forces and displacements are zero and that all frequencies are positive. The coordinates and normal modes energies of compounds **1-6** can be found in Table S1 and Table S2, respectively.

Table S3 compares the structural results between crystal and optimised geometries for **1-6**. The RMSD values are calculated following the Kabsch algorithm[11,12] as implemented by Kroman and Bratholm,[13] against the crystal structure. In order to have a transferable RMSD value across **1-6**, the structures were trimmed and the RMSDs were obtained considering only the metal atom, the 10 carbon atoms from the two cyclopentadienyl (Cp) rings and the directly bonded carbon atoms of the corresponding substituents. We observe a very good agreement between the optimised and crystal structures, with the maximum RMSD value of 0.358 Å for **3**.

Table S1. Cartesian coordinates of the optimised structures for **1-6.**

1							
PBE				PBE0			
Dy	-0.000003	0.00001	-0.258916	Dy	-0.000089	-0.000378	-0.242488
C	-2.50515	-0.376571	-0.743551	C	1.845444	0.612342	1.443009
C	-2.158845	-1.340476	0.263676	H	1.619017	1.058801	2.40003
C	2.505131	0.376552	-0.743599	C	2.150356	1.333188	0.265629
C	2.158869	1.34048	0.26362	C	2.489556	0.381198	-0.738328
C	-2.412753	0.931142	-0.146581	C	2.402296	-0.919314	-0.150393
C	2.018107	-0.777077	1.222325	C	2.018473	-0.771665	1.210066
C	-2.018092	0.777099	1.222338	C	2.253229	2.839601	0.212568
C	-1.844246	-0.61783	1.449205	H	2.290869	3.153765	-0.841519
C	1.844291	0.617859	1.44917	C	3.557347	3.28669	0.881626
C	2.412727	-0.931149	-0.146604	H	4.431145	2.799386	0.426809
C	-1.609018	2.54977	-1.923567	H	3.686634	4.376385	0.798662
C	-1.786357	-1.320898	-3.000842	H	3.549386	3.024469	1.951118
C	1.608808	-2.54975	-1.923509	C	1.059042	3.534733	0.864134
C	-2.91261	-0.659465	-2.184186	H	0.106308	3.265974	0.37837
C	-2.646702	2.276606	-0.816151	H	0.972441	3.273014	1.930097
C	2.646589	-2.276628	-0.816173	H	1.159853	4.628006	0.800519
C	1.786337	1.320948	-3.000867	C	2.896814	0.671551	-2.168867
C	2.912561	0.65942	-2.184247	H	3.088876	-0.2989	-2.644935
C	-2.271222	-2.854202	0.207639	C	4.203308	1.461042	-2.260333
C	2.271289	2.854201	0.207556	H	4.996437	0.97194	-1.676168
C	2.052998	-1.855226	2.291087	H	4.539934	1.525885	-3.306071
C	-2.052923	1.855267	2.291081	H	4.09333	2.487824	-1.883938
C	-1.081579	-3.567355	0.871892	C	1.781049	1.334601	-2.978951
C	1.081638	3.567396	0.871748	H	0.862507	0.714456	-3.007319
C	1.288385	-1.480026	3.566504	H	1.509339	2.324759	-2.583532
C	-1.288227	1.480073	3.566448	H	2.076062	1.471607	-4.03029

C	-4.090883	2.479713	-1.31074
C	-4.228879	-1.450778	-2.289737
C	4.228891	1.450627	-2.289821
C	-3.594485	-3.296305	0.86762
C	4.090725	-2.479797	-1.310871
C	3.594541	3.296285	0.86757
C	3.524759	-2.175643	2.633089
C	-3.52466	2.175699	2.633173
H	1.61232	1.070295	2.410124
H	2.302739	3.168833	-0.855505
H	4.466925	2.799184	0.401829
H	3.731172	4.392661	0.780234
H	3.595845	3.034453	1.945345
H	0.114464	3.298152	0.397101
H	1.004403	3.314485	1.948777
H	1.189705	4.667171	0.797142
H	3.102717	-0.322358	-2.657702
H	5.028851	0.963291	-1.698717
H	4.564594	1.503357	-3.344804
H	4.122364	2.48958	-1.922377
H	0.856543	0.701356	-3.011442
H	1.520864	2.326108	-2.616049
H	2.072952	1.439853	-4.065078
H	2.471338	-3.043871	-0.033629
H	4.239358	-3.522406	-1.655967
H	4.348147	-1.810255	-2.155088
H	4.816372	-2.28098	-0.498327
H	1.715805	-3.569885	-2.344268
H	0.564643	-2.50962	-1.528925
H	1.68477	-1.836053	-2.769129
H	1.595097	-2.782192	1.882963
H	3.583356	-2.977279	3.395975
H	4.093342	-2.508382	1.743257
H	4.031525	-1.275915	3.038175
H	1.308663	-2.31926	4.288318
H	1.748008	-0.605169	4.070982
H	0.23037	-1.231095	3.360852
H	-1.612238	-1.070247	2.410157
H	-1.595044	2.782222	1.88291
H	-4.093296	2.508434	1.743374
H	-4.031408	1.27598	3.038301
H	-3.583201	2.977344	3.396055
H	-0.230258	1.231033	3.360694
H	-1.308363	2.319342	4.288224
H	-1.747876	0.605278	4.071011
H	-2.471423	3.043861	-0.033625
H	-4.239579	3.52231	-1.65585
H	-4.348347	1.810142	-2.15492
H	-4.816462	2.280891	-0.498136

C	2.637442	-2.253745	-0.823691
H	2.461057	-3.020925	-0.053051
C	4.07516	-2.447813	-1.309476
H	4.225294	-3.478519	-1.664403
H	4.334204	-1.771993	-2.137299
H	4.790993	-2.260189	-0.49639
C	1.613773	-2.517074	-1.932281
H	1.738043	-3.518705	-2.371216
H	0.576059	-2.499898	-1.543326
H	1.682329	-1.789437	-2.755899
C	2.042232	-1.850832	2.266827
H	1.566101	-2.759648	1.862187
C	3.498858	-2.198176	2.596309
H	3.54662	-2.996443	3.352133
H	4.049657	-2.538299	1.707975
H	4.022239	-1.315653	2.996403
C	1.296884	-1.463642	3.538297
H	1.298478	-2.299776	4.252038
H	1.777777	-0.608595	4.039249
H	0.252502	-1.189284	3.337572
C	-1.845859	-0.612259	1.443081
H	-1.619618	-1.058682	2.400159
C	-2.018527	0.771789	1.210018
C	-2.402227	0.919439	-0.15046
C	-2.489792	-0.38111	-0.738302
C	-2.150901	-1.333096	0.265742
C	-2.042218	1.851021	2.266709
H	-1.56578	2.759689	1.862096
C	-3.498807	2.198713	2.595951
H	-4.049408	2.538936	1.707535
H	-4.022448	1.316325	2.996003
H	-3.54648	2.997011	3.351744
C	-1.297162	1.463696	3.538314
H	-0.252822	1.189035	3.337762
H	-1.298614	2.299865	4.252019
H	-1.778359	0.608807	4.039244
C	-2.637074	2.253857	-0.823868
H	-2.460601	3.021065	-0.053273
C	-4.074671	2.448225	-1.309864
H	-4.224512	3.478983	-1.664765
H	-4.333729	1.772534	-2.137789
H	-4.790688	2.260718	-0.496909
C	-1.613191	2.516839	-1.932349
H	-1.737093	3.518471	-2.371394
H	-0.575554	2.499393	-1.543196
H	-1.681843	1.789167	-2.755936
C	-2.896787	-0.671469	-2.168908
H	-3.088891	0.298962	-2.645005
C	-4.20316	-1.461129	-2.260609

H	-1.716076	3.569911	-2.344295	H	-4.539504	-1.526229	-3.306423
H	-0.564822	2.50965	-1.529068	H	-4.093181	-2.487816	-1.883954
H	-1.685032	1.83609	-2.769197	H	-4.996491	-0.971985	-1.676754
H	-3.10286	0.3223	-2.657626	C	-1.780775	-1.33435	-2.978794
H	-4.564621	-1.503487	-3.344708	H	-2.075143	-1.470385	-4.030444
H	-4.122251	-2.48974	-1.922349	H	-0.861945	-0.714565	-3.006152
H	-5.028856	-0.963536	-1.698578	H	-1.509687	-2.32493	-2.583997
H	-2.072982	-1.4398	-4.06505	C	-2.25349	-2.839514	0.212536
H	-0.856605	-0.701242	-3.011418	H	-2.291102	-3.153588	-0.841575
H	-1.52081	-2.326047	-2.616049	C	-3.557512	-3.286967	0.88156
H	-2.302622	-3.16886	-0.855416	H	-4.431377	-2.799531	0.427004
H	-4.466864	-2.799221	0.401854	H	-3.686736	-4.376638	0.798186
H	-3.731095	-4.392684	0.780289	H	-3.549472	-3.025154	1.951152
H	-3.59582	-3.034466	1.945394	C	-1.059147	-3.53447	0.864001
H	-0.114391	-3.298109	0.397274	H	-0.106433	-3.265455	0.378303
H	-1.004387	-3.314417	1.948917	H	-0.972614	-3.27291	1.930005
H	-1.189626	-4.667134	0.797311	H	-1.159674	-4.62776	0.800183

2

PBE				PBE0			
Dy	0.000001	0.220419	0.000008	Dy	0.000383	-0.190402	-0.001139
C	2.467909	0.866749	-0.345529	C	-2.43086	-0.866571	-0.375155
C	2.427455	-0.023327	0.814951	C	-2.43001	0.027258	0.756748
C	2.063428	-1.325959	0.322722	C	-2.08039	1.312146	0.261181
H	1.996091	-2.227827	0.938389	H	-2.04461	2.212523	0.853899
C	1.92568	-1.305651	-1.101779	C	-1.90882	1.272644	-1.140475
C	2.160367	0.043297	-1.486352	C	-2.11062	-0.066569	-1.508418
H	2.175704	0.393131	-2.522952	H	-2.0893	-0.426553	-2.525118
C	2.85685	2.353278	-0.545463	C	-2.79337	-2.348722	-0.564543
C	2.150034	3.319144	0.431544	C	-2.15102	-3.289442	0.462953
H	1.039481	3.246958	0.352115	H	-1.04621	-3.220103	0.451535
H	2.405967	4.368379	0.182677	H	-2.39289	-4.334167	0.21713
H	2.424347	3.159694	1.4887	H	-2.48779	-3.114659	1.490178
C	2.462489	2.825377	-1.966652	C	-2.31218	-2.838926	-1.940805
H	3.009716	2.281767	-2.760367	H	-2.81875	-2.32722	-2.770445
H	2.708873	3.899166	-2.079755	H	-2.52855	-3.911918	-2.044462
H	1.373642	2.714604	-2.162249	H	-1.2239	-2.709888	-2.074797
C	4.393644	2.494454	-0.429279	C	-4.32313	-2.495126	-0.539812
H	4.769509	2.19877	0.565711	H	-4.75602	-2.184531	0.418163
H	4.698698	3.545002	-0.613839	H	-4.61072	-3.542464	-0.721837
H	4.894763	1.85389	-1.181824	H	-4.77675	-1.874594	-1.326839
C	2.517178	0.244497	2.335545	C	-2.58184	-0.211141	2.264974
C	3.736607	1.09402	2.743513	C	-3.82904	-1.02287	2.62544
H	3.717939	2.117185	2.331134	H	-3.81543	-2.042921	2.227846
H	4.67483	0.609088	2.409131	H	-4.73305	-0.524704	2.245211
H	3.777042	1.185768	3.847546	H	-3.92103	-1.099415	3.719381
C	2.633645	-1.088147	3.111494	C	-2.70581	1.129115	3.004821
H	1.750994	-1.743128	2.974257	H	-1.81108	1.759044	2.894141
H	2.71885	-0.879692	4.196094	H	-2.83964	0.943939	4.080592

H	3.534495	-1.653182	2.80185	H	-3.57534	1.701302	2.650556
C	1.196859	0.924154	2.777969	C	-1.30765	-0.899551	2.784547
H	0.315835	0.25638	2.599524	H	-0.41265	-0.260862	2.626643
H	1.02499	1.905246	2.287466	H	-1.13414	-1.887868	2.333403
H	1.169359	1.116383	3.870944	H	-1.34074	-1.055411	3.874604
C	1.901064	-2.512457	-2.040523	C	-1.85175	2.463279	-2.079164
C	-2.42746	-0.023298	-0.81495	C	2.431087	0.027431	-0.756275
C	-2.4679	0.866787	0.345523	C	2.431	-0.866624	0.375447
C	-2.16037	0.043338	1.486354	C	2.109994	-0.066797	1.508616
H	-2.17571	0.393181	2.522951	H	2.087995	-0.426922	2.525243
C	-1.9257	-1.305617	1.101792	C	1.908743	1.272514	1.140786
C	-2.06345	-1.325932	-0.32271	C	2.081342	1.312288	-0.260743
H	-1.99611	-2.227803	-0.938371	H	2.046151	2.212819	-0.853276
C	-2.51719	0.244505	-2.335548	C	2.582273	-0.210974	-2.264588
C	-1.19686	0.924106	-2.778011	C	1.307003	-0.897974	-2.783402
H	-0.31585	0.256309	-2.599557	H	0.412656	-0.25828	-2.625299
H	-1.02495	1.905207	-2.287541	H	1.13268	-1.886225	-2.332302
H	-1.16937	1.116302	-3.870992	H	1.339089	-1.053879	-3.873485
C	-2.63372	-1.08815	-3.11147	C	2.70724	1.129191	-3.00443
H	-2.71894	-0.879713	-4.196072	H	2.840751	0.943945	-4.080228
H	-3.53458	-1.653151	-2.801793	H	3.577302	1.700607	-2.650237
H	-1.75109	-1.743156	-2.974243	H	1.813066	1.75989	-2.893597
C	-3.7366	1.094064	-2.743512	C	3.828318	-1.02407	-2.625863
H	-3.71789	2.117235	-2.33115	H	3.813847	-2.044125	-2.228312
H	-4.67483	0.609169	-2.40911	H	4.733091	-0.526902	-2.246161
H	-3.77704	1.185795	-3.847546	H	3.919552	-1.100658	-3.719864
C	-2.8568	2.353328	0.54544	C	2.792957	-2.34893	0.564665
C	-4.39358	2.494556	0.42925	C	4.322608	-2.496175	0.539021
H	-4.89473	1.854025	1.181807	H	4.777	-1.875986	1.325864
H	-4.6986	3.545118	0.61379	H	4.609716	-3.543692	0.720782
H	-4.76946	2.198867	-0.565735	H	4.755157	-2.185732	-0.41915
C	-2.46242	2.825433	1.966623	C	2.312355	-2.838859	1.941222
H	-1.37358	2.714638	2.162218	H	1.224191	-2.709531	2.075785
H	-3.00966	2.281845	2.760346	H	2.819521	-2.327142	2.770495
H	-2.70878	3.899229	2.079714	H	2.52855	-3.911885	2.044868
C	-2.14994	3.319153	-0.431576	C	2.149378	-3.289264	-0.46245
H	-1.03939	3.246912	-0.352147	H	1.044595	-3.219305	-0.450299
H	-2.40582	4.368403	-0.18272	H	2.390685	-4.334166	-0.216804
H	-2.42426	3.159704	-1.488731	H	2.485595	-3.114703	-1.489899
C	-1.90111	-2.512417	2.040542	C	1.851588	2.462966	2.079687
C	-3.3596	-3.033561	2.118991	C	3.281539	3.026185	2.161508
H	-3.72466	-3.348685	1.121063	H	3.632517	3.359258	1.173251
H	-4.04277	-2.248339	2.50017	H	3.984375	2.26445	2.53129
H	-3.42077	-3.906685	2.800235	H	3.316362	3.887909	2.845867
C	-1.43811	-2.118018	3.455687	C	1.404306	2.046933	3.482033
H	-0.40086	-1.725188	3.453917	H	0.390895	1.616864	3.477922
H	-1.45445	-3.003955	4.120787	H	1.386265	2.922893	4.146925
H	-2.09703	-1.353982	3.914512	H	2.088468	1.312217	3.932334
C	-0.99498	-3.635422	1.508202	C	0.915629	3.55093	1.554196

H	-1.30411	-3.975961	0.50062	H	1.212388	3.900377	0.554853
H	-1.03774	-4.51475	2.181293	H	0.92796	4.422957	2.22485
H	0.060573	-3.30377	1.447113	H	-0.12082	3.186648	1.491385
C	1.438033	-2.118068	-3.45566	C	-1.40463	2.047566	-3.481666
H	0.400784	-1.725244	-3.453868	H	-0.39102	1.617938	-3.477866
H	1.454369	-3.004007	-4.120756	H	-1.38708	2.92361	-4.14646
H	2.096942	-1.35403	-3.914503	H	-2.0886	1.312638	-3.931922
C	3.359554	-3.033596	-2.119	C	-3.28167	3.026605	-2.160682
H	4.042718	-2.248375	-2.500201	H	-3.98458	2.265022	-2.530624
H	3.420721	-3.906726	-2.800237	H	-3.31653	3.888549	-2.844764
H	3.724644	-3.348709	-1.121076	H	-3.63252	3.359375	-1.172279
C	0.994949	-3.63546	-1.508158	C	-0.91562	3.551056	-1.553564
H	1.037703	-4.514793	-2.181244	H	-0.92779	4.423129	-2.224158
H	-0.0606	-3.303809	-1.447055	H	0.120769	3.186598	-1.490732
H	1.304095	-3.975992	-0.50058	H	-1.21236	3.90048	-0.554208

3

PBE				PBE0			
Dy	-0.027002	0.210135	-0.28115	Dy	-0.026534	0.215381	-0.246892
C	-2.270493	-0.833526	-1.023418	C	2.203194	-1.183	-0.567628
C	-2.200668	-1.308663	0.327216	C	2.041707	-0.991471	0.838101
C	2.228142	-1.190134	-0.549164	C	2.196755	0.406732	1.122578
C	2.033042	-0.996512	0.863133	C	2.441026	1.079437	-0.119171
C	-2.450142	0.591753	-1.000218	C	2.452243	0.095628	-1.154657
C	2.481227	0.100247	-1.137521	C	2.438063	-2.48009	-1.329286
C	-2.292565	-0.159911	1.194679	H	2.426065	-2.202627	-2.393376
C	2.172481	0.414774	1.151241	C	3.845013	-3.01142	-1.035436
C	2.445838	1.092727	-0.09532	H	4.088369	-3.851156	-1.704006
C	-2.47186	1.014038	0.382284	H	4.607642	-2.23163	-1.174395
C	-2.142757	-1.723607	-2.256058	H	3.92312	-3.376582	-0.00079
C	-1.527216	-3.865491	0.446966	C	1.408896	-3.602391	-1.222151
C	-2.494627	-2.730508	0.810698	H	1.600517	-4.347037	-2.00984
C	-0.879574	-1.405375	-3.088133	H	1.447164	-4.142628	-0.266269
C	2.501931	-2.492017	-1.306589	H	0.383948	-3.235506	-1.357445
C	1.941924	-2.165799	1.84592	C	1.949181	-2.152938	1.817014
C	0.731217	-2.178111	2.795716	H	1.819972	-3.035883	1.180102
C	-2.491638	1.416663	-2.286467	C	3.240545	-2.388159	2.608869
C	1.479898	-3.636763	-1.229241	H	3.223648	-3.39327	3.057375
C	-1.200847	2.228211	-2.482858	H	4.133885	-2.315864	1.972515
C	2.258656	0.942509	2.582778	H	3.351365	-1.669456	3.432592
C	-2.434235	-0.280686	2.711644	C	0.751855	-2.149647	2.768365
C	2.999619	0.292315	-2.564883	H	0.639188	-3.13976	3.236095
C	-2.91499	2.340131	0.999748	H	0.860001	-1.423478	3.586766
C	2.783896	2.55631	-0.393346	H	-0.185164	-1.925322	2.240209
C	1.60516	3.539622	-0.289546	C	2.330346	0.925326	2.544946
C	2.185841	1.211941	-3.495646	H	1.849882	0.162889	3.172838
C	1.543476	2.270386	2.88793	C	3.799444	0.980488	2.991158
C	-2.16306	3.614876	0.586952	H	4.343404	0.067706	2.720107
C	-1.496298	0.591283	3.562922	H	4.330297	1.825746	2.537452

C	-3.40529	-1.77634	-3.137555	H	3.856402	1.101205	4.084071
C	-3.941413	-3.105483	0.420279	C	1.643211	2.249423	2.878676
C	3.917854	-3.010322	-0.97583	H	1.588259	2.375673	3.970335
C	3.239962	-2.392959	2.65034	H	2.194759	3.11321	2.485857
C	-3.735751	2.288146	-2.512848	H	0.612371	2.303835	2.496072
C	-3.898043	-0.15089	3.182243	C	2.75393	2.538696	-0.420755
C	3.719476	1.013009	3.08706	H	2.995192	2.546186	-1.489088
C	4.501906	0.657288	-2.568081	C	4.000047	3.093758	0.268652
C	-4.442668	2.533175	0.873371	H	4.309073	4.027357	-0.225954
C	4.028207	3.098622	0.33193	H	3.828511	3.333117	1.325856
H	2.517542	-2.210902	-2.379111	H	4.83915	2.385623	0.210985
H	4.196297	-3.839368	-1.656884	C	1.566924	3.490751	-0.280357
H	4.678222	-2.21167	-1.077575	H	0.727919	3.183318	-0.925051
H	3.972267	-3.397248	0.060811	H	1.200643	3.570057	0.750262
H	1.720921	-4.39682	-1.999513	H	1.841047	4.505612	-0.607742
H	1.482177	-4.163569	-0.25552	C	2.952103	0.287854	-2.58019
H	0.44832	-3.288256	-1.417969	H	2.909099	-0.702841	-3.052602
H	1.823618	-3.056179	1.202433	C	4.438425	0.672326	-2.596119
H	3.233212	-3.409265	3.093175	H	4.838752	0.591169	-3.618029
H	4.143394	-2.302798	2.016995	H	4.617185	1.702119	-2.255145
H	3.336667	-1.675164	3.487132	H	5.02393	0.003871	-1.948421
H	0.629637	-3.174831	3.270491	C	2.119742	1.187465	-3.496575
H	0.822662	-1.440921	3.617444	H	2.602916	1.270792	-4.481803
H	-0.211052	-1.967395	2.255846	H	1.120746	0.759217	-3.670468
H	1.75887	0.173428	3.202294	H	1.988952	2.210331	-3.112539
H	4.287	0.098982	2.837705	C	-2.258136	-0.832939	-0.992191
H	4.262658	1.869379	2.649599	C	-2.18239	-1.292138	0.353595
H	3.733374	1.136592	4.188887	C	-2.271961	-0.144722	1.203255
H	1.447449	2.404336	3.983808	C	-2.459498	1.011861	0.38681
H	2.104749	3.143609	2.506524	C	-2.44211	0.580182	-0.980735
H	0.518623	2.312857	2.465476	C	-2.148742	-1.730563	-2.211117
H	3.056718	2.555218	-1.462866	H	-1.993162	-2.742792	-1.816618
H	4.369333	4.030143	-0.163065	C	-0.914522	-1.420277	-3.069921
H	3.828481	3.350796	1.390079	H	0.020224	-1.371631	-2.472277
H	4.862679	2.371295	0.303978	H	-0.732903	-2.216079	-3.808154
H	0.762284	3.234442	-0.943009	H	-1.006815	-0.478111	-3.629167
H	1.222415	3.648086	0.741078	C	-3.421015	-1.792539	-3.060692
H	1.908197	4.54905	-0.634665	H	-4.295984	-2.028319	-2.439222
H	2.943816	-0.704726	-3.043895	H	-3.63457	-0.846487	-3.579185
H	4.91306	0.570784	-3.593721	H	-3.32867	-2.574148	-3.830162
H	4.692819	1.692136	-2.222311	C	-2.47393	-2.701274	0.852461
H	5.076925	-0.023579	-1.910632	H	-2.459582	-2.640952	1.949787
H	2.678973	1.28011	-4.486018	C	-1.518599	-3.83799	0.504346
H	1.170498	0.804105	-3.674933	H	-0.484853	-3.600816	0.779944
H	2.075763	2.247219	-3.115195	H	-1.811167	-4.741572	1.06055
H	-1.995237	-2.747909	-1.866884	H	-1.534835	-4.107203	-0.561524
H	0.047898	-1.353304	-2.46192	C	-3.911461	-3.073834	0.467928
H	-0.667244	-2.206752	-3.824113	H	-4.619366	-2.274446	0.731252
H	-0.960116	-0.457329	-3.655346	H	-4.001378	-3.258474	-0.612949

H	-4.297378	-2.023697	-2.530778	H	-4.222007	-3.99324	0.986927
H	-3.61308	-0.816908	-3.651265	C	-2.378565	-0.242313	2.71686
H	-3.296897	-2.55326	-3.920876	H	-2.085304	-1.272077	2.964439
H	-2.479044	-2.682823	1.917581	C	-1.409676	0.627299	3.516536
H	-0.488277	-3.624087	0.731074	H	-0.374609	0.469161	3.185676
H	-1.817582	-4.787039	0.990343	H	-1.622612	1.704066	3.453575
H	-1.536822	-4.118553	-0.631651	H	-1.455129	0.355845	4.582381
H	-4.657196	-2.305842	0.694233	C	-3.816482	-0.085563	3.221586
H	-4.0339	-3.279885	-0.670431	H	-4.514522	-0.714251	2.649572
H	-4.251206	-4.037882	0.933144	H	-3.880151	-0.385768	4.278506
H	-2.132764	-1.319911	2.950056	H	-4.167606	0.953687	3.155551
H	-0.443781	0.464769	3.249899	C	-2.908127	2.332657	0.991283
H	-1.73291	1.672824	3.523759	H	-2.698751	2.23443	2.062515
H	-1.562817	0.287753	4.627129	C	-4.429381	2.500328	0.880974
H	-4.578119	-0.782858	2.578038	H	-4.765211	3.325727	1.527695
H	-3.987067	-0.470373	4.23989	H	-4.748292	2.73051	-0.142279
H	-4.263406	0.892329	3.122006	H	-4.955247	1.587689	1.192411
H	-2.717491	2.225352	2.080267	C	-2.18406	3.603328	0.5552
H	-4.775832	3.359781	1.533119	H	-2.489385	4.444179	1.195985
H	-4.748062	2.785642	-0.15751	H	-1.091026	3.508642	0.648316
H	-4.990705	1.618143	1.166967	H	-2.416727	3.895376	-0.478167
H	-2.466705	4.458709	1.238234	C	-2.501141	1.388865	-2.266184
H	-1.064604	3.503585	0.693	H	-2.521473	0.643866	-3.068651
H	-2.379512	3.925759	-0.453552	C	-1.22739	2.203178	-2.481407
H	-2.509481	0.673097	-3.102339	H	-1.178021	2.634333	-3.493523
H	-1.135148	2.671232	-3.497756	H	-1.136717	3.030383	-1.766294
H	-1.108735	3.053819	-1.753501	H	-0.304787	1.585125	-2.419655
H	-0.272442	1.601671	-2.421467	C	-3.746614	2.242654	-2.48449
H	-4.662636	1.709715	-2.333604	H	-4.660463	1.662344	-2.293058
H	-3.75621	3.180931	-1.860597	H	-3.767085	3.134042	-1.844583
H	-3.754684	2.648596	-3.561135	H	-3.77829	2.591324	-3.528133

4

PBE				PBE0			
Dy	0.038732	0.319672	-0.184529	Dy	0.035128	0.29238	-0.184075
C	-2.393705	-0.262879	-1.021265	C	-2.203521	0.658384	1.089607
C	-2.494653	0.954795	-0.265598	C	-1.917999	-0.735472	1.200329
C	2.390364	-0.695407	-0.849049	C	-2.038491	-1.310715	-0.107809
C	2.258369	-1.082279	0.528211	C	-2.386696	-0.271556	-1.016112
C	2.226241	0.114636	1.323249	C	-2.481719	0.946512	-0.281593
C	2.348979	1.239042	0.443771	C	-2.368487	1.652983	2.211787
C	-2.207257	0.648842	1.111967	H	-1.52516	1.605313	2.914627
C	2.458154	0.740321	-0.895707	H	-2.344953	2.668114	1.794577
C	-2.032834	-1.319328	-0.120551	C	-3.672218	1.476819	2.991288
C	-1.91027	-0.755141	1.205165	H	-3.793354	2.283867	3.729119
C	-1.890802	0.319864	-3.483896	H	-4.544036	1.490035	2.322423
C	-2.105459	3.489948	-0.75361	H	-3.693306	0.522903	3.5346
C	-2.769549	-0.460363	-2.486898	C	-1.701216	-1.567149	2.452183
C	-3.033625	2.264731	-0.841717	H	-0.991855	-2.364765	2.174643

C	1.473458	-3.56016	0.774133
C	2.469997	-2.455921	1.154753
C	2.244961	2.707433	0.838899
C	0.850859	3.002875	1.422342
C	2.633056	-1.651804	-2.01073
C	-2.368963	1.63319	2.253679
C	2.354401	0.145832	2.829663
C	-2.07771	-2.817977	-0.406313
C	2.59416	1.576408	-2.161964
C	-1.153156	-3.336267	-1.522235
C	-1.69647	-1.60789	2.453126
C	1.628973	-1.535475	-3.175376
C	1.30711	2.370395	-2.461731
C	-1.052724	-0.900994	3.656661
C	-4.273318	-0.226897	-2.746435
C	-4.434216	2.602895	-0.292204
C	3.920255	-2.941971	0.938584
C	3.367074	3.212581	1.761055
C	3.81494	0.025178	3.305841
C	-3.528901	-3.288307	-0.652926
C	4.085446	-1.556094	-2.522248
C	3.851675	2.463839	-2.177374
C	-3.678273	1.452774	3.043723
C	-3.004243	-2.300944	2.894542
H	-1.517537	1.571925	2.959115
H	-2.343021	2.662237	1.848956
H	-3.792612	2.259382	3.79474
H	-4.560256	1.475703	2.375332
H	-3.700857	0.487235	3.583194
H	-0.992232	-2.415999	2.158869
H	-3.420145	-2.953212	2.105027
H	-2.822055	-2.928648	3.789842
H	-3.782198	-1.55599	3.153534
H	-0.191226	-0.273923	3.361034
H	-1.77065	-0.258475	4.200932
H	-0.685551	-1.654184	4.381622
H	-1.738	-3.316269	0.524171
H	-4.22085	-2.909131	0.123621
H	-3.908805	-2.941413	-1.634105
H	-3.580921	-4.395462	-0.650813
H	-0.112525	-2.99171	-1.380895
H	-1.135063	-4.444575	-1.519064
H	-1.479845	-3.023865	-2.533796
H	-2.590721	-1.528593	-2.704766
H	-4.892876	-0.781103	-2.014789
H	-4.559052	0.840956	-2.684224
H	-4.543315	-0.58104	-3.761562
H	-0.820676	0.034805	-3.391565
H	-2.184156	0.091878	-4.52839

C	-2.994573	-2.26244	2.893799
H	-3.393658	-2.926562	2.116533
H	-2.812355	-2.870029	3.7933
H	-3.777126	-1.528212	3.134448
C	-1.07298	-0.83922	3.638486
H	-0.225557	-0.209926	3.335954
H	-1.794944	-0.2028	4.167698
H	-0.699698	-1.572264	4.368912
C	-2.073814	-2.804073	-0.378269
H	-1.74464	-3.289891	0.552647
C	-3.509998	-3.278158	-0.636448
H	-4.204867	-2.906706	0.129909
H	-3.879881	-2.932301	-1.612797
H	-3.556225	-4.377756	-0.637796
C	-1.140462	-3.31991	-1.47434
H	-0.112432	-2.962441	-1.332014
H	-1.10672	-4.419818	-1.455953
H	-1.462413	-3.028445	-2.48453
C	-2.754767	-0.480891	-2.473374
H	-2.581756	-1.543565	-2.679683
C	-4.246479	-0.244414	-2.737081
H	-4.865236	-0.794975	-2.013852
H	-4.527831	0.816107	-2.673666
H	-4.51152	-0.593644	-3.746669
C	-1.872942	0.283731	-3.463903
H	-0.813537	-0.009374	-3.369492
H	-2.164368	0.057346	-4.500792
H	-1.9364	1.375691	-3.340267
C	-3.006654	2.246456	-0.871412
H	-3.145537	2.046956	-1.940562
C	-4.391414	2.605078	-0.324731
H	-5.066851	1.737728	-0.350767
H	-4.34296	2.965547	0.712124
H	-4.841731	3.407005	-0.929501
C	-2.069776	3.453005	-0.803189
H	-1.093035	3.244471	-1.269717
H	-2.504753	4.300217	-1.354838
H	-1.89103	3.799712	0.225008
C	2.207347	0.118034	1.316772
C	2.324676	1.233063	0.44223
C	2.443854	0.736188	-0.885365
C	2.385557	-0.688879	-0.83605
C	2.250655	-1.070906	0.530715
C	2.328102	0.151495	2.816646
H	1.900236	1.081095	3.218411
H	1.739716	-0.660561	3.265934
C	3.777661	0.019322	3.288942
H	3.841137	0.121107	4.382469
H	4.194579	-0.961021	3.019329

H	-1.965129	1.419079	-3.356767	H	4.42103	0.785682	2.834602
H	-3.167274	2.0773	-1.922617	C	2.219766	2.693171	0.835302
H	-5.104828	1.722567	-0.332494	H	2.298414	3.280199	-0.088659
H	-4.394118	2.952091	0.757326	C	3.337655	3.189377	1.750716
H	-4.894496	3.413561	-0.892155	H	4.32391	2.945833	1.32965
H	-1.116814	3.298988	-1.22174	H	3.277459	4.282334	1.86556
H	-2.551561	4.345795	-1.298943	H	3.28135	2.749017	2.755283
H	-1.933493	3.827139	0.287756	C	0.837266	2.988059	1.419951
H	1.914077	1.07616	3.239571	H	0.015413	2.738537	0.715486
H	1.77072	-0.679487	3.281352	H	0.653621	2.440756	2.355868
H	3.875897	0.123507	4.407723	H	0.694378	4.05984	1.626658
H	4.246031	-0.956491	3.030804	C	2.599043	1.56614	-2.143539
H	4.456354	0.805476	2.853421	H	2.730707	0.859011	-2.970896
H	2.325744	3.29799	-0.092803	C	3.854171	2.439889	-2.135294
H	4.361652	2.96618	1.340667	H	4.74589	1.82543	-1.943613
H	3.305468	4.313917	1.870934	H	3.984042	2.934911	-3.109711
H	3.309302	2.774595	2.775278	H	3.823738	3.22502	-1.36657
H	0.023307	2.747958	0.712118	C	1.331344	2.363172	-2.46228
H	0.663649	2.456635	2.367824	H	0.443321	1.705698	-2.57199
H	0.699243	4.083131	1.621861	H	1.107887	3.125842	-1.700095
H	2.715406	0.864036	-2.997632	H	1.407183	2.888043	-3.42694
H	4.756437	1.851969	-1.993491	C	2.63094	-1.642273	-1.98893
H	3.965496	2.957814	-3.16319	H	2.507877	-2.654481	-1.578859
H	3.827618	3.259481	-1.407472	C	4.07322	-1.541182	-2.496304
H	0.408933	1.706558	-2.537085	H	4.792362	-1.655335	-1.673132
H	1.100144	3.153396	-1.703713	H	4.276727	-2.325254	-3.241393
H	1.35124	2.879303	-3.445964	H	4.271675	-0.570556	-2.975173
H	2.505397	-2.671822	-1.599251	C	1.632347	-1.530404	-3.144756
H	4.810364	-1.673963	-1.694168	H	0.5917	-1.621258	-2.795816
H	4.286497	-2.34669	-3.272732	H	1.721525	-0.585392	-3.700498
H	4.289415	-0.579596	-3.00559	H	1.788994	-2.343074	-3.870226
H	0.579162	-1.594441	-2.821429	C	2.463304	-2.436162	1.156465
H	1.741283	-0.595829	-3.752103	H	2.349084	-2.281885	2.240186
H	1.765309	-2.369783	-3.89241	C	3.900047	-2.92296	0.930232
H	2.345711	-2.303709	2.246312	H	4.636426	-2.139581	1.160264
H	4.658151	-2.150613	1.174234	H	4.113768	-3.792646	1.569829
H	4.133328	-3.81589	1.586038	H	4.060589	-3.235828	-0.11196
H	4.091305	-3.258723	-0.109293	C	1.466815	-3.530341	0.787113
H	0.427485	-3.234655	0.934297	H	0.430113	-3.199904	0.942229
H	1.572635	-3.878347	-0.282297	H	1.565559	-3.856709	-0.258186
H	1.645487	-4.459226	1.399204	H	1.631958	-4.417881	1.416558

5

PBE				PBE0			
Dy	-0.056895	-0.349115	-0.101932	Dy	-0.059286	-0.325235	-0.09164
C	2.333059	-0.278207	0.94178	C	-2.158503	0.725708	-1.264377
C	2.425895	-1.127854	-0.214854	C	-2.111855	1.399043	-0.008767
C	-2.408058	-0.671667	-1.036286	C	-2.327181	0.429963	1.016982
C	2.081259	1.06163	0.491037	C	-2.515736	-0.837001	0.389645

C	-2.525388	-0.855544	0.378837
C	-2.160202	0.71826	-1.288138
C	2.229206	-0.310989	-1.378461
C	-2.342021	0.422086	1.010451
C	-2.122688	1.398302	-0.023882
C	2.02079	1.041037	-0.951147
C	1.637396	-1.77913	2.914353
C	2.587132	-0.684605	2.389148
C	1.919635	-3.601796	-0.818637
C	2.892224	-2.580868	-0.198699
C	-2.420751	-1.77907	-2.082226
C	-2.785278	-2.169919	1.103519
C	-1.024493	-1.923895	-2.718508
C	2.109407	2.337596	1.32447
C	-1.591622	-3.137998	0.980882
C	2.396241	-0.766173	-2.806793
C	-2.244729	1.375683	-2.641785
C	-2.596378	0.757381	2.474891
C	2.080974	2.286583	-1.822965
C	-2.192936	2.901664	0.200074
C	1.017014	2.444884	2.404156
C	-1.684079	0.052154	3.495503
C	-1.078151	3.744191	-0.439358
C	1.316462	2.230643	-3.155944
C	4.065049	-1.050343	2.638776
C	4.307523	-2.708369	-0.799219
C	-3.531752	-1.641237	-3.136582
C	-4.120148	-2.829455	0.712192
C	3.506676	2.603786	1.922975
C	-4.087776	0.573966	2.825336
C	3.556367	2.672577	-2.062491
C	-3.590089	3.425364	-0.195398
H	-1.802121	2.384151	-2.649684
H	-3.307876	1.48684	-2.941382
H	-1.752816	0.794382	-3.443577
H	-2.094464	3.062064	1.293641
H	-3.762259	3.336905	-1.286606
H	-3.695247	4.494901	0.075176
H	-4.39279	2.860637	0.318425
H	-0.079038	3.362437	-0.158259
H	-1.148229	4.793449	-0.08983
H	-1.129224	3.769521	-1.544917
H	-2.381237	1.839376	2.588252
H	-4.733833	1.131851	2.119605
H	-4.296096	0.944425	3.848897
H	-4.394524	-0.490661	2.786684
H	-1.829297	-1.046339	3.527511
H	-1.883776	0.431769	4.517577
H	-0.614247	0.250518	3.284429

C	-2.404758	-0.653482	-1.014886
C	-2.248117	1.381936	-2.610778
H	-1.805354	2.381464	-2.619925
H	-3.305501	1.4954	-2.898912
H	-1.766695	0.802465	-3.408896
C	-2.161574	2.896004	0.211942
H	-2.081213	3.057375	1.297803
C	-3.530843	3.441	-0.208608
H	-3.681336	3.358731	-1.295254
H	-3.62248	4.503942	0.060874
H	-4.346758	2.892357	0.284568
C	-1.024036	3.705195	-0.405753
H	-0.047991	3.317993	-0.085643
H	-1.089165	4.75483	-0.082094
H	-1.039085	3.706443	-1.504295
C	-2.555978	0.757134	2.479257
H	-2.336136	1.828657	2.597094
C	-4.031621	0.577026	2.850213
H	-4.68073	1.146062	2.168852
H	-4.219234	0.930456	3.875338
H	-4.342612	-0.477415	2.799956
C	-1.632913	0.043731	3.468542
H	-1.774478	-1.047078	3.487863
H	-1.813873	0.407321	4.491353
H	-0.574821	0.246441	3.243655
C	-2.786619	-2.143313	1.107716
H	-2.867861	-1.902587	2.174594
C	-4.122779	-2.777647	0.717923
H	-4.943093	-2.058401	0.856422
H	-4.328945	-3.655612	1.348778
H	-4.149803	-3.109724	-0.329602
C	-1.614078	-3.119603	0.979036
H	-1.437953	-3.435111	-0.061413
H	-1.776365	-4.03544	1.567742
H	-0.67273	-2.689536	1.379539
C	-2.438746	-1.751466	-2.058101
H	-2.628556	-2.693698	-1.528286
C	-3.563302	-1.603231	-3.081786
H	-4.533418	-1.491951	-2.575674
H	-3.615131	-2.49541	-3.724074
H	-3.424819	-0.732472	-3.736147
C	-1.067387	-1.898811	-2.722108
H	-0.767097	-0.992279	-3.268657
H	-1.039311	-2.7372	-3.434892
H	-0.265028	-2.14085	-1.990603
C	2.202002	-0.313287	-1.382292
C	2.401057	-1.133021	-0.235079
C	2.330999	-0.296604	0.919251
C	2.094515	1.038993	0.482624

H	-2.870636	-1.924017	2.177688	C	2.016565	1.028244	-0.946907
H	-4.95647	-2.114906	0.841472	C	2.341221	-0.759698	-2.809425
H	-4.319135	-3.71098	1.354079	H	2.401912	-1.848754	-2.894187
H	-4.13868	-3.174033	-0.340186	H	1.512653	-0.427572	-3.447041
H	-1.422708	-3.48019	-0.060857	H	3.262811	-0.350218	-3.252402
H	-1.730395	-4.047605	1.599619	C	2.84908	-2.583338	-0.233439
H	-0.642716	-2.683674	1.360694	H	2.95401	-2.872513	0.819503
H	-2.619169	-2.727265	-1.548304	C	4.244186	-2.721773	-0.851496
H	-4.518979	-1.528648	-2.646936	H	4.61968	-3.748705	-0.725379
H	-3.56877	-2.544738	-3.777615	H	4.246238	-2.496632	-1.927342
H	-3.383349	-0.768631	-3.799632	H	4.955445	-2.036256	-0.368063
H	-0.711843	-1.012685	-3.267251	C	1.860974	-3.580855	-0.840473
H	-0.97158	-2.77331	-3.429404	H	0.880777	-3.542712	-0.336444
H	-0.230323	-2.163313	-1.963674	H	1.695101	-3.421646	-1.915878
H	2.431277	-1.864512	-2.892887	H	2.234069	-4.609383	-0.722534
H	1.590529	-0.409073	-3.473397	C	2.597999	-0.71375	2.352825
H	3.346657	-0.378917	-3.229613	H	2.41095	0.173514	2.971802
H	2.984625	-2.865258	0.865719	C	4.066814	-1.089497	2.575294
H	4.696048	-3.736949	-0.658211	H	4.266828	-1.230955	3.648341
H	4.322214	-2.490869	-1.884726	H	4.341172	-2.022731	2.063104
H	5.008951	-2.005664	-0.308232	H	4.735438	-0.299474	2.204662
H	0.922508	-3.57181	-0.330019	C	1.654683	-1.79944	2.877994
H	1.769916	-3.45206	-1.906212	H	0.59864	-1.486707	2.816755
H	2.305261	-4.632426	-0.685706	H	1.756873	-2.753484	2.33983
H	2.383795	0.213034	3.002887	H	1.849613	-2.004392	3.941616
H	4.252314	-1.174584	3.724266	C	2.138523	2.301722	1.321188
H	4.354874	-1.996835	2.142241	H	1.961132	3.133345	0.623031
H	4.739044	-0.256592	2.262488	C	3.528274	2.541229	1.92119
H	0.571813	-1.475543	2.825352	H	4.314582	2.461955	1.156888
H	1.761541	-2.746751	2.388138	H	3.584442	3.547128	2.363882
H	1.811411	-1.968651	3.992674	H	3.763056	1.819167	2.716644
H	1.917134	3.166803	0.613822	C	1.053259	2.409758	2.393946
H	4.298749	2.524605	1.153133	H	0.048962	2.237648	1.974371
H	3.551463	3.62262	2.356848	H	1.202394	1.694318	3.216211
H	3.754042	1.889171	2.732533	H	1.051488	3.415328	2.841395
H	0.008604	2.25853	1.981456	C	2.070397	2.270969	-1.809247
H	1.172335	1.730827	3.237633	H	1.615689	3.086878	-1.230106
H	1.006216	3.460615	2.848051	C	3.53425	2.654829	-2.052032
H	1.622312	3.110438	-1.24086	H	3.600244	3.581581	-2.642051
H	3.624367	3.608416	-2.652613	H	4.070929	2.813827	-1.106012
H	4.096871	2.828335	-1.108951	H	4.062587	1.863693	-2.606584
H	4.089391	1.878607	-2.624358	C	1.30617	2.21255	-3.130628
H	1.182769	3.25466	-3.557641	H	1.166538	3.2294	-3.526772
H	1.858468	1.653705	-3.929468	H	1.845429	1.643992	-3.900606
H	0.310638	1.785347	-3.036657	H	0.31039	1.764059	-3.009061

6

PBE				PBE0			
Dy	-0.670579	0.050361	0.28411	Dy	-0.655735	0.02075	0.260937

C	1.603138	-0.718192	1.079878
C	1.627729	0.715977	1.052956
C	-3.017627	-1.063324	0.262455
C	-3.158769	0.224063	0.87501
C	1.582535	-1.190112	-0.273842
C	-2.716022	-0.864536	-1.12196
C	-2.950314	1.219102	-0.133914
C	1.62765	1.134689	-0.321077
C	-2.674231	0.548294	-1.36749
C	1.607101	-0.044149	-1.140957
C	0.013412	-1.439996	2.901442
C	0.130453	2.374943	2.238757
C	1.433099	-1.600227	2.311923
C	1.479724	1.620942	2.272992
C	0.400048	-3.463073	-0.394015
C	-3.289482	-2.386284	0.924408
C	-3.559624	0.483196	2.301424
C	1.66201	-2.642672	-0.726723
C	-2.714253	-1.935559	-2.175959
C	-3.142482	2.699775	0.039428
C	1.741998	2.579999	-0.791987
C	-2.629705	1.198882	-2.720769
C	1.824712	-0.05253	-2.648228
C	0.708763	-0.736053	-3.456121
C	0.575485	3.033968	-1.689563
C	2.541828	-1.451174	3.367042
C	2.677677	2.55513	2.517912
C	2.953883	-3.333032	-0.247181
C	3.118225	2.883873	-1.417626
C	3.22241	-0.597806	-3.009421
H	-3.119921	-0.245379	3.012589
H	-4.661476	0.408148	2.421603
H	-3.276083	1.498868	2.639762
H	-2.804565	3.06739	1.028975
H	-4.218338	2.965013	-0.042094
H	-2.61343	3.285261	-0.736495
H	-2.081052	2.159931	-2.723334
H	-3.660847	1.418194	-3.07189
H	-2.167042	0.546316	-3.484065
H	-1.941373	-1.781703	-2.952045
H	-3.694286	-1.958324	-2.698813
H	-2.562127	-2.943056	-1.745526
H	-2.61109	-3.190577	0.577292
H	-4.323125	-2.727834	0.702891
H	-3.207888	-2.328186	2.027028
H	1.492016	-2.645672	1.958047
H	3.534178	-1.602078	2.899098
H	2.420654	-2.20903	4.16676
H	2.553531	-0.456268	3.853

C	-3.114401	0.188012	0.924128
C	-2.929303	1.213392	-0.042314
C	-2.694282	0.595535	-1.299249
C	-2.736787	-0.814475	-1.110299
C	-2.997873	-1.064882	0.262917
C	-3.474392	0.392516	2.363697
H	-2.999057	-0.342638	3.031469
H	-4.562048	0.291171	2.511861
H	-3.200217	1.3958	2.719442
C	-3.108677	2.680839	0.193472
H	-2.687436	3.016086	1.153408
H	-4.180203	2.939479	0.213428
H	-2.651561	3.28463	-0.602106
C	-2.6742	1.297578	-2.620434
H	-2.064975	2.212002	-2.614005
H	-3.696988	1.596416	-2.903604
H	-2.298756	0.651233	-3.424145
C	-2.75734	-1.840152	-2.199957
H	-1.993577	-1.666259	-2.96976
H	-3.735016	-1.831013	-2.709384
H	-2.613715	-2.856509	-1.809646
C	-3.248823	-2.407281	0.878047
H	-2.569025	-3.18434	0.498143
H	-4.273729	-2.747838	0.657226
H	-3.153624	-2.383977	1.972723
C	1.614556	-0.755599	1.023118
C	1.591987	-1.161387	-0.340406
C	1.602287	0.013736	-1.147642
C	1.621645	1.144847	-0.280869
C	1.630511	0.667321	1.061378
C	1.464075	-1.687364	2.210013
H	1.513177	-2.70864	1.813038
C	2.588157	-1.585013	3.239802
H	3.562003	-1.72933	2.749938
H	2.47592	-2.362529	4.010575
H	2.619594	-0.613643	3.752952
C	0.067126	-1.551012	2.831726
H	-0.124398	-0.550878	3.257183
H	-0.094466	-2.270637	3.648807
H	-0.742801	-1.795287	2.106093
C	1.651184	-2.584781	-0.856752
H	1.703883	-2.515153	-1.95022
C	2.925534	-3.310475	-0.418437
H	3.817472	-2.729663	-0.695394
H	2.994186	-4.29457	-0.906128
H	2.966869	-3.478365	0.66781
C	0.383312	-3.387949	-0.553276
H	0.217983	-3.536306	0.525307
H	0.426998	-4.388027	-1.010736

H	-0.189324	-0.418239	3.29093	H	-0.507822	-2.887318	-0.970478
H	-0.17023	-2.13445	3.746172	C	1.780405	0.072158	-2.650725
H	-0.788494	-1.713308	2.164257	H	1.776131	1.135512	-2.922113
H	1.719582	-2.61929	-1.830338	C	3.151631	-0.465398	-3.072629
H	3.845606	-2.744238	-0.538733	H	3.957787	0.03734	-2.518238
H	3.044645	-4.340998	-0.698901	H	3.316786	-0.292174	-4.146773
H	2.986591	-3.460387	0.853218	H	3.250774	-1.545772	-2.893518
H	0.243214	-3.592299	0.696566	C	0.637759	-0.561954	-3.442787
H	0.458637	-4.479684	-0.832158	H	0.538712	-1.642381	-3.261262
H	-0.508032	-2.982218	-0.816886	H	0.790227	-0.424439	-4.523908
H	1.819228	1.006118	-2.967903	H	-0.321004	-0.089591	-3.179642
H	4.014027	-0.070687	-2.441353	C	1.714277	2.602304	-0.687441
H	3.423046	-0.456217	-4.090194	H	1.667738	3.188575	0.23978
H	3.320673	-1.679727	-2.793177	C	3.065316	2.94181	-1.323274
H	0.620346	-1.819471	-3.240706	H	3.89167	2.629493	-0.667831
H	0.894224	-0.631601	-4.543781	H	3.150719	4.026773	-1.486834
H	-0.271726	-0.269239	-3.235853	H	3.208122	2.448281	-2.294962
H	1.682728	3.209962	0.115898	C	0.531413	3.073918	-1.53563
H	3.935387	2.578567	-0.734731	H	0.450787	2.535469	-2.490901
H	3.221935	3.969751	-1.614184	H	0.61415	4.146939	-1.765252
H	3.271215	2.355841	-2.378724	H	-0.424042	2.934837	-0.99823
H	0.513228	2.461273	-2.635673	C	1.494004	1.510782	2.315133
H	0.673216	4.105859	-1.953923	H	1.451919	0.81496	3.162956
H	-0.401118	2.91733	-1.169049	C	2.689593	2.423651	2.587524
H	1.431585	0.958847	3.157852	H	3.61673	1.832889	2.6134
H	3.614156	1.966042	2.568571	H	2.577775	2.926265	3.560272
H	2.559404	3.096465	3.477989	H	2.816723	3.202411	1.823033
H	2.804912	3.311892	1.720348	C	0.156198	2.263804	2.324952
H	0.029737	3.047406	1.362419	H	0.053213	2.968539	1.485399
H	-0.02268	2.992284	3.146812	H	0.01473	2.83759	3.253429
H	-0.757125	1.684648	2.249418	H	-0.723986	1.578436	2.308137

Table S2. Normal mode frequencies (cm-1) of the optimised structures for **1**-**6**.

1		**2**		**3**	
PBE	PBE0	PBE	PBE0	PBE	PBE0
33.3385	34.3233	23.1243	22.2299	17.1767	14.1414
36.2946	36.5805	26.0275	29.8151	37.6242	38.241
40.5996	42.7025	36.2251	35.0399	43.8842	45.3834
44.4676	46.6092	39.1615	37.6349	48.7629	51.604
45.6114	49.0479	46.703	46.0906	53.1542	56.9576
54.8968	56.7669	54.8745	53.8915	60.6904	61.0615
60.676	64.4615	58.1584	59.958	67.8596	69.7844
69.6708	72.0849	58.3594	61.9804	70.5732	73.469
73.5098	78.3309	73.6171	74.9589	75.4409	77.9084
79.1293	83.9695	79.8924	84.6071	79.5652	82.8262
82.1886	84.6889	89.4375	91.1801	83.1739	86.4693
92.2723	94.7567	93.082	95.6007	85.0432	89.138

92.3497	96.1069	94.4977	96.9901	95.055	100.0064
100.4738	103.4304	119.1209	126.9998	101.4639	104.1413
102.4837	104.1386	124.178	129.6767	109.2628	113.4891
103.159	111.2537	125.6245	130.0535	109.4528	117.0595
113.3583	120.0041	135.7611	138.0596	115.4662	121.2683
131.3263	135.6426	173.3917	180.2106	122.3568	128.8558
137.7601	145.7535	173.9985	180.6888	126.6593	132.5103
138.9089	147.2805	179.9919	188.7814	131.3536	139.3871
143.5528	151.2924	186.5741	197.5413	133.9566	143.4991
161.0031	166.7778	199.158	207.731	149.5146	152.4821
161.2095	167.5169	202.3212	210.395	153.584	161.8836
166.3545	172.1928	202.627	210.7734	156.5874	163.2312
166.4122	172.648	215.7107	225.2834	162.5403	171.8769
178.1576	186.139	217.428	226.8131	164.7945	173.2187
190.3483	198.7855	224.3868	230.1312	175.0651	181.8521
191.3991	200.6462	226.2828	233.8938	176.7737	183.7628
200.9163	210.4211	228.9092	237.3887	180.0727	185.0494
212.6352	218.6757	236.2663	244.5231	181.3115	188.1231
213.3752	219.3098	244.3911	251.8893	185.9593	191.5303
215.632	225.2804	252.5625	260.3852	186.7556	195.0456
219.3983	226.6519	253.1195	262.4456	193.3992	200.5781
224.6121	233.6824	255.0547	264.1894	195.9383	202.608
226.3237	235.1354	255.4407	265.532	196.341	204.5171
227.4995	236.211	266.028	269.4248	205.2257	212.432
230.1655	239.3408	268.4603	276.4689	205.8838	214.5426
231.6553	239.9788	271.0988	280.1786	209.726	216.2489
237.0955	246.2568	272.3114	281.1351	211.4947	221.2638
242.9705	251.0309	285.2831	296.5244	217.8346	225.8599
243.7354	252.9048	285.7375	296.6688	219.5968	227.7744
248.9652	255.8614	291.6681	299.3211	225.0564	233.7336
249.2995	256.7867	292.2347	303.8998	229.1283	238.7547
251.7818	263.6464	296.057	309.2311	229.6034	240.2207
255.8733	266.692	297.0818	310.0887	234.2295	243.6587
257.3761	269.6601	299.7775	311.682	236.163	247.6684
261.0013	274.6875	300.3319	312.825	241.0583	251.5765
263.9753	275.3728	328.8174	346.7889	243.9303	254.2628
267.0222	280.7134	330.1655	347.0753	246.9839	256.9697
270.1006	281.5811	341.2372	357.2126	248.6541	259.9056
272.0479	283.0341	342.6577	358.1709	252.7028	264.2449
285.1209	296.6801	344.3275	359.0178	254.9534	264.6561
285.2117	296.9492	344.9553	359.9855	257.9282	267.9278
309.2754	320.3865	347.4	367.6611	265.3235	273.9212
313.4355	324.2766	348.5788	368.1583	267.4101	276.4992
336.7744	349.3942	359.416	374.6251	269.7005	281.0165
338.798	351.0266	359.494	375.3219	271.599	282.3926
366.8477	379.9234	371.2353	384.8014	273.6773	284.8092
368.1834	381.3725	375.2829	389.9974	276.0425	287.5049
387.1413	403.7574	382.2257	395.5445	276.3723	288.6519

391.529	407.7572	382.3937	396.024	276.8393	289.4877
418.035	432.1937	388.6941	403.9028	279.3696	291.7093
419.4562	433.8104	388.7945	404.5826	284.3131	299.7639
430.4139	445.3289	413.2102	429.1304	287.8526	301.7537
432.6829	447.7506	417.3926	433.4838	289.8863	305.3537
454.9002	471.2286	425.5473	443.3925	297.1507	309.0669
454.9525	471.2669	426.5022	444.4146	310.7875	321.7333
522.7382	543.7106	452.6678	468.4185	325.1796	336.8089
523.4099	544.8013	455.0405	470.3945	337.7442	352.179
532.1365	551.1179	464.1646	479.8676	347.7893	358.3217
532.6065	551.5082	464.4433	480.1736	350.9404	363.9772
541.4051	563.9574	536.9216	557.3088	376.9549	391.8812
544.7323	566.8806	539.1215	558.7209	383.7234	398.051
569.0781	590.4521	542.3497	562.9414	425.517	441.4377
569.8194	591.6501	543.4169	563.8476	428.0985	443.2676
608.0421	629.0742	561.3757	585.165	429.2385	443.9665
608.1076	629.1368	563.7615	587.6792	436.8869	452.2089
669.5972	696.951	579.3997	602.005	450.5063	466.8199
669.6619	697.0151	580.2798	602.7028	455.3588	471.1233
675.7827	703.5541	630.3497	655.9905	466.1847	483.2582
676.5595	704.0583	630.4733	656.2982	468.6086	485.6563
716.2577	749.0575	655.7743	693.2288	490.3376	509.1009
721.308	753.8401	656.8536	693.4041	495.4783	515.0614
744.7059	771.7489	687.9171	726.6784	519.7574	539.2691
745.163	772.3036	694.8971	733.5153	522.1801	540.5072
809.1032	850.2561	793.9587	833.3582	531.864	553.2393
813.4418	854.5774	798.0419	833.4551	535.5162	554.6621
863.0569	896.3709	802.2721	839.0634	539.911	560.2357
864.4271	897.7433	802.3044	840.8117	543.0413	567.7333
866.4641	899.7045	808.2233	853.3991	550.805	573.0739
866.5446	900.0164	808.502	855.1369	556.06	579.7502
875.2705	909.0468	821.2495	855.9714	560.692	581.9375
876.2252	910.4974	821.9383	856.0392	562.6181	585.091
886.1151	918.0699	831.0197	883.2718	668.4104	691.6271
886.61	919.7473	831.3588	883.5916	668.763	692.5572
888.5303	920.7027	896.7522	931.208	684.6219	715.6737
891.0124	923.3114	897.0333	931.5072	688.8738	720.1736
891.3738	924.0449	897.936	933.5857	701.5159	733.9393
891.9135	925.287	898.2167	934.3554	715.1441	747.7655
895.078	927.7824	902.21	938.9114	734.6638	762.2053
895.3103	927.8544	902.2179	939.0215	739.4653	767.8679
897.0674	930.9871	903.7813	939.905	760.0468	787.7526
898.5513	933.0374	904.5978	940.0615	760.6994	788.3701
928.5239	963.0363	908.392	943.6118	862.3093	896.8965
928.5598	963.1639	908.5867	943.708	867.6641	901.378
930.7394	965.8153	910.6894	946.1611	868.8185	902.9101
931.1026	966.1142	910.7896	946.2767	873.1474	906.5351
934.318	968.7064	913.6521	946.6209	877.5444	910.8732

934.4451	968.7776	915.7856	949.6935	882.9383	915.6932
937.1435	970.8554	915.8378	949.7431	885.612	918.0447
937.7122	971.3985	917.7213	950.4933	886.335	919.0112
966.9874	1004.0695	919.164	953.0994	887.8297	919.5061
967.4322	1004.1312	920.0369	953.342	890.3045	922.18
1012.0248	1049.959	938.1722	975.8632	890.4329	922.5358
1012.4184	1050.5075	940.2231	977.8843	891.8534	925.668
1034.7613	1071.4778	974.7525	1014.974	894.2653	926.9956
1036.557	1073.1091	975.8154	1016.2226	895.9672	928.6729
1045.0449	1082.1367	985.421	1024.2585	896.6414	930.9837
1046.5939	1083.8535	986.4229	1024.3701	898.3446	932.1246
1069.1876	1108.6189	994.4173	1031.9586	903.2012	938.6834
1070.5288	1109.8314	994.7491	1032.151	904.072	940.1108
1089.5813	1130.36	995.7347	1033.1823	904.4767	940.5743
1090.5585	1131.4521	995.9792	1034.2263	909.1908	945.4044
1098.0563	1143.8214	997.5451	1035.1868	926.813	961.5851
1098.1636	1144.1067	998.0619	1035.7791	930.0395	965.4355
1099.6252	1145.602	1000.1316	1037.0625	932.4657	966.7678
1099.9098	1146.2768	1000.3676	1037.7709	933.7813	968.0552
1103.5049	1149.7033	1005.9108	1044.8276	934.0789	968.377
1103.8778	1150.2346	1006.414	1045.4071	934.4599	968.798
1106.8068	1154.1502	1077.0709	1129.1264	934.9063	969.1616
1107.0913	1154.6117	1077.989	1130.2219	935.325	969.5856
1125.2316	1168.6247	1129.4444	1184.3462	939.0531	973.2931
1128.2716	1171.4716	1129.8033	1184.6988	939.1922	973.6898
1136.4162	1179.2487	1146.7894	1192.532	987.9598	1025.1186
1136.7449	1179.7355	1150.447	1195.6107	991.0122	1027.8524
1147.637	1191.9545	1167.3573	1217.255	1002.137	1041.8216

3			5		
1148.4937	1192.9251	1168.217	1217.89	1003.694	1042.7131
1156.8501	1201.6684	1173.7643	1227.7495	1038.584	1076.0099
1159.9613	1205.2196	1176.4931	1228.9236	1040.751	1078.2652
1169.1969	1214.8125	1178.1497	1231.7146	1060.007	1099.455
1171.2801	1216.8546	1179.5295	1232.2696	1060.789	1100.7644
1253.4034	1304.6929	1181.0769	1234.1623	1067.124	1106.9591
1254.2455	1305.4899	1181.4173	1234.6036	1070.881	1110.1209
1267.9996	1320.6423	1185.4478	1238.6891	1081.277	1122.3655
1268.8268	1321.4743	1185.7803	1238.8557	1082.153	1122.9515
1273.8399	1325.8048	1200.8105	1253.7234	1092.694	1137.86
1274.4225	1326.228	1200.9561	1253.8165	1096.064	1141.9111
1285.4887	1335.0457	1208.6889	1261.2213	1098.493	1144.2276
1286.6454	1336.3713	1209.445	1262.5071	1102.318	1148.2952
1286.658	1336.5388	1213.6312	1265.53	1103.328	1150.0595
1287.2995	1337.3085	1214.6249	1267.2188	1105.497	1150.8506
1294.6871	1343.8421	1269.3398	1315.7749	1106.06	1152.0162
1295.0505	1344.1524	1270.2171	1316.7736	1108.931	1152.6559
1296.9695	1347.6355	1310.5133	1365.1811	1109.606	1153.7964
1297.9298	1348.8541	1310.6839	1365.3964	1110.535	1156.9877
1306.7394	1356.3003	1324.3816	1375.811	1113.463	1161.2236
1308.0198	1357.5592	1324.4434	1376.3614	1115.017	1163.5467
1326.4149	1378.1135	1326.0166	1377.3759	1126.646	1170.6545
1328.2603	1380.8998	1327.283	1379.5126	1130.888	1174.9331
1329.2121	1381.5413	1328.69	1380.2162	1143.286	1187.8495
1330.3286	1382.4324	1329.0703	1380.7313	1143.963	1188.8005

1330.7205	1382.9764	1329.2264	1380.9725	1151.386	1197.3568
1331.9977	1383.55	1330.3518	1382.5698	1153.675	1199.8747
1332.401	1383.9806	1331.8198	1387.2048	1159.118	1205.5115
1333.5646	1385.8416	1332.2809	1387.2893	1159.82	1206.6438
1335.6447	1387.9732	1337.8424	1391.9042	1192.726	1242.9593
1336.8731	1390.021	1338.5244	1393.2292	1193.468	1244.1288
1349.2506	1399.4506	1354.7858	1406.786	1263.011	1312.9988
1349.3493	1399.5072	1355.0578	1406.8068	1265.406	1315.7502
1350.5742	1400.5407	1359.8142	1409.8837	1265.816	1316.8259
1350.5984	1400.5642	1360.4654	1412.0066	1268.026	1318.1953
1354.0799	1404.1166	1362.8347	1415.3199	1269.906	1322.3953
1354.8922	1404.8286	1364.9398	1416.5645	1274.27	1324.8057
1355.721	1406.1366	1367.9983	1418.9188	1276.764	1328.8864
1357.7343	1408.2245	1369.2182	1420.4831	1278.738	1330.2555
1382.0276	1437.8019	1387.806	1437.8715	1282.832	1333.754
1384.9166	1441.6427	1389.178	1439.11	1284.05	1336.0392
1387.5063	1442.9019	1389.8307	1439.7073	1288.232	1339.6014
1389.7033	1444.3851	1393.9032	1443.8973	1289.036	1339.8047
1395.4234	1446.4181	1395.6392	1444.9557	1292.37	1347.0012
1398.3054	1449.8538	1398.1721	1447.9324	1297.309	1348.6931
1399.2589	1450.6827	1398.7443	1448.3672	1301.206	1356.3674
1399.8115	1450.7261	1398.8569	1449.3534	1302.862	1357.2194
1400.4805	1453.7582	1399.5115	1449.5408	1306.218	1360.7312
1401.6277	1454.4781	1401.0972	1451.0362	1307.79	1361.0671
1404.2487	1456.722	1401.4774	1452.1136	1313.294	1362.4168

1404.786	1457.698	1402.1898	1452.6959	1313.776	1363.2675
1406.5504	1459.062	1402.5989	1452.699	1326.928	1378.822
1406.7131	1459.2921	1403.3834	1454.2646	1329.678	1381.4537
1409.176	1461.2106	1404.6457	1454.4689	1330.423	1381.9623
1410.164	1461.7587	1408.7147	1459.1592	1331.002	1382.2752
1410.3033	1461.9675	1409.2357	1460.7123	1331.091	1382.6734
1411.5161	1462.7844	1411.1613	1462.5704	1332.709	1384.023
1411.763	1463.1913	1412.3823	1464.2508	1334.619	1386.2277
1412.6901	1464.6092	1413.1108	1464.947	1336.011	1387.9367
1413.9734	1467.0064	1420.3567	1471.6453	1337.326	1389.8551
1414.6944	1468.6329	1422.2109	1473.2426	1338.137	1391.461
1419.9525	1470.8958	1423.092	1474.4373	1340.631	1393.673
1422.2401	1473.0523	1423.4373	1474.4697	1344.469	1395.231
1422.3086	1473.3749	1425.329	1476.2528	1346.461	1399.5005
1424.3067	1475.4355	1426.0087	1476.4971	1347.842	1401.6142
1424.4539	1475.5262	1429.5298	1480.9378	1349.617	1402.5754
1426.0332	1477.1118	1429.5928	1481.1845	1351.401	1404.7949
1426.1469	1477.3975	1432.5131	1483.0869	1353.334	1405.7698
1426.7548	1478.3339	1433.7299	1484.7981	1354.934	1406.6452
1428.9201	1480.8034	1435.0644	1486.3718	1356.104	1407.0201
1429.0553	1480.9922	1438.7495	1490.0919	1358.187	1408.8665
1431.8401	1485.7968	1440.0886	1491.5426	1362.705	1415.1523
1433.0564	1486.0446	1442.0243	1493.1245	1364.186	1419.0824
1433.353	1489.1358	1443.8503	1495.6757	1372.758	1429.4919
1435.4878	1492.0436	1444.6072	1495.9845	1375.655	1432.1334

1437.2443	1493.0886	1450.4548	1502.9654	1387.955	1439.5994
1438.3384	1494.2503	1451.0293	1503.5168	1391.558	1444.7819
1464.4806	1531.3951	1481.2706	1543.0691	1392.597	1444.9518
1465.3729	1532.1581	1483.135	1544.4726	1395.078	1449.3586
2901.143	2992.5671	2884.2812	2980.118	1396.105	1449.7605
2903.6223	2997.514	2887.5381	2982.6776	1399.308	1451.1509
2909.5626	3001.2285	2920.3288	3010.9196	1400.792	1452.6796
2911.8537	3004.9174	2924.226	3018.1435	1402.919	1454.3035
2957.7036	3047.3438	2958.0746	3040.9509	1403.122	1456.2187
2957.7266	3047.4557	2958.1289	3041.1287	1404.72	1456.5165
2963.58	3056.6906	2967.489	3051.087	1405.056	1457.2587
2963.6565	3056.7533	2967.5287	3051.1543	1406.817	1458.2948
2972.4622	3057.3908	2970.424	3055.5198	1407.036	1459.0909
2972.5457	3057.4628	2971.0603	3056.2848	1408.21	1459.4579
2973.1521	3058.1948	2976.1207	3059.4514	1408.694	1460.8794
2973.1957	3058.254	2976.4155	3059.6242	1409.759	1461.6754
2975.8538	3064.0417	2976.4303	3060.2729	1410.026	1463.0299
2975.8617	3064.1057	2978.0338	3061.3767	1411.229	1463.4469
2978.9521	3064.1278	2979.5792	3063.3792	1412.464	1465.0815
2979.2505	3064.412	2979.6275	3063.426	1413.013	1465.9383
2979.2881	3065.413	2985.0393	3069.5456	1414.208	1466.794
2979.579	3065.4471	2985.0808	3069.5894	1414.89	1467.8148
2979.757	3071.0521	2998.8025	3095.2805	1415.49	1468.9956
2979.8379	3071.0716	2999.239	3095.7043	1416.164	1469.9189
2982.4023	3081.0483	3026.785	3116.9305	1416.719	1471.5819
2982.5019	3081.1872	3027.7424	3118.3375	1417.748	1472.6098

3006.9868	3099.0582	3036.1958	3130.0016	1422.759	1474.0436
3008.6127	3099.8755	3036.2288	3130.3663	1424.121	1476.3207
3009.2233	3102.668	3042.3972	3142.4753	1425.099	1476.5286
3009.8525	3103.9422	3042.7576	3142.7842	1425.73	1477.2061
3015.9971	3114.06	3052.8048	3142.8599	1426.336	1478.2373
3016.5056	3114.1389	3052.8432	3143.0883	1427.351	1479.8725
3040.5353	3129.5814	3054.5512	3143.6086	1427.668	1480.8171
3040.6047	3129.699	3054.6311	3143.9627	1429.495	1481.8836
3049.5524	3141.822	3055.4766	3144.5656	1429.63	1483.4117
3049.6484	3141.9201	3056.7348	3144.9421	1432.626	1483.8323
3053.4554	3143.1667	3057.006	3145.4368	1433.828	1485.4991
3053.5229	3143.2093	3057.0575	3145.4527	1434.097	1488.15
3054.8147	3144.2971	3057.3153	3145.7494	1434.856	1489.1681
3054.8261	3144.3052	3057.324	3145.9438	1436.88	1492.36
3055.8276	3147.7576	3059.6713	3148.0578	1438.676	1493.0136
3055.875	3147.7769	3059.966	3148.0831	1440.437	1494.3947
3057.9008	3148.6034	3060.0727	3148.8027	1440.669	1496.2694
3057.9675	3148.6198	3060.5319	3148.9165	1443.129	1497.7067
3059.3403	3149.6803	3060.5408	3148.9378	1444.394	1498.8913
3059.4047	3149.7691	3060.9188	3149.2074	1445.392	1500.6861
3060.9665	3151.8187	3063.9686	3155.0085	2864.541	2964.8254
3061.0336	3151.8385	3066.429	3156.6968	2875.45	2979.8325
3061.8364	3152.8424	3066.6243	3156.763	2969.136	3055.6919
3061.8398	3152.9522	3067.2101	3156.8668	2969.646	3058.5905
3067.3869	3158.2457	3068.2369	3157.2829	2971.56	3059.3777

3067.4897	3158.3475	3068.2763	3157.4802	2973.974	3059.8943
3068.78	3160.0791	3093.6295	3189.1479	2975.093	3060.6195
3068.8129	3160.1016	3093.7526	3189.1964	2975.212	3060.7507
3070.9158	3160.9988	3099.4055	3191.1133	2976.133	3062.1757
3070.9289	3161.0474	3099.4202	3191.3055	2977.303	3062.9335
3074.7033	3166.5185	3104.4991	3202.3213	2977.749	3064.373
3074.7371	3166.5462	3104.5131	3202.3375	2978.502	3064.6321
3075.8815	3166.5536	3181.2154	3256.5974	2978.822	3064.7576
3078.7368	3169.5471	3181.2559	3256.6982	2979.847	3065.9075
3152.8842	3242.6346	3181.324	3259.3662	2980.253	3066.2883
3152.9327	3242.6575	3181.4157	3259.5128	2980.34	3066.5112
				2980.466	3069.1538
				2981.185	3071.0395
				2982.96	3072.2603
				2986.08	3075.7754
				2987.109	3078.7819
				2990.434	3087.4585
				2990.706	3097.5485
				2990.852	3099.3156
				3007.47	3099.8372
				3008.413	3101.0018
				3008.846	3108.3248
				3021.605	3118.7876
				3028.047	3127.9074
				3036.136	3129.5874
				3036.977	3134.7557
				3037.038	3136.6135
				3041.897	3137.322
				3044.414	3137.9527
				3046.112	3139.258
				3047.915	3140.026
				3049.536	3142.5956
				3051.571	3143.6156
				3051.629	3145.2093
				3053.602	3146.0074
				3055.203	3147.0422
				3056.118	3147.9386
				3058.118	3148.193

3058.56	3149.146
3058.682	3149.5736
3058.797	3149.7454
3059.332	3149.9259
3060.11	3151.8843
3060.956	3152.3351
3061.801	3155.566
3064.263	3156.0188
3065.53	3157.6442
3068.067	3158.9664
3069.276	3162.426
3069.975	3162.7413
3071.111	3163.7388
3072.802	3164.5477
3073.337	3165.3992
3073.866	3166.6559
3076.615	3168.5835
3079.037	3169.8964
3080.608	3170.6772
3081.594	3175.8613
3082.253	3177.75
3084.376	3180.4862
3085.484	3181.9945
3093.272	3187.3812
3097.364	3191.2898
3099.521	3194.4406
3103.371	3196.5566

4		**5**		**6**	
PBE	PBE0	PBE	PBE0	PBE	PBE0
33.0309	36.2052	34.9896	35.8665	28.266	25.7439
43.2	44.2261	37.5414	40.0426	31.9309	32.3455
47.5954	48.9191	43.4185	45.5047	57.8908	55.7236
51.5542	53.9195	49.9304	51.4876	58.7828	60.1034
56.8148	59.6007	57.026	60.7497	62.3133	61.7285
61.3809	63.3088	61.9631	62.7774	65.3495	63.7971
61.9203	65.7519	67.6729	70.2074	68.1294	68.7646
68.5572	69.8008	69.5367	70.7477	83.7339	82.9846
75.921	79.4191	73.4234	74.4879	93.6018	90.8727
80.8416	83.0048	79.0534	81.9443	99.7946	98.857
89.7547	92.6624	89.5717	94.5667	102.7626	101.5878
96.1474	98.1177	93.2145	96.5351	105.9669	109.7365
101.0309	105.0812	95.3669	98.2723	114.698	119.7494
108.229	112.0068	102.4047	105.0184	118.6672	122.4174
109.357	113.2489	104.9673	109.7109	125.7277	130.5669
117.5448	125.5068	117.5681	123.1123	126.7035	133.7591
127.8701	134.3517	124.1503	133.7837	129.6112	135.4443
132.7823	138.2439	128.8243	135.1498	132.7371	138.1357

139.0245	146.8371	136.2269	143.6004	138.5881	144.112
143.5955	150.1602	148.2446	155.5876	142.3175	150.1432
144.9438	152.1991	152.8735	161.9217	154.3017	160.8871
151.6991	160.1111	159.282	166.9211	159.2412	165.1961
154.597	162.8447	167.2993	172.5701	164.606	172.1261
165.0711	172.1786	171.0163	177.3077	169.767	174.4127
169.2389	176.1964	172.888	180.1067	171.1999	177.4328
170.1087	178.2614	174.5604	183.1777	178.7352	184.1434
177.106	183.1937	183.1412	189.7847	183.4165	189.6623
179.7558	187.2072	184.8943	193.3542	189.4323	199.2967
182.4906	189.2179	187.9837	196.4783	196.5192	202.8199
185.5464	193.6158	188.2586	197.8834	206.7114	211.6732
188.2131	197.6139	193.0986	204.5625	209.5781	214.9163
191.5172	201.2717	199.9863	208.7485	212.7687	217.4931
192.2885	201.5339	209.8899	216.2484	214.4378	220.0714
197.5326	208.3466	211.9083	218.388	222.5415	226.8359
201.7504	210.9816	214.8608	221.892	224.5477	228.6212
203.9886	213.8455	221.052	228.8408	225.3238	229.9477
210.1403	217.4482	222.328	228.9514	228.7927	235.8192
213.1659	219.1105	225.4147	234.5035	231.7169	236.6181
218.0466	225.8	227.2789	236.1382	236.8126	248.2635
220.2188	227.5336	228.8565	236.8857	244.0524	252.8619
224.0084	232.1328	229.9014	239.0734	252.6667	261.3697
229.008	235.8574	232.5427	241.0722	271.61	280.6829
230.4971	237.3232	234.9573	244.6545	274.4029	282.3052
235.0913	242.8721	235.8487	247.0894	276.2482	284.7581
239.3247	249.1141	240.4316	250.3243	277.8817	285.8687
242.4807	251.5757	241.0642	251.5254	278.4008	286.2794
245.7466	254.861	247.7536	258.1855	281.1461	289.0125
246.3691	257.383	251.3879	262.1769	292.1433	304.3968
251.7684	261.1113	252.7172	263.6008	300.5767	310.5668
252.2749	264.1397	254.6673	266.6368	322.3705	336.6762
254.9786	265.465	258.0804	269.5505	339.1566	350.306
257.5958	270.2735	260.9186	273.9169	341.143	351.2627
266.1894	276.0362	263.8044	277.6414	372.1508	384.4438
270.0206	281.3638	269.1317	279.8288	386.3197	404.9259
272.4395	284.8298	282.2183	290.0797	390.0236	408.1184
274.7026	287.6841	284.5437	297.1019	413.9322	427.3337
276.1201	290.272	289.2919	298.9306	416.0278	429.5729
283.7727	296.8473	304.0533	312.7163	464.4655	480.4336
286.7423	300.43	316.0792	327.1891	464.7876	481.3202
291.3465	304.9037	317.1521	327.5043	492.2529	512.3529
291.8595	305.7703	321.9798	333.7704	507.3152	526.1252
296.7492	312.757	334.9689	345.4409	536.0017	553.7054
311.958	323.3546	339.6666	351.6395	536.6641	554.0927
320.0107	333.2457	371.0348	383.9053	538.0789	555.1745
328.8368	340.5243	376.3215	388.875	539.0056	559.6819
341.4118	353.0709	408.8167	425.9236	543.6059	563.3086

346.9399	360.0182	419.3169	434.6848	557.0937	580.7211
386.6428	399.6187	421.0166	435.478	568.518	591.1757
392.5992	405.9294	426.1532	442.6675	586.3802	606.1804
418.8727	433.5823	438.6544	454.2678	611.0263	638.0429
422.8304	437.249	439.0939	454.6895	623.2965	649.7212
435.5777	450.8658	448.0141	463.6826	703.3257	736.2417
438.4445	454.1941	451.1671	467.2364	716.6105	742.1151
448.3786	464.6602	510.7776	530.0412	722.2632	756.0514
465.3707	482.1409	515.4199	536.9125	743.4186	771.1179
481.8886	499.828	521.9767	541.0757	744.1079	772.4035
491.1271	510.3269	528.4464	549.6433	791.2337	818.1751
506.8056	526.9573	537.3443	559.481	791.5532	818.503
510.0198	529.9085	547.3539	566.7689	853.8667	887.4441
526.1207	546.3418	548.4753	568.5378	863.8632	896.889
529.9616	551.0665	555.3472	577.7702	871.1364	903.8664
537.947	558.0229	564.3835	584.7044	882.4286	914.5117
545.1683	564.7976	568.2897	589.982	884.5528	918.1654
550.2455	572.0751	669.7999	699.4506	892.2751	923.5075
554.2275	575.7221	675.6203	702.3473	893.8741	926.9006
561.7516	584.5478	679.5284	703.3239	896.8396	930.9253
569.819	592.4858	680.0484	707.5927	898.8549	934.25
667.4801	692.9095	699.9922	732.2841	900.3552	935.1107
668.9988	693.8337	712.0082	745.231	918.6807	953.7198
685.3016	712.7467	738.7553	765.973	922.8642	955.9791
691.5397	721.5868	741.0055	768.869	925.2625	960.9081
705.6262	737.641	774.6672	802.5062	928.4308	964.1562
716.5448	749.558	775.871	804.244	933.3713	967.8361
723.6981	751.2878	862.6081	896.6288	935.3366	969.9661
737.1688	764.6255	867.6355	901.3723	937.0866	972.1325
758.9596	786.8589	869.3571	903.2964	983.5657	1021.7404
767.1774	795.3419	875.7846	909.6885	984.1484	1022.3256
787.2749	813.4606	885.0462	916.9083	989.1858	1025.7246
788.4513	816.4873	885.8872	918.6177	991.3682	1028.2334
862.7287	896.7857	889.4431	921.6444	993.8174	1031.1817
868.3626	902.3226	890.0767	923.2773	994.1709	1033.3892
870.3354	904.7029	891.0224	923.6783	995.1437	1034.2268
876.9291	910.5448	892.6177	925.1278	1040.1295	1077.1471
883.233	916.1922	893.1524	926.074	1040.806	1077.6149
885.2644	917.672	893.9173	927.2366	1060.686	1099.5608
888.2271	920.5369	895.052	930.4053	1062.3259	1100.5552
888.8169	921.7523	897.1433	931.3072	1071.2082	1110.3676
890.4563	922.951	899.4557	934.7505	1078.5376	1118.61
891.6628	924.8283	901.4457	935.4136	1086.252	1126.9824
892.925	926.0158	927.4236	962.6705	1089.487	1130.2113

				8	
894.288	926.7441	929.6972	965.2599	1102.6651	1150.2834
894.9095	929.094	931.3991	965.8037	1105.3533	1153.6811
896.362	931.6262	932.7571	967.1005	1108.9167	1156.836
901.6756	938.0449	933.0481	967.4075	1110.171	1158.6841
903.4424	938.523	934.0938	968.7598	1113.0247	1162.2914
926.8153	962.2863	937.0702	971.1427	1126.9117	1170.3791
930.0497	965.5693	937.2226	971.1732	1141.8024	1186.2357
931.7719	966.3908	963.8523	998.6045	1142.8804	1186.5944
932.1519	966.8534	966.4412	1001.4945	1145.5432	1187.4717
934.0059	968.2122	981.9087	1017.4865	1148.216	1188.8399
934.8491	969.8712	985.2204	1023.2743	1167.6923	1215.1159
936.4311	970.5216	1001.6257	1039.0876	1171.9417	1218.6285
937.9121	972.1014	1002.1912	1040.0033	1277.9225	1329.5357
955.5633	990.9205	1019.3071	1057.1047	1279.4638	1330.9535
960.53	995.6274	1019.8854	1057.6742	1281.0924	1334.3001
992.6018	1029.6781	1065.4593	1104.984	1287.428	1338.3977
996.884	1034.5684	1067.5427	1106.7383	1289.0388	1339.9044
1007.6027	1044.4554	1078.0837	1118.3334	1289.87	1340.7818
1008.5155	1045.7665	1079.1799	1119.1843	1291.9018	1342.333
1031.4545	1068.9718	1097.8993	1141.023	1300.201	1353.1833
1041.2399	1082.7026	1099.4661	1143.033	1304.9414	1356.9779
1042.382	1083.8684	1100.6622	1147.4918	1311.2664	1357.5536
1050.6933	1089.3924	1101.8808	1148.1937	1325.6583	1377.4128
1067.529	1106.6264	1104.2937	1150.6249	1331.7202	1383.606
1068.7597	1108.034	1105.2718	1151.4677	1333.5181	1386.155
1074.475	1114.9931	1106.0843	1152.672	1335.185	1387.7726

9			4	4	
1078.9518	1119.1322	1107.4359	1153.757	1337.268	1388.0662
1086.4246	1128.2037	1108.8255	1154.5165	1340.2516	1388.9616
1097.6294	1141.7034	1110.1017	1157.8773	1341.8477	1390.3785
1099.7706	1145.2418	1115.8757	1158.2653	1347.7835	1395.2306
1100.742	1146.5397	1117.8495	1160.4457	1348.5297	1395.3748
1101.1897	1147.2735	1131.5831	1175.2399	1349.2634	1400.4447
1103.3948	1149.491	1134.1583	1178.0897	1351.5619	1401.7997
1104.825	1150.3437	1146.8524	1191.9756	1352.0875	1402.1599
1105.3251	1152.9737	1148.8142	1194.2027	1352.3653	1402.2807
1106.2992	1153.4924	1158.4484	1203.1662	1353.6213	1402.7066
1109.8776	1156.5068	1159.8868	1205.1049	1355.9147	1404.1902
1114.5059	1158.0643	1175.4444	1222.5366	1369.0912	1424.8499
1115.7674	1158.6088	1176.0688	1223.3788	1370.6982	1427.9171
1131.5345	1175.3589	1263.1178	1312.8465	1371.6061	1429.9858
1133.8142	1177.8944	1268.3308	1318.656	1383.7074	1442.2967
1146.2311	1191.4176	1274.0972	1324.7137	1389.6656	1442.9606
1148.7601	1194.1952	1277.0592	1328.3711	1390.1629	1443.3151
1160.5209	1206.553	1279.5992	1330.6868	1390.4375	1444.9311
1164.0602	1210.6479	1281.1615	1332.5872	1393.0718	1447.7483
1173.6195	1220.9489	1282.3194	1334.0889	1396.3256	1449.6491
1175.3501	1222.9017	1286.2702	1336.5035	1398.0878	1450.0753
1238.4793	1283.8426	1289.8543	1340.7153	1399.22	1451.6645
1242.0244	1286.8981	1292.5968	1343.1868	1401.6827	1453.5131
1261.4411	1310.0807	1293.345	1345.5881	1401.997	1454.2478
1271.744	1321.8989	1297.2043	1347.944	1404.325	1455.8839

3			1	1	
1272.997			1348.524	1404.708	
4	1323.8193	1297.8461	6	8	1456.3977
1273.959			1353.178	1406.577	
8	1325.9936	1301.8559	8	7	1458.0343
1274.919			1359.291	1407.883	
9	1326.7313	1308.1637	7	4	1459.0532
1278.310			1360.058		
1	1329.6982	1309.9082	7	1408.801	1461.2984
1280.921			1378.902	1412.289	
4	1332.4355	1326.2967	8	7	1463.6248
1285.750			1380.582	1412.770	
5	1336.4855	1329.0427	5	5	1464.111
1287.506			1382.184	1413.878	
8	1338.8386	1330.6738	1	4	1465.2496
1288.079				1414.978	
4	1339.0112	1331.3113	1382.884	7	1465.3435
1288.575			1384.664	1415.464	
6	1340.3479	1331.6855	8	5	1466.0153
1289.951			1386.382	1416.558	
2	1342.6638	1333.9912	6	6	1468.4268
1296.685					
2	1347.0421	1334.7726	1387.533	1417.436	1469.0365
1297.494			1388.988	1422.100	
4	1349.2221	1336.4476	5	4	1472.4718
1299.632				1423.795	
9	1350.5399	1342.7432	1391.416	5	1474.5111
1301.220			1392.375	1425.099	
1	1351.8296	1343.0649	1	5	1476.9974
1312.433			1398.192	1425.837	
1	1361.4395	1346.4698	7	9	1479.0502
1313.620			1399.402	1428.730	
4	1363.1537	1348.3324	8	4	1482.0308
1329.114			1401.205	1431.735	
2	1381.5358	1349.6376	6	6	1483.3593
1331.221			1401.351	1433.171	
6	1382.8418	1350.5697	5	6	1485.6328
1331.684			1402.374	1437.620	
6	1383.2368	1352.1276	6	8	1487.3876
			1403.484	1438.779	
1332.116	1383.849	1352.8998	8	7	1490.6792
1333.787			1406.717	1439.934	
6	1386.2517	1355.8934	5	9	1493.5594
1334.222			1407.320	1440.090	
8	1387.3513	1356.5714	5	1	1494.5269
			1424.902	1443.481	
1334.98	1387.9157	1367.6176	5	1	1505.9467
1336.065			1427.739	1443.809	
8	1389.2801	1371.099	8	5	1507.995
1339.548	1390.4059	1374.7307	1432.945	1465.339	1528.8394

5			6	7	
1342.3524	1393.3205	1375.9947	1433.1449	1468.7583	1531.7072
1347.9759	1398.8399	1389.9061	1442.5705	2842.5008	2934.1357
1349.369	1401.1021	1390.988	1444.0017	2859.1355	2949.0714
1350.3378	1401.649	1392.904	1447.656	2947.0286	3032.1591
1350.8609	1402.3348	1395.5224	1449.7085	2955.9474	3037.9131
1351.6023	1402.5109	1398.4355	1450.8298	2959.7709	3047.517
1352.5289	1403.3133	1399.0684	1451.5826	2961.7626	3050.6103
1352.8226	1403.5937	1400.1184	1453.4363	2963.1377	3051.442
1354.0313	1405.8049	1400.9874	1454.4712	2966.2536	3056.6136
1363.7298	1422.3309	1402.3348	1455.7955	2968.5381	3057.0206
1371.3678	1429.5736	1403.5677	1456.4556	2973.6854	3057.6875
1380.3573	1438.0809	1406.2365	1457.6289	2977.1104	3062.5767
1384.3226	1438.2704	1406.9841	1458.0719	2978.1192	3062.8337
1387.0318	1443.211	1407.6563	1458.7277	2978.6441	3063.3958
1388.5403	1445.1563	1409.7219	1461.2283	2980.1653	3065.2528
1390.7305	1446.7679	1410.4912	1461.3958	2980.3686	3065.712
1393.0293	1449.3709	1410.9705	1462.0108	2987.9734	3080.8493
1397.8805	1450.7775	1412.5912	1463.8986	3000.385	3092.1593
1400.3225	1452.352	1412.9061	1464.1863	3007.8764	3107.1632
1401.9477	1453.8308	1413.3558	1464.6976	3015.643	3112.4896
1404.7581	1455.8341	1414.7602	1466.0999	3015.8424	3114.9251
1405.6917	1457.0752	1415.2245	1467.7523	3018.7918	3114.9888
1406.1505	1457.8621	1417.7764	1468.9706	3019.8316	3115.5519
1407.8932	1459.1428	1418.9652	1471.8647	3023.1767	3117.8341
1408.202	1459.9791	1422.0385	1473.649	3024.568	3118.3835

7			2	1	
1409.429			1474.820	3026.339	
1	1461.8492	1423.4447	8	8	3121.2125
1410.838				3027.951	
9	1462.4111	1425.3652	1476.478	5	3121.3994
1411.451				3035.073	
3	1462.6549	1426.3441	1477.728	5	3123.2628
1411.456				3035.567	
2	1462.8022	1426.5591	1478.06	1	3130.6666
1412.191			1479.141	3039.636	
3	1463.0042	1426.7077	3	3	3132.7071
1413.041			1480.799	3039.880	
4	1464.4851	1429.1808	3	1	3135.0247
1413.627			1482.646	3047.819	
1	1464.9902	1430.3045	4	4	3140.6778
1415.019			1483.068	3049.843	
6	1466.9225	1431.367	6	2	3142.6564
1415.345			1484.285	3053.532	
2	1467.4868	1431.8895	7	6	3143.6297
1417.419			1486.548	3054.905	
9	1469.0021	1434.8573	1	1	3147.6796
1417.567			1489.118	3056.303	
5	1469.9606	1436.1519	2	3	3148.6796
1417.964			1490.357	3058.282	
3	1471.0943	1437.4712	2	4	3148.9123
1420.586			1491.984	3059.023	
6	1472.8239	1440.3061	5	3	3149.2362
1421.281			1493.307	3059.746	
4	1474.2735	1441.4305	6	8	3150.8649
1423.181			1507.205	3060.336	
3	1475.4113	1444.1341	3	4	3152.0036
1425.593			1507.995	3062.044	
2	1477.7838	1445.6066	6	9	3152.3115
1426.817			1509.053	3062.192	
7	1478.4074	1447.2334	8	1	3152.498
1427.073			1512.593	3062.229	
4	1478.9033	1449.8301	2	8	3153.3965
1427.376			2968.991	3062.499	
2	1479.6015	2873.6949	4	3	3154.4863
1429.301				3065.381	
5	1481.2027	2896.8043	2991.172	5	3157.298
1430.982			3046.586	3068.278	
4	1482.2336	2955.5692	5	3	3160.4867
1431.557			3049.851	3071.698	
4	1483.6419	2962.9342	9	3	3164.1659
1432.873			3050.081	3072.271	
1	1486.4818	2965.6483	9	8	3164.7081
1434.355			3056.621	3072.640	
1	1487.8866	2970.5758	3	1	3165.6902
1436.341	1489.0582	2971.8078	3057.680	3075.365	3167.3142

8			8		
1437.018	1490.377	2972.5054	3060.368	3076.0835	3168.7925
1439.2349	1493.744	2974.3266	3061.4397		
1440.1057	1494.497	2975.3096	3063.8387		
1442.197	1497.5545	2976.0794	3064.0495		
1442.931	1504.0422	2978.2931	3064.2995		
1443.7045	1505.3275	2978.6672	3064.6049		
1444.8593	1509.09	2978.8566	3064.6763		
2884.4412	2981.2764	2979.3652	3067.4205		
2891.3754	2987.1698	2979.7865	3069.2528		
2948.803	3042.6502	2980.2635	3070.5247		
2954.364	3048.8622	2981.6172	3072.1442		
2963.6117	3051.5321	2982.6706	3074.0586		
2966.8555	3054.8404	2984.8775	3082.5203		
2974.2412	3060.8518	2985.4212	3084.9135		
2977.1831	3062.5253	2993.0321	3095.0536		
2977.3315	3062.8167	3002.2476	3096.4107		
2977.7327	3063.3315	3005.0265	3099.4021		
2978.6882	3063.7863	3013.2798	3111.3985		
2979.3338	3064.0236	3014.958	3115.0077		
2979.8198	3064.994	3018.1433	3119.3777		
2980.2262	3065.186	3025.8343	3124.1644		
2980.2935	3066.676	3030.3822	3124.789		
2980.4459	3066.9388	3037.3502	3128.6481		
2981.222	3070.4781	3042.1319	3133.2305		
2985.069	3071.7285	3046.2956	3138.711		

9			
2985.7615	3072.5974	3049.1305	3140.1918
2985.89	3079.1742	3050.0557	3142.6156
2986.3449	3082.5245	3051.7856	3143.559
2989.4403	3085.2289	3052.1207	3145.4692
3001.2736	3095.6039	3053.8249	3146.7724
3003.4424	3096.2831	3054.732	3147.6616
3004.3496	3098.7042	3055.3207	3148.161
3005.1873	3101.1494	3055.7796	3148.9431
3014.3254	3114.1684	3057.6088	3149.4246
3023.2959	3119.5136	3058.3256	3149.6858
3027.023	3125.1384	3058.7305	3150.5543
3028.6689	3126.1202	3060.2519	3150.889
3029.8711	3127.9459	3060.8364	3151.4229
3033.3155	3129.8277	3061.0386	3152.3155
3038.1867	3130.2871	3061.2427	3152.4032
3040.1785	3134.5016	3061.4596	3153.0239
3042.8791	3138.5205	3061.7995	3153.1455
3049.9676	3143.3007	3062.2086	3154.2065
3051.216	3143.8656	3064.0819	3155.1336
3052.6327	3144.2175	3065.9312	3156.3846
3052.7563	3146.1718	3066.0511	3157.2302
3053.5549	3146.5788	3068.8889	3161.0297
3056.6045	3148.0604	3070.1025	3163.5812
3058.4226	3148.6401	3072.4133	3163.9113
3058.697	3149.5481	3073.2693	3165.199

			2
3059.0414	3150.5759	3080.0675	3170.7952
3059.4967	3150.6349	3080.8051	3175.3168
3060.5189	3151.0657	3083.9017	3176.4655
3061.0797	3152.8912	3099.3498	3196.6768
3061.1743	3153.3009	3106.056	3204.2017
3061.4839	3153.6361		
3061.9218	3154.6297		
3062.1707	3155.4029		
3066.2042	3157.3822		
3067.8642	3159.4438		
3069.0945	3160.063		
3069.5073	3160.3155		
3069.6524	3160.7247		
3070.8012	3162.2838		
3071.1129	3164.7543		
3073.2376	3165.7144		
3077.2274	3169.1037		
3078.6455	3169.7183		
3079.4512	3169.9469		
3080.9132	3172.7557		
3081.307	3173.7476		
3082.3608	3174.6379		
3084.2277	3176.7837		

Table S3. Comparison of structural parameters between crystal/PBE/PBE0 optimised structures for compounds **1**-**6**. Cp^1 and Cp^2 in **6** refer to lightest and heaviest cyclopentadienyl rings, respectively. Values for **1**, **3**-**5** are taken from Table 1 in reference [14]. All angles and distances measured with respect to the Cp centroids. RMSD values do not consider hydrogen atoms.

	$Cp^1 - Dy$ (Å)	$Dy - Cp^2$ (Å)	$Cp - Dy - Cp$ (degrees)	RMSD crystal *vs* PBE	RMSD crystal *vs* PBE0
1	2.29(1) / 2.291 / 2.279	2.29(1) / 2.291 / 2.279	147.2(8) / 146.10 / 146.94	0.098	0.103
2	2.318 / 2.309 / 2.290	2.314 / 2.309 / 2.290	152.7 / 151.45 / 153.43	0.080	0.105
3	2.340(7) / 2.351 / 2.335	2.340(7) / 2.345 / 2.333	162.1(7) / 158.06 / 158.9	0.266	0.308
4	2.302(6)/ 2.323 / 2.311	2.302(6) / 2.331 / 2.318	161.1(2) / 155.67 / 156.69	0.358	0.223
5	2.298(5) / 2.318 / 2.306	2.298(5) / 2.323 / 2.309	156.6(3) / 155.11 / 156.10	0.088	0.084
6	2.296 / 2.308 / 2.297	2.284 / 2.290 / 2.277	162.5 / 160.10 / 162.06	0.273	0.100

The predicted Infra-Red (IR) spectra from DFT can be compared to the experimental IR to assess how accurate the calculated normal modes are. Figure S2-Figure S7 show that the IR profiles obtained with PBE and PBE0 are very similar, but the spectra from PBE0 are consistently shifted towards higher energies. In an attempt to improve the agreement with the experiment, we build a composite spectrum for each

molecule including the spectrum of the isolated counterion $[B(C_6F_5)]^+$ (Figure S8-Figure S12). From this comparison, a set of optimized linear corrections for the PBE energies for **1**-**6** is presented in Table S4. However, due to the moderate improvement between predicted and experimental IR and the small impact on the calculated rates (see main text), calibration of normal modes is not recommended.

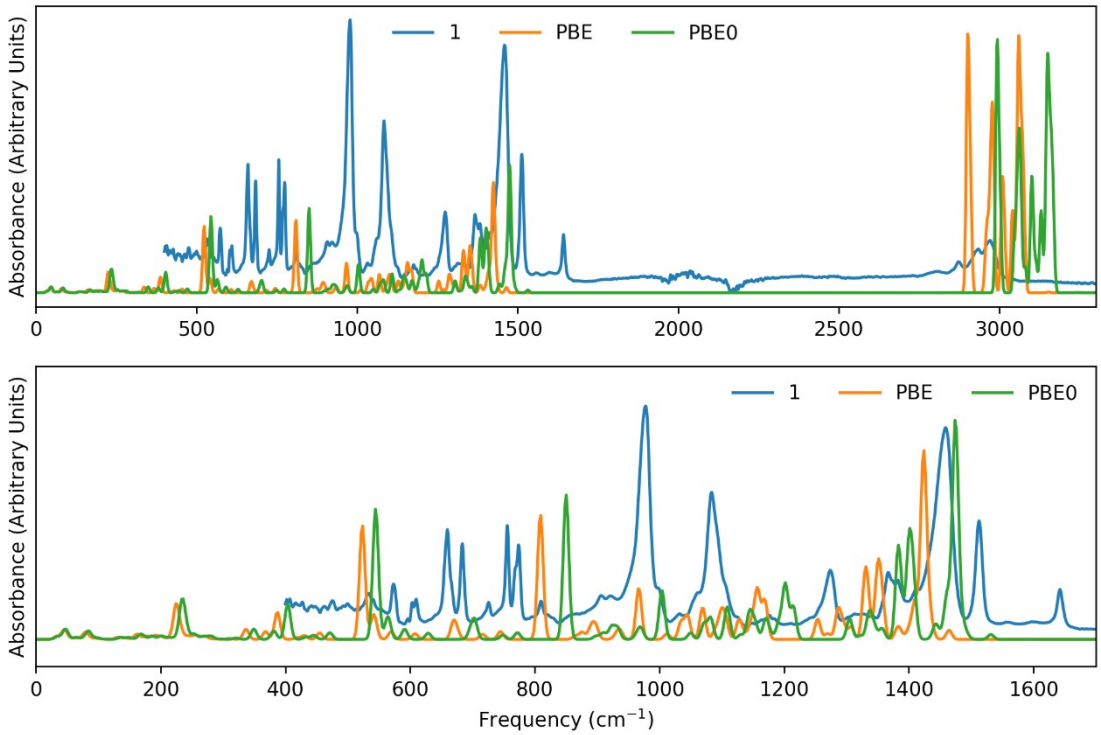

Figure S2. Comparison of IR spectra for **1**.

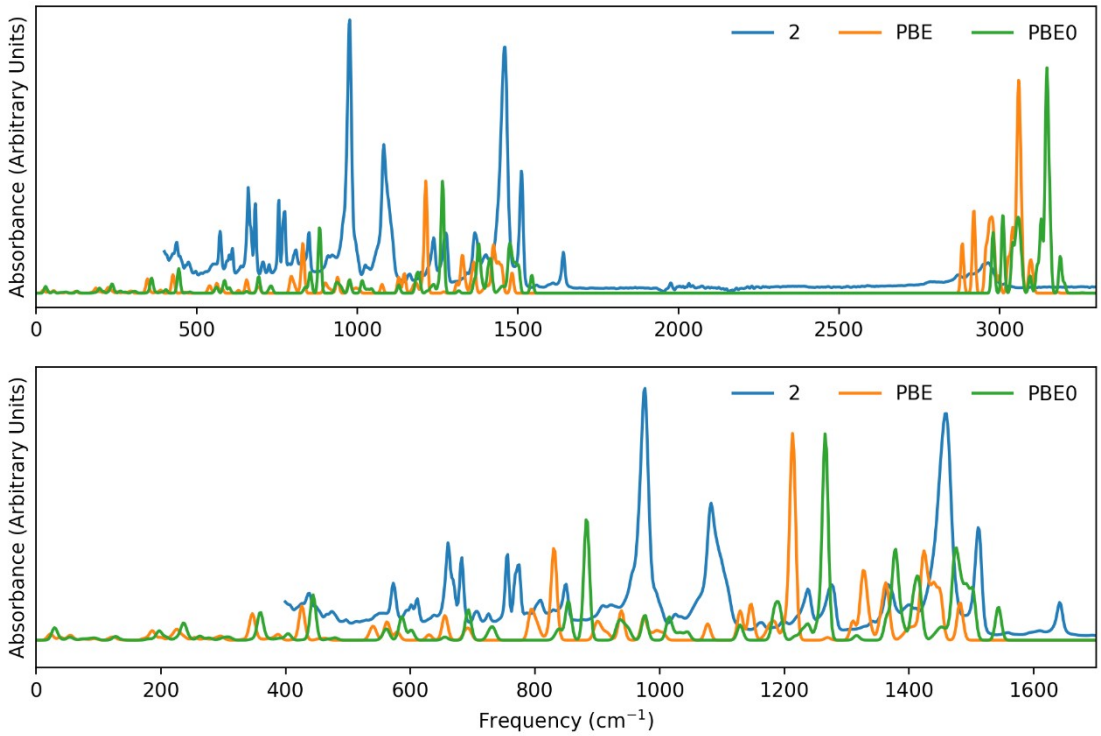

Figure S3. Comparison of IR spectra for **2**.

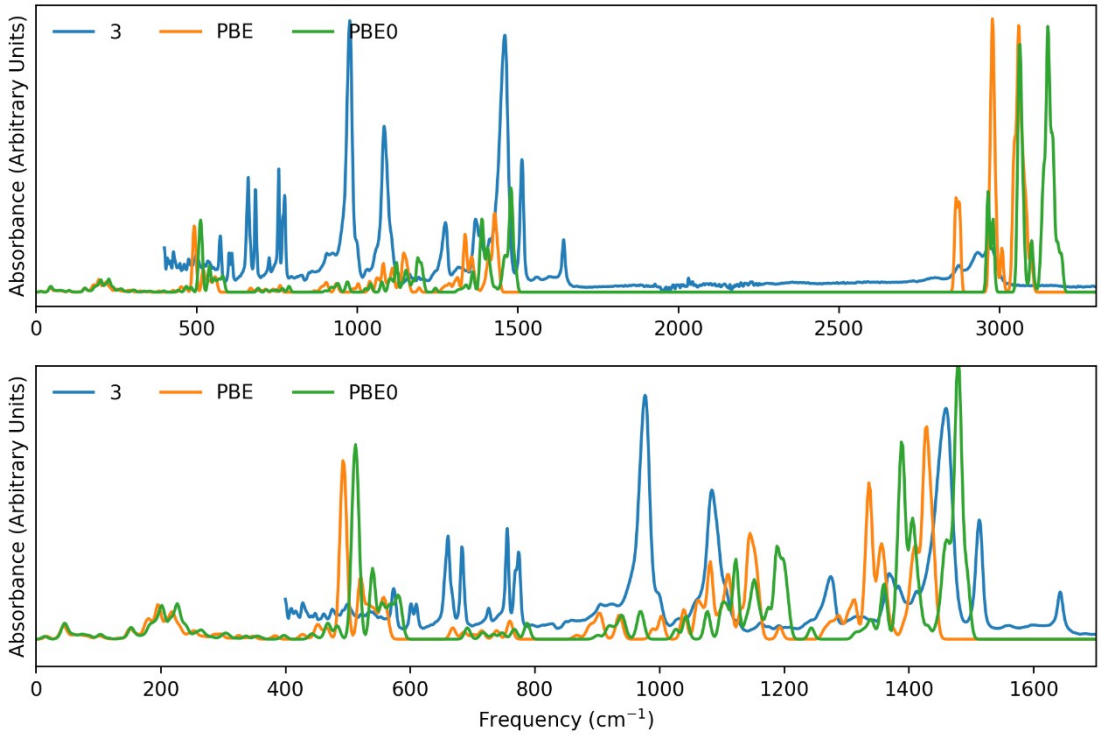

Figure S4. Comparison of IR spectra for **3**.

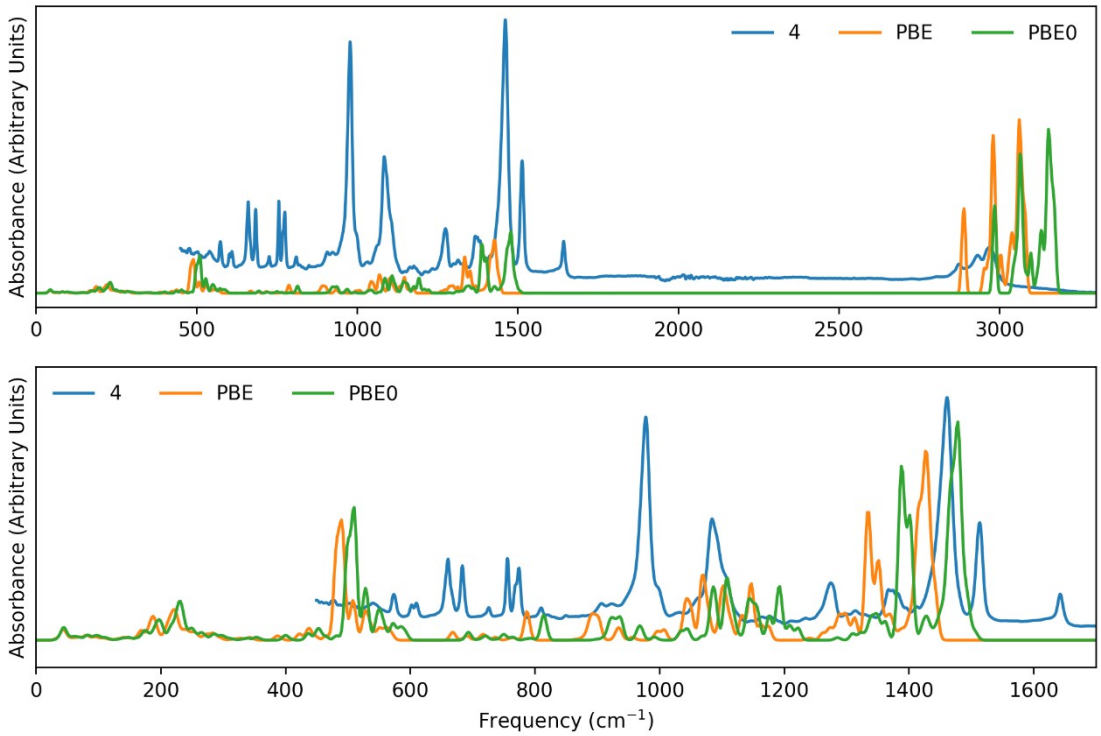

Figure S5. Comparison of IR spectra for **4**.

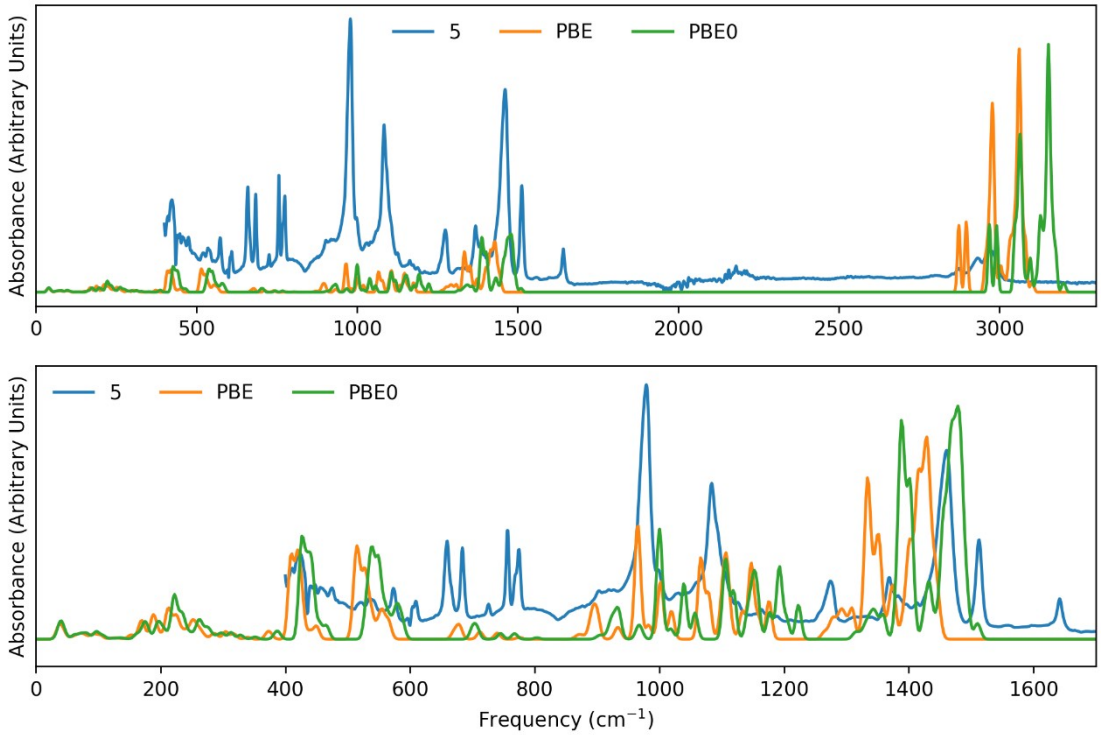

Figure S6. Comparison of IR spectra for **5**.

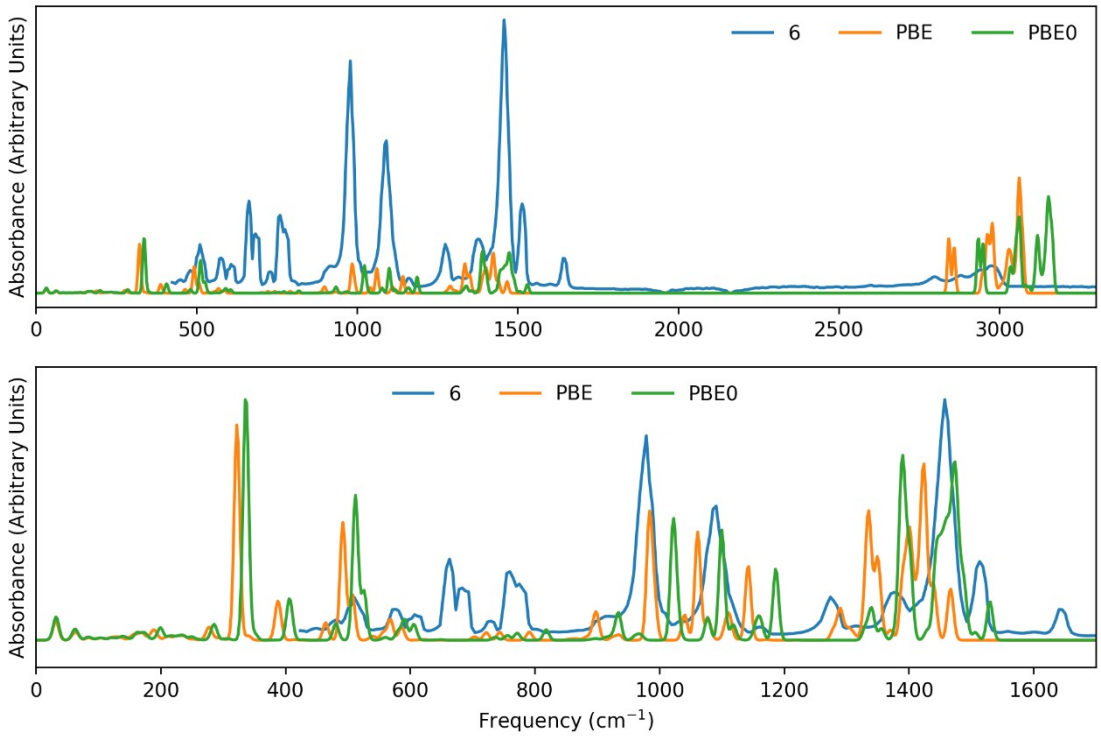

Figure S7. Comparison of IR spectra for **6**.

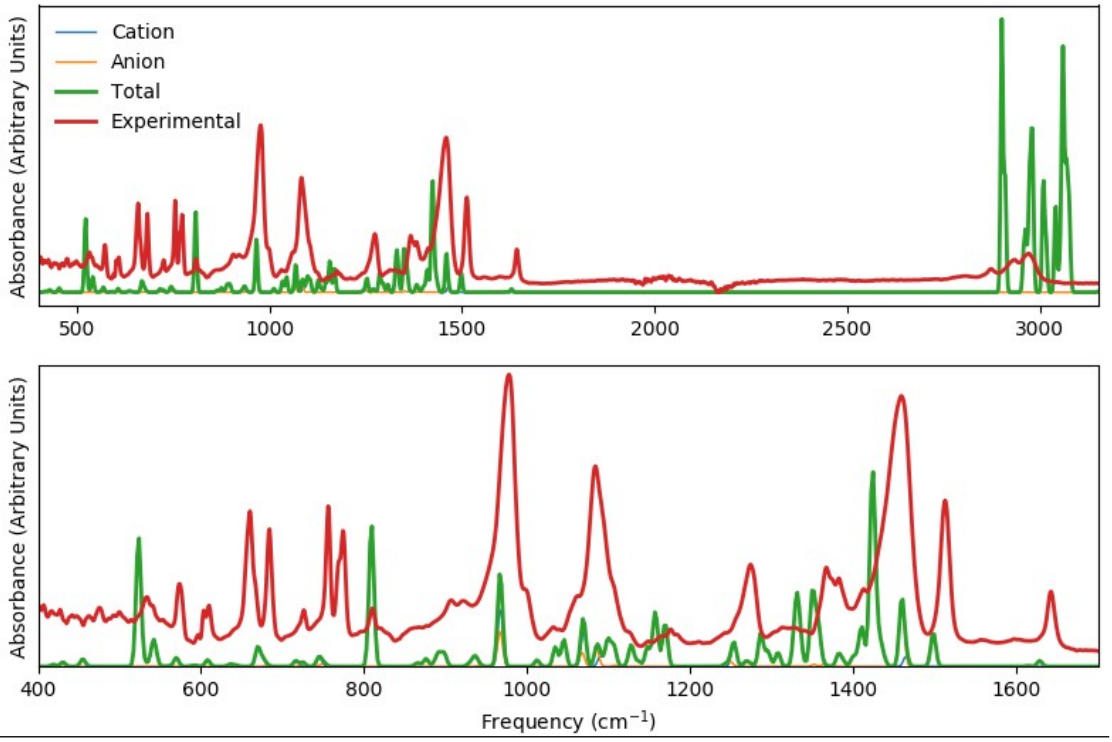

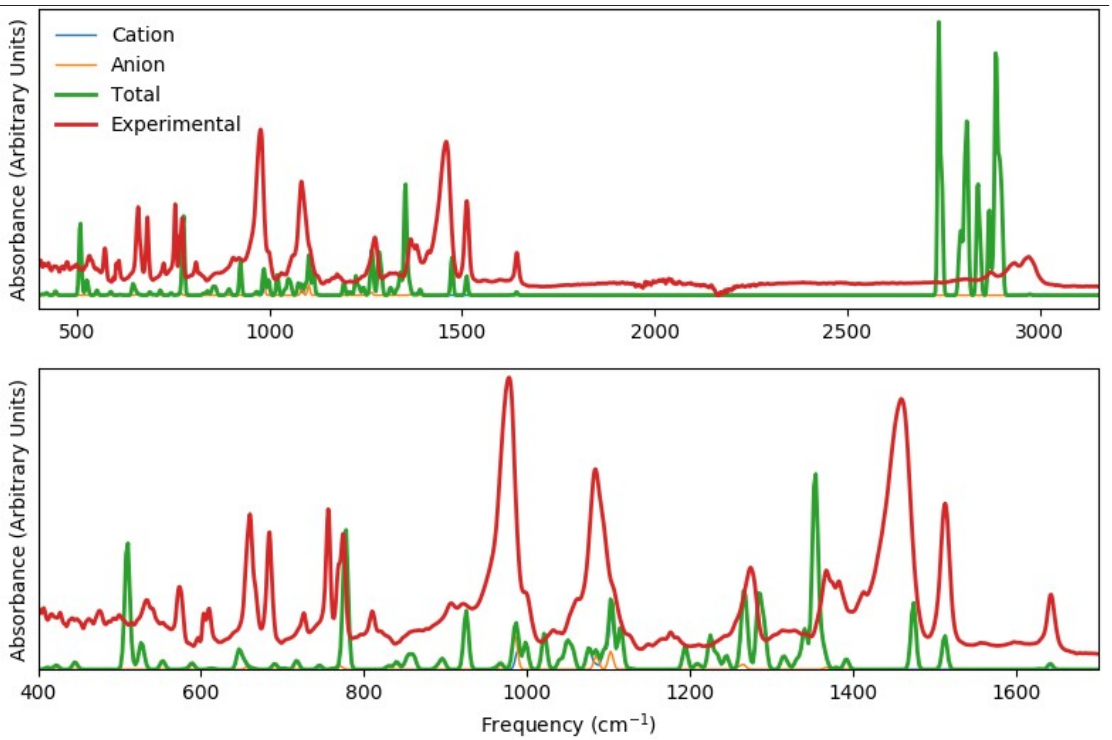

Figure S8. Comparison of experimental and PBE IR spectra without (top) and with (bottom) calibration for **1**, using the parameters from Table S4

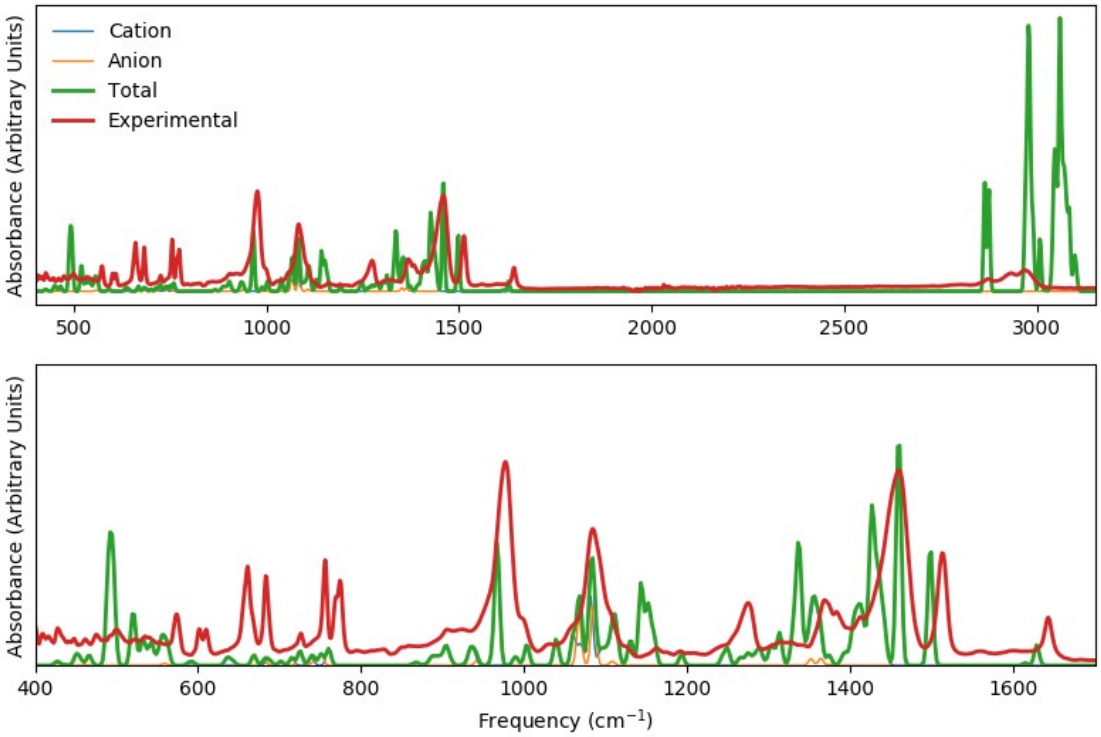

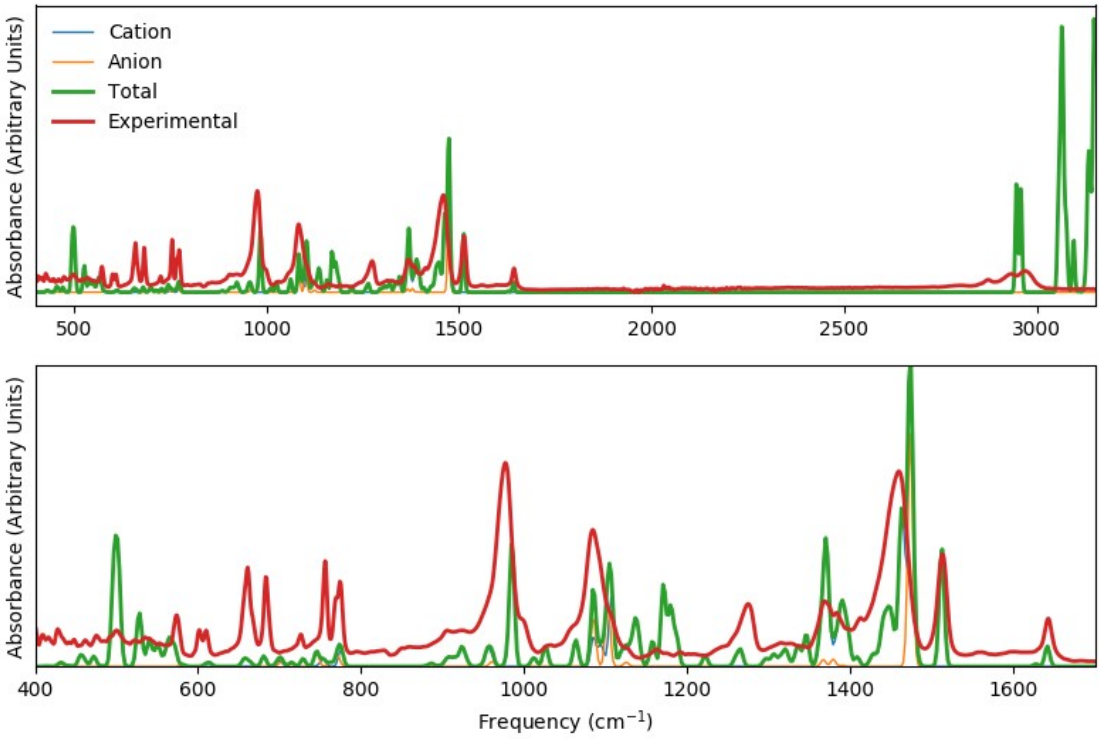

Figure S9. Comparison of experimental and PBE IR spectra without (top) and with (bottom) calibration for **3**, using the parameters from Table S4.

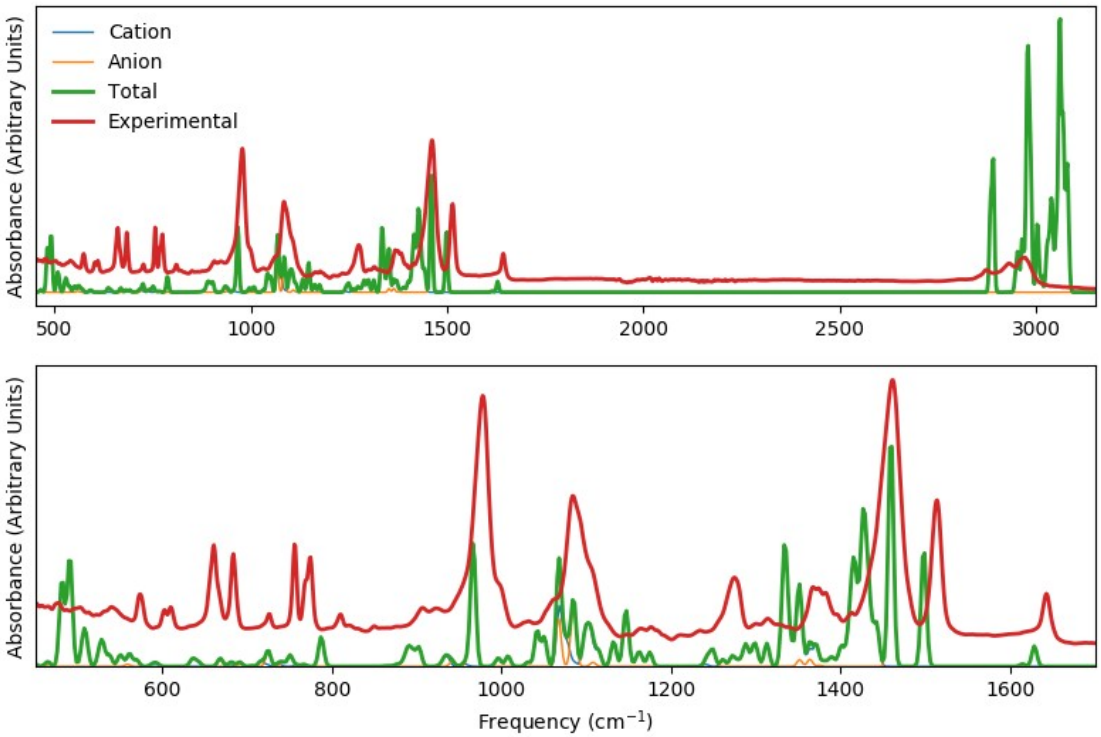

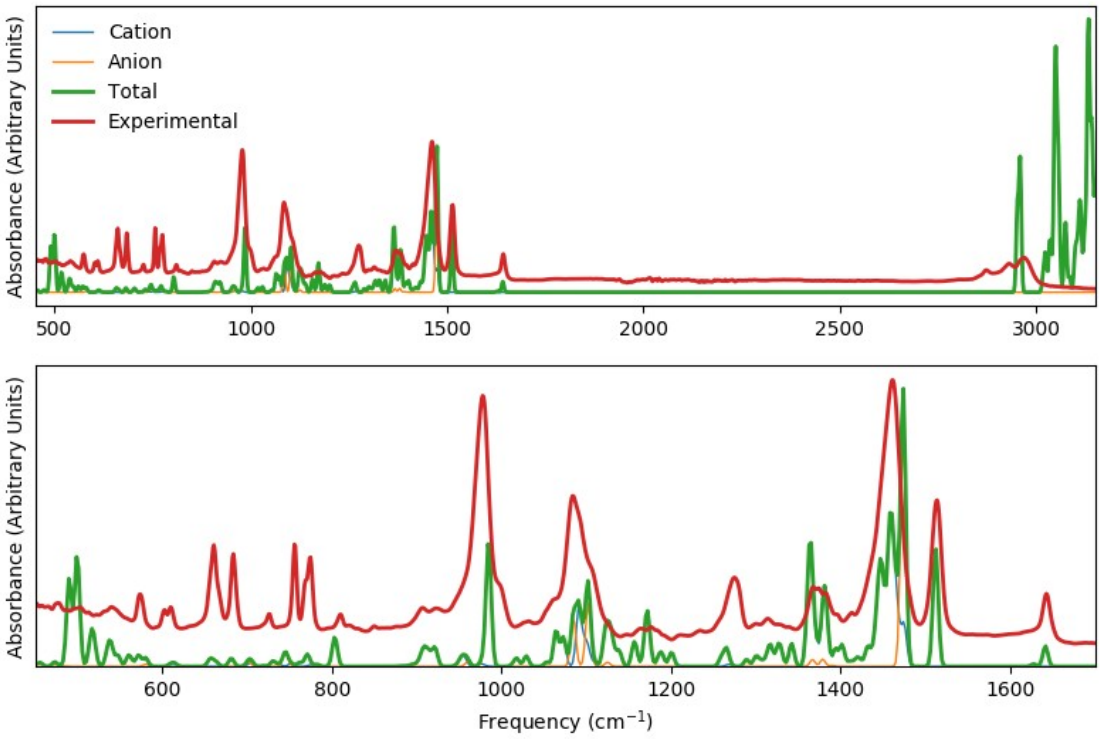

Figure S10. Comparison of experimental and PBE IR spectra without (top) and with (bottom) calibration for **4**, using the parameters from Table S4.

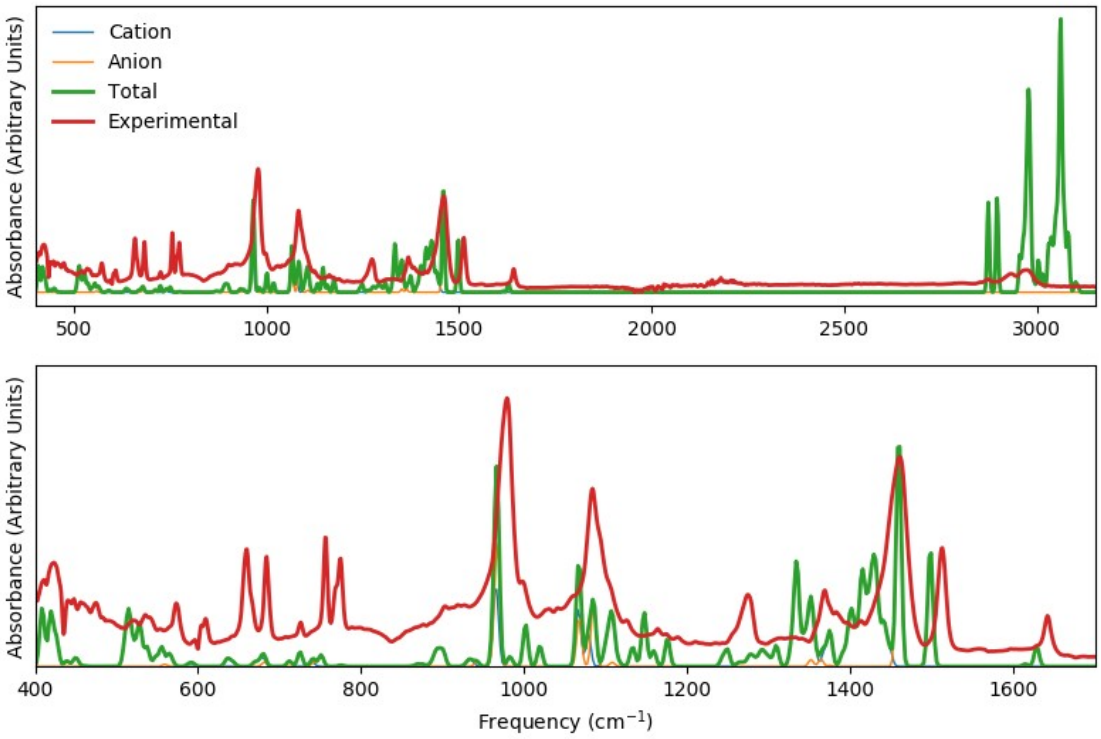

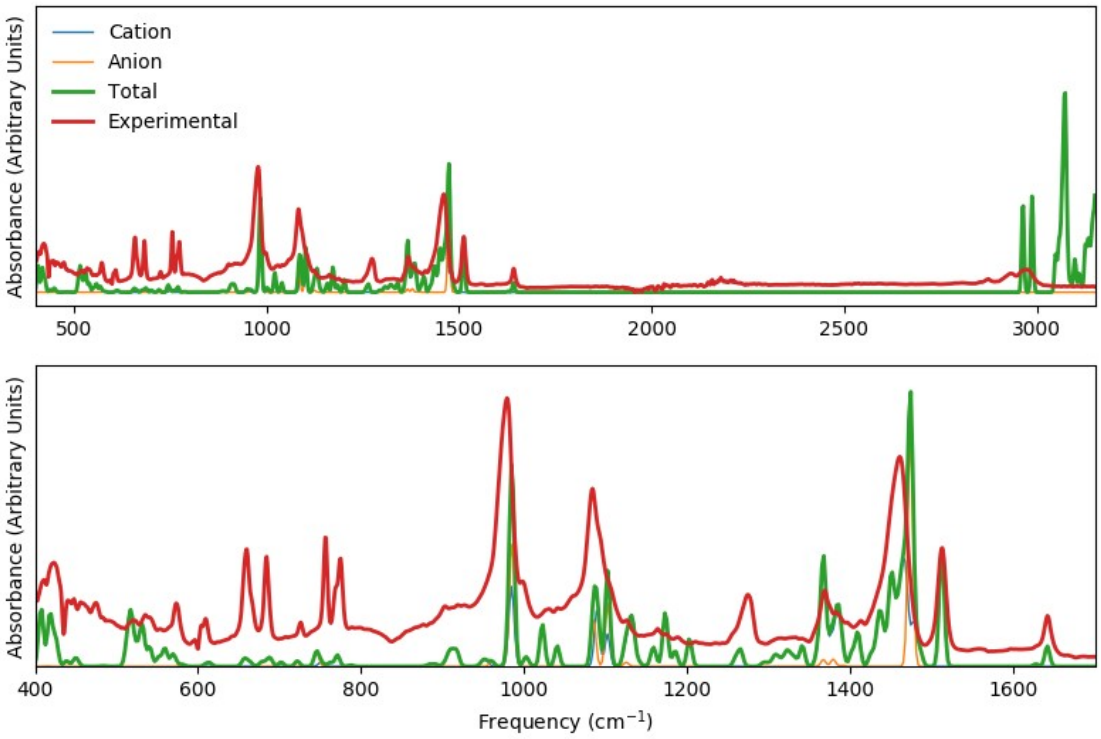

Figure S11. Comparison of experimental and PBE IR spectra without (top) and with (bottom) calibration for **5**, using the parameters from Table S4.

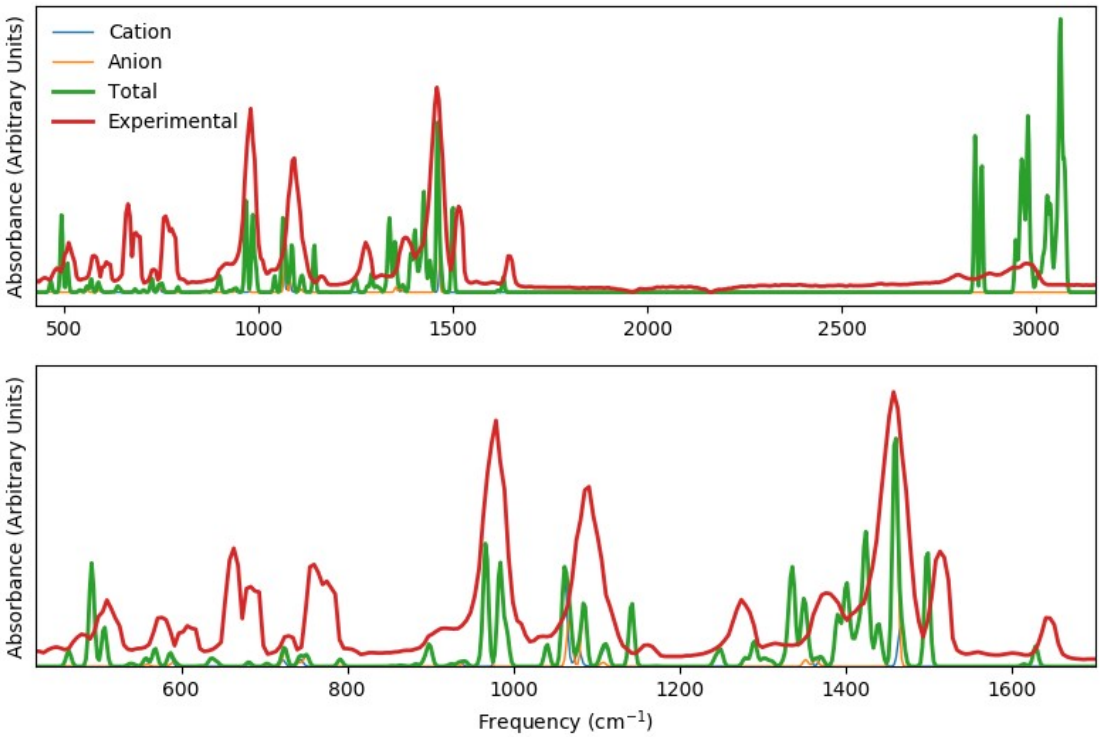

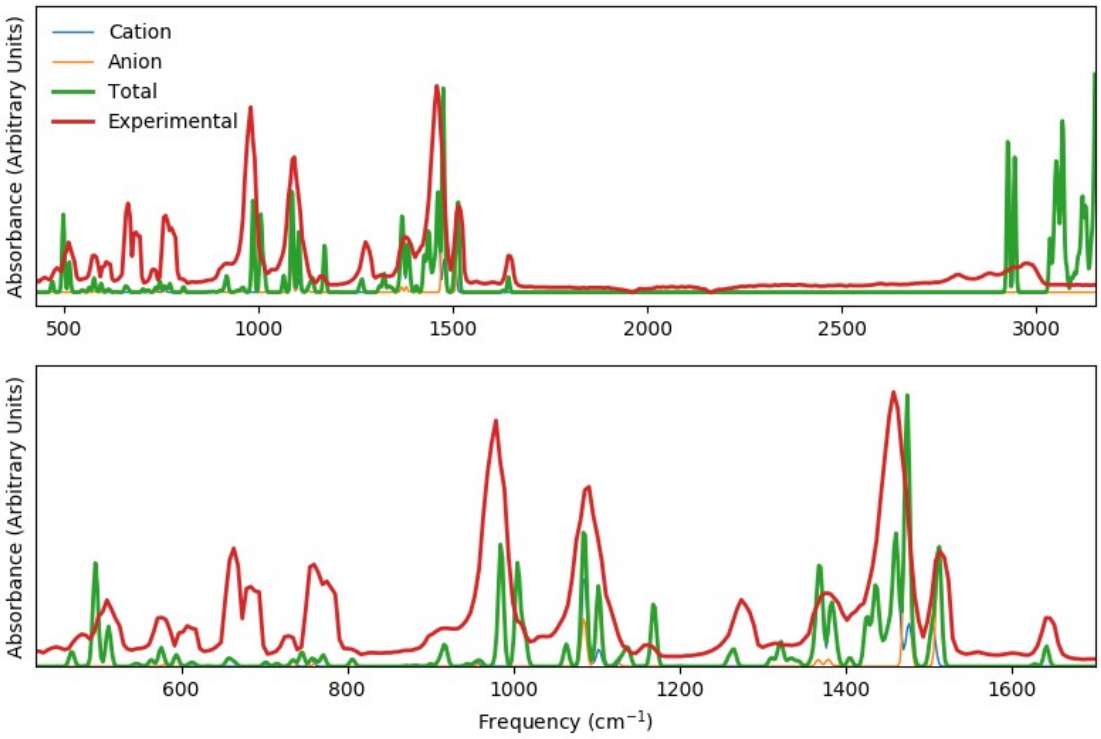

Figure S12. Comparison of experimental and PBE IR spectra without (top) and with (bottom) calibration for **6**, using the parameters from Table S4.

Table S4. Calibration applied to the PBE normal mode energies.

compound	Cation	Anion
1	$0.937\,x+19.141$	$0.992\,x+26$
2	$0.9485\,x+69.33$	$0.992\,x+26$
3	$1.032\,x-9.245$	$0.992\,x+26$
4	$1.025\,x-3.646$	$0.992\,x+26$
5	$1.037\,x-16.536$	$0.992\,x+26$
6	$1.034-12.167$	$0.992\,x+26$

S3. CASSCF-SO calculations: Electronic structure

We adopt two approaches to describe the electronic structure of **1-6**: "full" and "low" differing in the quality of the ANO-RCC[15,16] basis sets and the spin multiplicities considered (Table S5). Both approaches employ the resolution of the identity decomposition (RICD acCD) of the two-electron integrals,[17] as regular Cholesky decomposition results in discontinuous CASSCF energies along the potential energy surfaces. The molecular orbitals (MOs) were optimised in state-averaged CASSCF calculations, where the active space was defined by the nine *4f* electrons in the seven *4f* orbitals of Dy(III). The wavefunction was then mixed by spin orbit coupling where the corresponding states of appropriate multiplicity were included. The resulting spin orbit wavefunctions were decomposed into CFPs using SINGLE_ANISO[18] with a fixed reference frame extracted from the equilibrium geometry. The two different approaches were applied to the optimised and crystal geometries (Table S6 – Table S9). The "low" approach was employed to perform the ab initio spin dynamics calculations.

Table S5. Definition of the "low" and "full" CASSCF-SO approaches. 1st and 2nd refer to the 10 coordinating carbon atoms of the cyclopentadienyl ring and the remaining atoms, respectively.

	"low"	"full"
Basis sets	Dy : VTZP 1st : VDZP 2nd : VDZ	Dy : VQZP 1st : VTZP 2nd : VDZP
Spin multiplicities	6	6 / 4 / 2
State Averaged roots	21	21 / 224 / 490
States in RASSI	21	21 / 128 / 130

Table S6. Electronic structure of **1-6** calculated with "low" CASSCF-SO using the PBE optimised geometries. Each row corresponds to a Kramers doublet. Last column reports the CF energies from the CASSCF-SO crystal field parameters.

Energy (cm^{-1})	**Energy (K)**	**g1**	**g2**	**g3**	**Angle**	**Wavefunction**	**<Jz>**	**Energy^{CF} (cm^{-1})**
				1				
0.00	0.00	0.00	0.00	19.97	--	100% $\lvert \pm 15/2 \rangle$	±7.5	0.00

414.45	596.30	0.00	0.00	17.10	0.2	100% $\lvert\pm 13/2\rangle$	±6.5	421.18
687.61	989.32	0.00	0.00	14.46	0.4	100% $\lvert\pm 11/2\rangle$	±5.5	686.00
874.90	1258.78	0.02	0.03	11.79	0.1	100% $\lvert\pm 9/2\rangle$	±4.5	875.20
1035.22	1489.45	0.56	0.67	9.09	0.1	100% $\lvert\pm 7/2\rangle$	±3.5	1038.49
1166.90	1678.90	1.13	2.97	6.13	0.1	60% $\lvert\pm 5/2\rangle$ + 34% $\lvert\mp 5/2\rangle$	±0.7	1171.06
1248.77	1796.70	2.39	7.97	9.53	89.2	74% $\lvert\pm 3/2\rangle$ + 22% $\lvert\mp 1/2\rangle$	±0.9	1254.67
1384.89	1992.54	0.13	0.33	18.38	90.0	65% $\lvert\pm 1/2\rangle$ + 23% $\lvert\mp 3/2\rangle$ + 7% $\lvert\mp 1/2\rangle$	±0.0	1381.58
				2				
0.00	0.00	0.00	0.00	19.99	--	100% $\lvert\pm 15/2\rangle$	±7.5	0.00
460.98	663.24	0.00	0.00	17.08	1.6	100% $\lvert\pm 13/2\rangle$	±6.5	469.57
728.38	1047.96	0.00	0.00	14.45	2.8	100% $\lvert\pm 11/2\rangle$	±5.5	724.53
900.42	1295.50	0.00	0.01	11.79	2.8	100% $\lvert\pm 9/2\rangle$	±4.5	900.72
1057.68	1521.76	0.06	0.06	9.12	3.6	100% $\lvert\pm 7/2\rangle$	±3.5	1063.05
1207.60	1737.46	1.05	1.29	6.43	1.9	97% $\lvert\pm 5/2\rangle$	±2.5	1213.38
1324.41	1905.51	3.36	3.97	7.37	90.0	85% $\lvert\pm 3/2\rangle$ + 8% $\lvert\mp 1/2\rangle$	±1.2	1328.20
1407.80	2025.49	0.89	4.48	15.57	89.6	72% $\lvert\pm 1/2\rangle$ + 18% $\lvert\mp 1/2\rangle$ + 6% $\lvert\pm 3/2\rangle$	±0.3	1404.47
				3				
0.00	0.00	0.00	0.00	20.00	--	100% $\lvert\pm 15/2\rangle$	±7.5	0.00
478.43	688.35	0.00	0.00	17.08	2.1	100% $\lvert\pm 13/2\rangle$	±6.5	488.45
742.03	1067.61	0.00	0.00	14.46	2.9	100% $\lvert\pm 11/2\rangle$	±5.5	736.95
911.22	1311.03	0.04	0.04	11.84	3.2	100% $\lvert\pm 9/2\rangle$	±4.5	910.25
1068.40	1537.18	0.55	0.64	9.14	5.9	98% $\lvert\pm 7/2\rangle$	±3.5	1074.14
1224.96	1762.43	0.24	1.42	6.35	6.9	94% $\lvert\pm 5/2\rangle$+ 2% $\lvert\pm 3/2\rangle$	±2.4	1232.44
1351.46	1944.44	3.10	6.92	7.23	89.8	78% $\lvert\pm 3/2\rangle$ + 10% $\lvert\mp 1/2\rangle$ + 5% $\lvert\pm 1/2\rangle$	±1.1	1355.67
1466.5	2110.0	0.64	2.76	16.97	89.3	76% $\lvert\pm 1/2\rangle$ +	±0.2	1462.93

4	1					8%$\lvert\mp 1/2\rangle$ + 12%$\lvert\mp 3/2\rangle$		
				4				
0.00	0.00	0.00	0.00	20.00	--	100%$\lvert\pm 15/2\rangle$	±7.5	0.00
478.67	688.70	0.00	0.00	17.07	1.1	100%$\lvert\pm 13/2\rangle$	±6.5	488.40
749.63	1078.54	0.00	0.00	14.45	1.3	100%$\lvert\pm 11/2\rangle$	±5.5	744.66
924.19	1329.70	0.01	0.01	11.80	0.9	100%$\lvert\pm 9/2\rangle$	±4.5	923.50
1085.10	1561.20	0.26	0.29	9.11	2.9	100%$\lvert\pm 7/2\rangle$	±3.5	1090.66
1241.48	1786.21	0.09	0.68	6.38	4.1	98%$\lvert\pm 5/2\rangle$	±2.5	1248.38
1365.55	1964.71	3.20	6.37	7.04	89.0	77%$\lvert\pm 3/2\rangle$ + 10%$\lvert\mp 1/2\rangle$ + 10%$\lvert\mp 3/2\rangle$	±1.0	1369.48
1470.66	2115.95	0.71	3.20	16.61	90.0	51%$\lvert\pm 1/2\rangle$ + 36%$\lvert\mp 1/2\rangle$ + 7%$\lvert\mp 3/2\rangle$	±0.0	1467.08
				5				
0.00	0.00	0.00	0.00	20.00	--	100%$\lvert\pm 15/2\rangle$	±7.5	0.00
475.70	684.43	0.00	0.00	17.07	1.2	100%$\lvert\pm 13/2\rangle$	±6.5	485.13
745.35	1072.38	0.00	0.00	14.45	1.7	100%$\lvert\pm 11/2\rangle$	±5.5	740.38
919.38	1322.78	0.02	0.03	11.81	1.9	100%$\lvert\pm 9/2\rangle$	±4.5	918.63
1079.71	1553.45	0.42	0.49	9.11	3.3	99%$\lvert\pm 7/2\rangle$	±3.5	1085.06
1235.20	1777.16	0.25	0.67	6.39	3.5	98%$\lvert\pm 5/2\rangle$	±2.5	1241.80
1357.57	1953.23	3.21	6.19	7.20	88.9	86%$\lvert\pm 3/2\rangle$ + 10%$\lvert\mp 1/2\rangle$	±1.2	1361.42
1460.99	2102.02	0.72	3.20	16.57	89.7	78%$\lvert\pm 1/2\rangle$ + 8%$\lvert\mp 1/2\rangle$ + 9%$\lvert\mp 3/2\rangle$	±0.3	1457.13
				6				
0.00	0.00	0.00	0.00	20.00	--	100%$\lvert\pm 15/2\rangle$	±7.5	0.00
530.41	763.13	0.00	0.00	17.04	1.0	100%$\lvert\pm 13/2\rangle$	±6.5	543.62
807.70	1162.09	0.00	0.00	14.45	1.6	100%$\lvert\pm 11/2\rangle$	±5.5	800.34
971.40	1397.62	0.00	0.01	11.82	0.6	100%$\lvert\pm 9/2\rangle$	±4.5	970.51
1128.12	1623.11	0.27	0.29	9.11	2.4	99%$\lvert\pm 7/2\rangle$	±3.5	1135.81

1291.70	1858.45	0.28	0.77	6.35	2.7	99% $\lvert\pm 5/2\rangle$	±2.5	1301.35
1430.00	2057.44	3.25	5.65	7.12	88.8	87% $\lvert\pm 3/2\rangle$ + 10% $\lvert\mp 1/2\rangle$	±1.2	1434.85
1544.69	2222.45	0.77	3.62	16.37	90.0	58% $\lvert\pm 1/2\rangle$ + 31% $\lvert\mp 1/2\rangle$ + 6% $\lvert\mp 3/2\rangle$	±0.1	1540.66

Table S7. Electronic structure of **1-6** calculated with "low" CASSCF-SO using the crystal geometries. Each row corresponds to a Kramers doublet. Last column reports the CF energies from the CASSCF-SO crystal field parameters.

Energy (cm^{-1})	**Energy (K)**	**g1**	**g2**	**g3**	**Angle**	**Wavefunction**	**<Jz>**	**Energy^{CF} (cm^{-1})**
				1				
0.00	0.00	0.00	0.00	19.98	--	99% $\lvert\pm 15/2\rangle$	±7.5	0.00
452.99	651.74	0.00	0.00	17.07	1.31	99% $\lvert\pm 13/2\rangle$	±6.5	461.29
739.26	1063.62	0.00	0.00	14.45	1.98	99% $\lvert\pm 11/2\rangle$	±5.5	736.41
932.34	1341.42	0.04	0.04	11.80	1.76	99% $\lvert\pm 9/2\rangle$	±4.5	932.16
1098.60	1580.62	0.62	0.72	9.09	3.71	99% $\lvert\pm 7/2\rangle$	±3.5	1102.91
1244.21	1790.13	0.03	1.35	6.27	4.83	93% $\lvert\pm 5/2\rangle$ + 3% $\lvert\pm 1/2\rangle$	±2.3	1249.58
1341.86	1930.63	2.66	8.10	9.24	89.96	71% $\lvert\pm 3/2\rangle$ + 22% $\lvert\mp 1/2\rangle$	±0.9	1347.34
1476.73	2124.68	0.26	0.83	18.22	89.57	71% $\lvert\pm 1/2\rangle$ + 19% $\lvert\mp 3/2\rangle$	±0.2	1473.40
				2				
0.00	0.00	0.00	0.00	19.99	--	99% $\lvert\pm 15/2\rangle$	±7.5	0.00
489.45	704.21	0.00	0.00	17.06	1.84	99% $\lvert\pm 13/2\rangle$	±6.5	499.53
773.79	1113.30	0.00	0.00	14.45	3.38	99% $\lvert\pm 11/2\rangle$	±5.5	769.27
955.21	1374.33	0.00	0.01	11.81	3.33	99% $\lvert\pm 9/2\rangle$	±4.5	955.31
1118.62	1609.43	0.05	0.05	9.13	5.03	98% $\lvert\pm 7/2\rangle$	±3.5	1124.85
1276.01	1835.89	0.77	0.96	6.42	3.34	96% $\lvert\pm 5/2\rangle$ + 2% $\lvert\pm 3/2\rangle$	±2.5	1282.84
1399.91	2014.14	3.36	4.38	7.18	89.70	80% $\lvert\pm 3/2\rangle$ + 10% $\lvert\mp 1/2\rangle$ + 8% $\lvert\mp 3/2\rangle$	±1.1	1404.25
1490.5	2144.6	0.87	4.34	15.70	89.36	80% $\lvert\pm 1/2\rangle$ +	±0.4	1487.06

8	0					9%$\lvert\mp 1/2\rangle$ + 5%$\lvert\pm 3/2\rangle$ + 5%$\lvert\mp 3/2\rangle$		
				3				
0.00	0.00	0.00	0.00	20.00	--	100%$\lvert\pm 15/2\rangle$	±7.5	0.00
549.08	789.99	0.00	0.00	17.03	1.41	100%$\lvert\pm 13/2\rangle$	±6.5	560.82
881.33	1268.03	0.00	0.00	14.38	1.78	100%$\lvert\pm 11/2\rangle$	±5.5	874.82
1098.18	1580.03	0.00	0.00	11.75	2.04	100%$\lvert\pm 9/2\rangle$	±4.5	1097.50
1287.02	1851.72	0.02	0.02	9.10	4.52	99%$\lvert\pm 7/2\rangle$	±3.5	1294.42
1462.22	2103.79	0.13	0.18	6.41	5.36	97%$\lvert\pm 5/2\rangle$+ 1%$\lvert\pm 3/2\rangle$	±2.5	1470.70
1599.32	2301.05	3.38	4.99	6.37	86.89	89%$\lvert\pm 3/2\rangle$ + 7%$\lvert\mp 1/2\rangle$ + 2%$\lvert\pm 1/2\rangle$	±1.3	1603.74
1699.68	2445.45	0.87	4.38	15.68	89.44	76%$\lvert\pm 1/2\rangle$ + 8%$\lvert\mp 1/2\rangle$ + 12%$\lvert\mp 3/2\rangle$	±0.2	1695.41
				4				
0.00	0.00	0.00	0.00	20.00	--	100%$\lvert\pm 15/2\rangle$	±7.5	0.00
567.94	817.13	0.00	0.00	17.01	1.56	100%$\lvert\pm 13/2\rangle$	±6.5	583.50
864.63	1244.00	0.00	0.00	14.43	2.26	100%$\lvert\pm 11/2\rangle$	±5.5	855.81
1040.14	1496.52	0.02	0.03	11.82	2.59	100%$\lvert\pm 9/2\rangle$	±4.5	1038.87
1211.09	1742.48	0.42	0.47	9.11	5.12	100%$\lvert\pm 7/2\rangle$	±3.5	1220.13
1393.70	2005.22	0.04	0.86	6.35	5.42	97%$\lvert\pm 5/2\rangle$	±2.5	1405.24
1553.04	2234.47	3.39	5.12	5.36	89.52	88%$\lvert\pm 3/2\rangle$ + 6%$\lvert\mp 1/2\rangle$ + 2%$\lvert\mp 3/2\rangle$	±1.3	1558.43
1670.98	2404.15	0.92	4.93	15.39	89.49	56%$\lvert\pm 1/2\rangle$ + 35%$\lvert\mp 1/2\rangle$ + 5%$\lvert\mp 3/2\rangle$	±0.1	1665.86
				5				
0.00	0.00	0.00	0.00	20.00	--	100%$\lvert\pm 15/2\rangle$	±7.5	0.00
503.48	724.40	0.00	0.00	17.06	1.52	100%$\lvert\pm 13/2\rangle$	±6.5	514.44
787.33	1132.78	0.00	0.00	14.44	2.06	100%$\lvert\pm 11/2\rangle$	±5.5	781.58
969.48	1394.8	0.00	0.01	11.81	2.59	100%$\lvert\pm 9/2\rangle$	±4.5	968.57

1137.51	5 1636.61	0.32	0.35	9.11	4.21	99% $\lvert\pm 7/2\rangle$	±3.5	1143.90
1302.96	1874.66	0.14	0.74	6.36	4.16	97% $\lvert\pm 5/2\rangle$	±2.5	1311.04
1436.28	2066.48	3.21	6.01	7.13	88.41	82% $\lvert\pm 3/2\rangle$ + 10% $\lvert\mp 1/2\rangle$ + 5% $\lvert\mp 3/2\rangle$	±1.1	1440.82
1547.58	2226.60	0.74	3.37	16.49	89.36	51% $\lvert\pm 1/2\rangle$ + 36% $\lvert\mp 1/2\rangle$ + 7% $\lvert\pm 3/2\rangle$	±0.1	1543.60
				6				
0.00	0.00	0.00	0.00	20.01	--	100% $\lvert\pm 15/2\rangle$	±7.5	0.00
579.22	833.36	0.00	0.00	17.00	0.78	100% $\lvert\pm 13/2\rangle$	±6.5	595.41
881.96	1268.93	0.00	0.00	14.43	1.37	100% $\lvert\pm 11/2\rangle$	±5.5	872.51
1057.67	1521.74	0.01	0.01	11.81	1.44	100% $\lvert\pm 9/2\rangle$	±4.5	1056.51
1228.55	1767.60	0.13	0.16	9.09	2.28	100% $\lvert\pm 7/2\rangle$	±3.5	1238.02
1410.73	2029.72	0.33	0.64	6.35	2.24	99% $\lvert\pm 5/2\rangle$	±2.5	1422.52
1570.65	2259.79	3.48	4.46	4.79	88.01	85% $\lvert\pm 3/2\rangle$ + 9% $\lvert\mp 3/2\rangle$	±1.1	1576.04
1683.30	2421.88	0.99	5.60	14.85	89.71	88% $\lvert\pm 1/2\rangle$ + 6% $\lvert\mp 1/2\rangle$ + 4% $\lvert\pm 3/2\rangle$	±0.4	1678.18

Table S8. Electronic structure of **1-6** calculated with "full" CASSCF-SO using the PBE optimised geometries. Each row corresponds to a Kramers doublet. Last column reports the CF energies from the CASSCF-SO crystal field parameters.

Energy (cm^{-1})	**Energy (K)**	**g1**	**g2**	**g3**	**Angle**	**Wavefunction**	**<Jz>**	**Energy^{CF} (cm^{-1})**
				1				
0.00	0.00	0.00	0.00	19.87	--	100% $\lvert\pm 15/2\rangle$	±7.5	0.00
416.26	598.90	0.00	0.00	17.05	0.10	100% $\lvert\pm 13/2\rangle$	±6.5	420.87
691.18	994.45	0.00	0.00	14.42	0.09	100% $\lvert\pm 11/2\rangle$	±5.5	690.11
883.09	1270.56	0.01	0.02	11.76	0.03	100% $\lvert\pm 9/2\rangle$	±4.5	883.38
1044.82	1503.25	0.53	0.62	9.07	0.13	100% $\lvert\pm 7/2\rangle$	±3.5	1046.96

1174.84	1690.32	1.28	3.05	6.10	0.10	93% $\lvert\pm 5/2\rangle$ + 5% $\lvert\pm 1/2\rangle$	± 2.3	1177.63
1255.57	1806.47	2.37	7.78	9.62	89.43	72% $\lvert\pm 3/2\rangle$ + 22% $\lvert\mp 3/2\rangle$	±0.9	1259.79
1386.31	1994.58	0.14	0.35	18.32	89.90	62% $\lvert\pm 1/2\rangle$ + 22% $\lvert\mp 3/2\rangle$ + 10% $\lvert\mp 1/2\rangle$	±0.0	1383.98
				2				
0.00	0.00	0.00	0.00	19.89	--	100% $\lvert\pm 15/2\rangle$	±7.5	0.00
460.60	662.70	0.00	0.00	17.03	1.57	100% $\lvert\pm 13/2\rangle$	±6.5	466.21
727.23	1046.32	0.00	0.00	14.40	2.39	100% $\lvert\pm 11/2\rangle$	±5.5	724.67
903.59	1300.06	0.00	0.01	11.74	2.73	100% $\lvert\pm 9/2\rangle$	±4.5	904.17
1062.92	1529.29	0.07	0.07	9.10	3.50	100% $\lvert\pm 7/2\rangle$	±3.5	1066.62
1211.03	1742.40	1.03	1.28	6.45	2.05	97% $\lvert\pm 5/2\rangle$	±2.5	1214.67
1326.02	1907.83	2.47	3.67	5.48	90.00	82% $\lvert\pm 3/2\rangle$ + 11% $\lvert\mp 3/2\rangle$	±1.0	1328.21
1396.96	2009.90	1.09	6.28	14.11	89.64	88% $\lvert\pm 1/2\rangle$ + 6% $\lvert\mp 1/2\rangle$ + 2% $\lvert\pm 3/2\rangle$	±0.4	1395.19
				3				
0.00	0.00	0.00	19.90	--	--	100% $\lvert\pm 15/2\rangle$	±7.5	0.00
479.56	0.00	0.00	17.03	2.13	2.13	100% $\lvert\pm 13/2\rangle$	±6.5	486.31
744.50	0.00	0.00	14.42	2.66	2.66	100% $\lvert\pm 11/2\rangle$	±5.5	741.05
920.27	0.04	0.04	11.79	2.74	2.74	100% $\lvert\pm 9/2\rangle$	±4.5	919.69
1080.60	0.51	0.59	9.11	5.54	5.54	98% $\lvert\pm 7/2\rangle$	±3.5	1084.40
1234.83	0.49	1.61	6.33	6.75	6.75	95% $\lvert\pm 5/2\rangle$+ 2% $\lvert\pm 3/2\rangle$	±2.4	1239.70
1355.95	3.04	6.99	7.59	89.75	89.75	81% $\lvert\pm 3/2\rangle$ + 14% $\lvert\mp 1/2\rangle$	±1.2	1358.84
1468.92	0.60	2.44	17.12	89.39	89.39	72% $\lvert\pm 1/2\rangle$ + 10% $\lvert\mp 1/2\rangle$ + 11% $\lvert\mp 3/2\rangle$	±0.2	1466.54
				4				
0.00	0.00	0.00	0.00	19.90	--	100% $\lvert\pm 15/2\rangle$	±7.5	0.00

479.74	690.23	0.00	0.00	17.03	1.13	100% $\lvert \pm 13/2 \rangle$	±6.5	486.21
751.56	1081.33	0.00	0.00	14.41	1.34	100% $\lvert \pm 11/2 \rangle$	±5.5	748.20
932.27	1341.32	0.01	0.01	11.77	0.68	100% $\lvert \pm 9/2 \rangle$	±4.5	931.93
1095.90	1576.75	0.25	0.27	9.09	2.60	100% $\lvert \pm 7/2 \rangle$	±3.5	1099.65
1250.10	1798.60	0.13	0.69	6.38	3.81	98% $\lvert \pm 5/2 \rangle$	±2.5	1254.65
1369.31	1970.12	3.19	6.49	7.09	88.90	83% $\lvert \pm 3/2 \rangle$ + 11% $\lvert \mp 1/2 \rangle$	±1.1	1372.10
1469.96	2114.93	0.70	3.06	16.65	90.00	46% $\lvert \pm 1/2 \rangle$ + 41% $\lvert \mp 1/2 \rangle$ + 6% $\lvert \mp 3/2 \rangle$	±0.0	1467.68
				5				
0.00	0.00	0.00	0.00	19.90	--	100% $\lvert \pm 15/2 \rangle$	±7.5	0.00
476.70	685.87	0.00	0.00	17.03	1.29	100% $\lvert \pm 13/2 \rangle$	±6.5	483.07
747.42	1075.36	0.00	0.00	14.41	1.63	100% $\lvert \pm 11/2 \rangle$	±5.5	744.19
927.66	1334.69	0.02	0.02	11.77	1.65	100% $\lvert \pm 9/2 \rangle$	±4.5	927.44
1090.68	1569.23	0.39	0.45	9.09	3.05	99% $\lvert \pm 7/2 \rangle$	±3.5	1094.46
1243.94	1789.75	0.20	0.66	6.38	3.37	98% $\lvert \pm 5/2 \rangle$	±2.5	1248.47
1361.57	1958.98	3.20	6.30	7.27	88.80	86% $\lvert \pm 3/2 \rangle$ + 11% $\lvert \mp 1/2 \rangle$	±1.2	1364.48
1460.66	2101.55	0.70	3.06	16.62	89.70	52% $\lvert \pm 1/2 \rangle$ + 34% $\lvert \mp 1/2 \rangle$ + 7% $\lvert \pm 3/2 \rangle$	±0.1	1458.38
				6				
0.00	0.00	0.00	0.00	19.90	--	100% $\lvert \pm 15/2 \rangle$	±7.5	0.00
529.36	761.62	0.00	0.00	17.00	1.02	100% $\lvert \pm 13/2 \rangle$	±6.5	538.13
804.37	1157.31	0.00	0.00	14.41	1.55	100% $\lvert \pm 11/2 \rangle$	±5.5	799.38
973.79	1401.06	0.01	0.01	11.78	0.50	100% $\lvert \pm 9/2 \rangle$	±4.5	973.26
1132.55	1629.47	0.24	0.26	9.09	2.23	100% $\lvert \pm 7/2 \rangle$	±3.5	1137.58
1292.35	1859.39	0.29	0.73	6.35	2.66	98% $\lvert \pm 5/2 \rangle$	±2.5	1298.51
1423.19	2047.64	3.22	5.86	7.35	88.84	85% $\lvert \pm 3/2 \rangle$ + 11% $\lvert \mp 1/2 \rangle$	±1.2	1426.39
1533.02	2205.66	0.74	3.33	16.53	90.00	46% $\lvert \pm 1/2 \rangle$ + 41% $\lvert \mp 1/2 \rangle$ +	±0.0	1530.32

						$7\%\lvert\mp 3/2\rangle$ + $5\%\lvert\pm 3/2\rangle$		

Table S9. Electronic structure of **1-6** calculated with "full" CASSCF-SO using the crystal geometries. Each row corresponds to a Kramers doublet. Last column reports the CF energies from the CASSCF-SO crystal field parameters.

Energy (cm^{-1})	**Energy (K)**	**g1**	**g2**	**g3**	**Angle**	**Wavefunction**	**<Jz>**	**Energy^{CF} (cm^{-1})**
				1				
0.00	0.00	0.00	0.00	19.88	--	$100\%\lvert\pm 15/2\rangle$	±7.5	0.00
455.37	655.17	0.00	0.00	17.03	1.22	$100\%\lvert\pm 13/2\rangle$	±6.5	460.98
743.46	1069.67	0.00	0.00	14.40	1.53	$100\%\lvert\pm 11/2\rangle$	±5.5	741.54
942.01	1355.33	0.03	0.04	11.76	1.72	$100\%\lvert\pm 9/2\rangle$	±4.5	942.01
1110.81	1598.20	0.59	0.67	9.07	3.44	$99\%\lvert\pm 7/2\rangle$	±3.5	1113.66
1254.94	1805.57	0.06	1.37	6.25	4.50	$92\%\lvert\pm 5/2\rangle$ + $3\%\lvert\mp 5/2\rangle$	±2.3	1258.48
1350.17	1942.59	2.65	8.15	9.13	89.87	$74\%\lvert\pm 3/2\rangle$ + $19\%\lvert\mp 1/2\rangle$ + $3\%\lvert\pm 1/2\rangle$	±1.0	1354.08
1479.64	2128.86	0.26	0.82	18.17	89.53	$57\%\lvert\pm 1/2\rangle$ + $20\%\lvert\mp 3/2\rangle$ + $17\%\lvert\mp 1/2\rangle$	±0.1	1477.33
				2				
0.00	0.00	0.00	0.00	19.89	--	$100\%\lvert\pm 15/2\rangle$	±7.5	0.00
488.65	703.05	0.00	0.00	17.02	1.88	$100\%\lvert\pm 13/2\rangle$	±6.5	495.15
770.98	1109.27	0.00	0.00	14.40	2.94	$100\%\lvert\pm 11/2\rangle$	±5.5	767.94
956.54	1376.24	0.00	0.01	11.76	3.27	$100\%\lvert\pm 9/2\rangle$	±4.5	956.93
1122.17	1614.54	0.05	0.05	9.11	4.87	$98\%\lvert\pm 7/2\rangle$	±3.5	1126.36
1277.54	1838.08	0.83	1.01	6.44	3.44	$96\%\lvert\pm 5/2\rangle$	±2.5	1281.76
1399.35	2013.34	2.84	3.67	5.39	89.42	$90\%\lvert\pm 3/2\rangle$ + $4\%\lvert\mp 1/2\rangle$	±1.3	1401.81
1476.06	2123.70	1.07	6.11	14.27	89.41	$86\%\lvert\pm 1/2\rangle$ + $4\%\lvert\mp 1/2\rangle$ + $8\%\lvert\pm 3/2\rangle$	±0.4	1474.05
				3				
0.00	0.00	0.00	0.00	19.90	--	$100\%\lvert\pm 15/2\rangle$	±7.5	0.00

550.90	792.62	0.00	0.00	16.99	1.41	100% $\lvert\pm 13/2\rangle$	±6.5	558.69
881.13	1267.75	0.00	0.00	14.35	1.58	100% $\lvert\pm 11/2\rangle$	±5.5	876.71
1102.70	1586.52	0.00	0.00	11.72	1.85	100% $\lvert\pm 9/2\rangle$	±4.5	1102.39
1293.84	1861.54	0.02	0.03	9.08	4.13	98% $\lvert\pm 7/2\rangle$	±3.5	1298.76
1466.48	2109.93	0.15	0.20	6.42	5.02	98% $\lvert\pm 5/2\rangle$+ 1% $\lvert\pm 3/2\rangle$	±2.5	1471.93
1598.52	2299.90	3.40	4.94	6.35	86.76	90% $\lvert\pm 3/2\rangle$ + 8% $\lvert\mp 1/2\rangle$	±1.3	1601.46
1693.26	2436.22	0.88	4.38	15.62	89.45	62% $\lvert\pm 1/2\rangle$ + 28% $\lvert\mp 1/2\rangle$ + 5% $\lvert\mp 3/2\rangle$	±0.2	1690.40
				4				
0.00	0.00	0.00	0.00	19.90	--	100% $\lvert\pm 15/2\rangle$	±7.5	0.00
571.16	821.77	0.00	0.00	16.98	1.63	100% $\lvert\pm 13/2\rangle$	±6.5	581.51
868.77	1249.96	0.00	0.00	14.39	2.08	100% $\lvert\pm 11/2\rangle$	±5.5	862.83
1054.41	1517.06	0.01	0.02	11.78	2.24	100% $\lvert\pm 9/2\rangle$	±4.5	1053.71
1231.22	1771.44	0.39	0.42	9.09	4.79	99% $\lvert\pm 7/2\rangle$	±3.5	1237.31
1412.50	2032.26	0.04	0.87	6.37	5.31	97% $\lvert\pm 5/2\rangle$	±2.5	1420.07
1565.60	2252.53	3.40	5.22	5.40	89.92	90% $\lvert\pm 3/2\rangle$ + 6% $\lvert\mp 1/2\rangle$	±1.3	1569.25
1677.18	2413.08	0.92	4.79	15.41	89.52	47% $\lvert\pm 1/2\rangle$ + 44% $\lvert\mp 1/2\rangle$ + 5% $\lvert\mp 3/2\rangle$	±0.0	1673.89
				5				
0.00	0.00	0.00	0.00	19.90	--	100% $\lvert\pm 15/2\rangle$	±7.5	0.00
506.44	728.65	0.00	0.00	17.01	1.54	100% $\lvert\pm 13/2\rangle$	±6.5	513.77
792.58	1140.34	0.00	0.00	14.40	1.91	100% $\lvert\pm 11/2\rangle$	±5.5	788.70
982.86	1414.10	0.00	0.00	11.77	2.24	100% $\lvert\pm 9/2\rangle$	±4.5	982.35
1155.30	1662.20	0.30	0.31	9.09	3.94	99% $\lvert\pm 7/2\rangle$	±3.5	1159.57
1319.43	1898.36	0.22	0.77	6.36	4.04	97% $\lvert\pm 5/2\rangle$	±2.5	1324.71
1448.02	2083.36	3.20	6.13	7.22	88.52	76% $\lvert\pm 3/2\rangle$ + 11% $\lvert\mp 1/2\rangle$ + 11% $\lvert\pm 1/2\rangle$	±0.9	1451.13

1555.14	2237.48	0.72	3.20	16.55	89.40	41% $\lvert\pm 1/2\rangle$ + 46% $\lvert\mp 1/2\rangle$ + 7% $\lvert\mp 3/2\rangle$	±0.0	1552.49
				6				
0.00	0.00	0.00	0.00	19.90	--	100% $\lvert\pm 15/2\rangle$	±7.5	0.00
580.50	835.20	0.00	0.00	16.97	0.79	100% $\lvert\pm 13/2\rangle$	±6.5	591.21
881.24	1267.90	0.00	0.00	14.39	1.19	100% $\lvert\pm 11/2\rangle$	±5.5	874.84
1064.95	1532.21	0.01	0.01	11.77	1.27	100% $\lvert\pm 9/2\rangle$	±4.5	1064.30
1239.84	1783.84	0.13	0.15	9.08	2.16	100% $\lvert\pm 7/2\rangle$	±3.5	1246.12
1419.23	2041.95	0.42	0.72	6.36	2.22	99% $\lvert\pm 5/2\rangle$	±2.5	1426.83
1571.76	2261.39	3.48	4.57	5.00	88.33	91% $\lvert\pm 3/2\rangle$ + 6% $\lvert\mp 1/2\rangle$	±1.3	1575.29
1678.07	2414.36	0.98	5.37	14.95	89.70	63% $\lvert\pm 1/2\rangle$ + 31% $\lvert\mp 1/2\rangle$ + 4% $\lvert\pm 3/2\rangle$	±0.2	1674.76

Table S10. Comparison of crystal field splitting (cm^{-1}) of the ground $^6H_{15/2}$ multiplet obtained at different levels of theories for **6**.

Kramers doublet	"low" CASSCF-SO on DFT-PBE **6** (this work)	XMS-CASPT2 on DFT-PBE0 **6** (ref. [19])[a]
1	0.00	0
2	530.41	539
3	807.70	824
4	971.40	992
5	1128.12	1143
6	1291.70	1293
7	1430.00	1414
8	1544.69	1536

[a] SA-CASSCF/XMS-CASPT2/SO-RASSI with only sextets included in the XMS-CASPT2 and SO-RASSI calculations (see Table S16 in ref. 19).

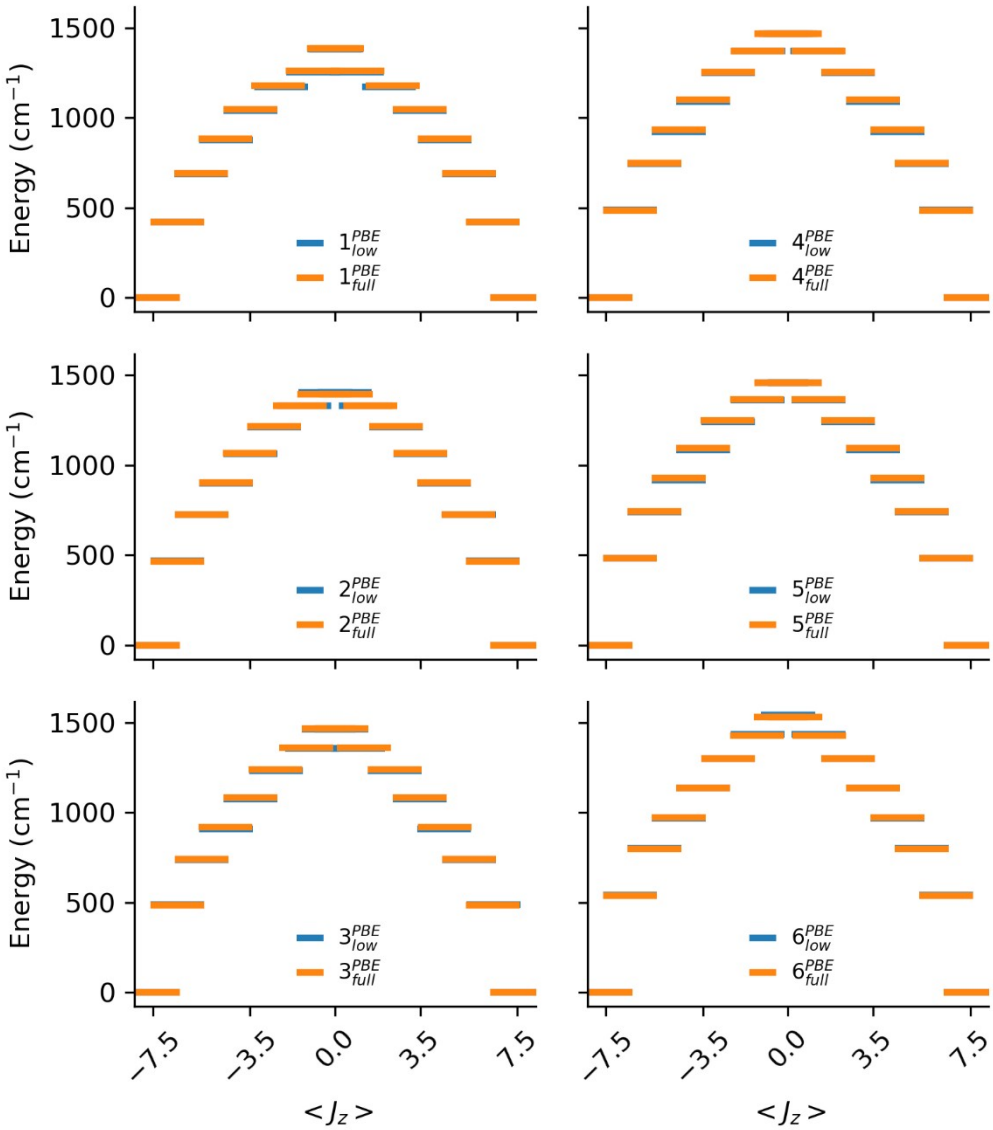

Figure S13. Comparison of the static electronic structure of compounds **1-6** calculated with the crystal field parameters obtained from "low" and "full" CASSCF-SO calculations, at the PBE optimised geometries.

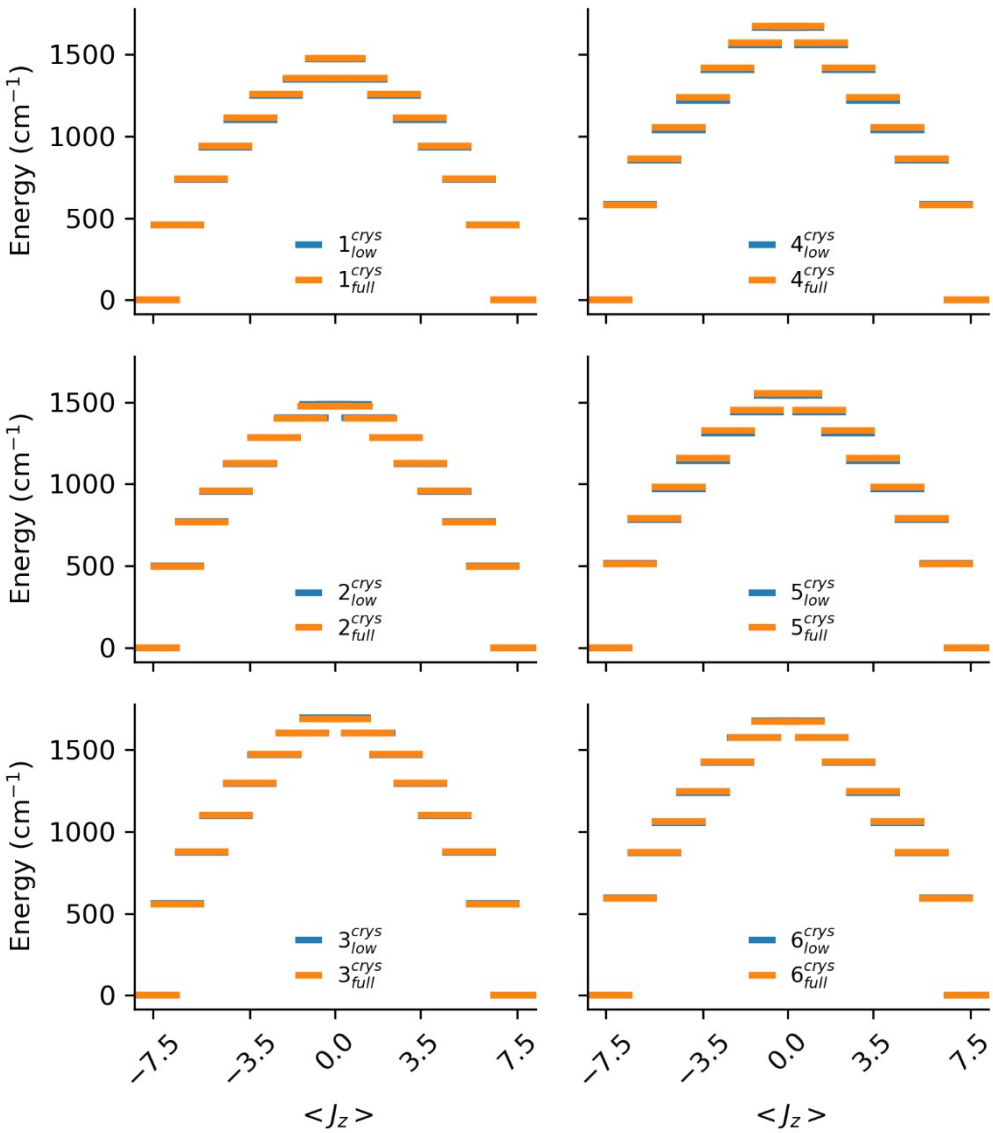

Figure S14. Comparison of the static electronic structure of compounds **1-6** calculated with the crystal field parameters obtained from "low" and "full" CASSCF-SO calculations, at the crystal geometries.

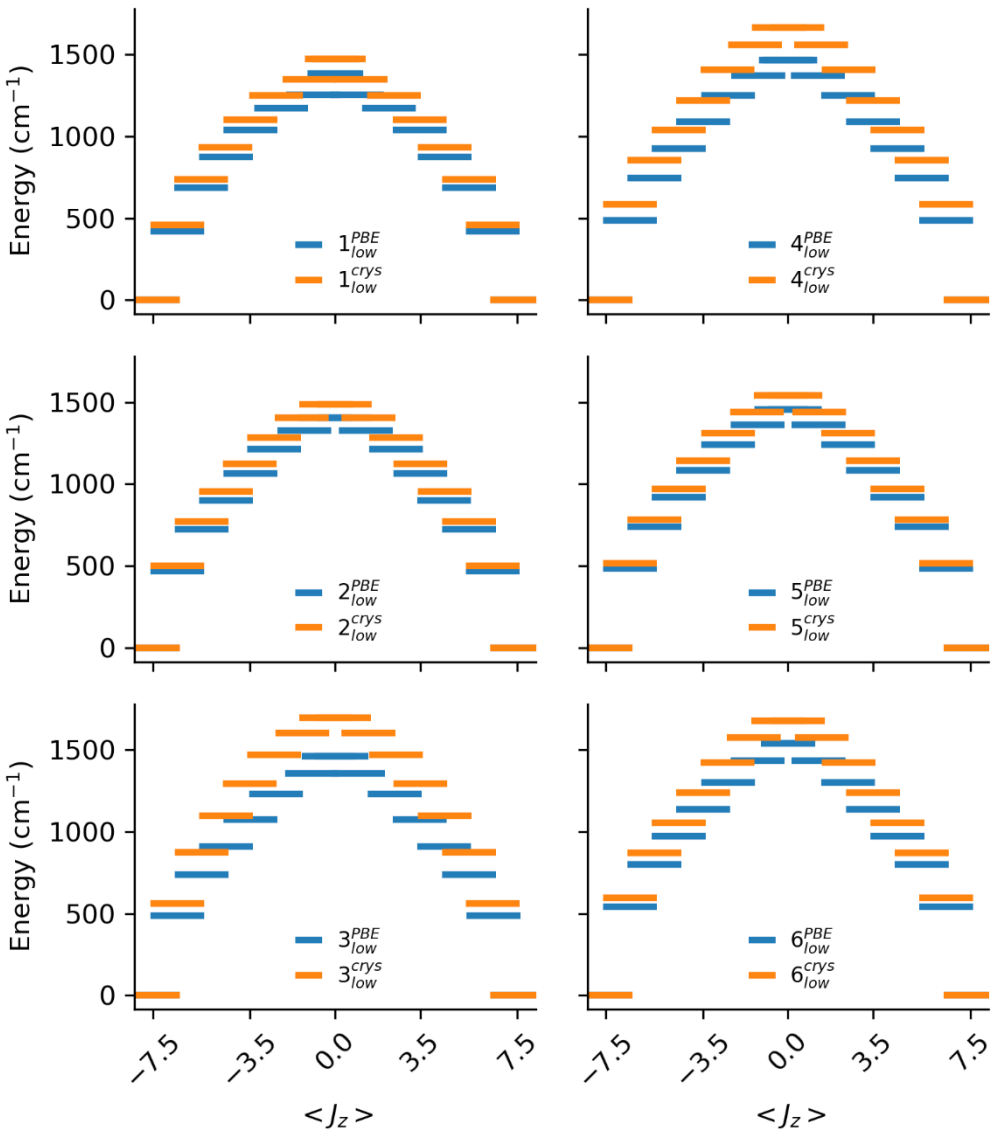

Figure S15. Comparison of the static electronic structure of compounds **1-6** calculated with the crystal field parameters obtained from "low" CASSCF-SO calculations, at the crystal and PBE optimised geometries.

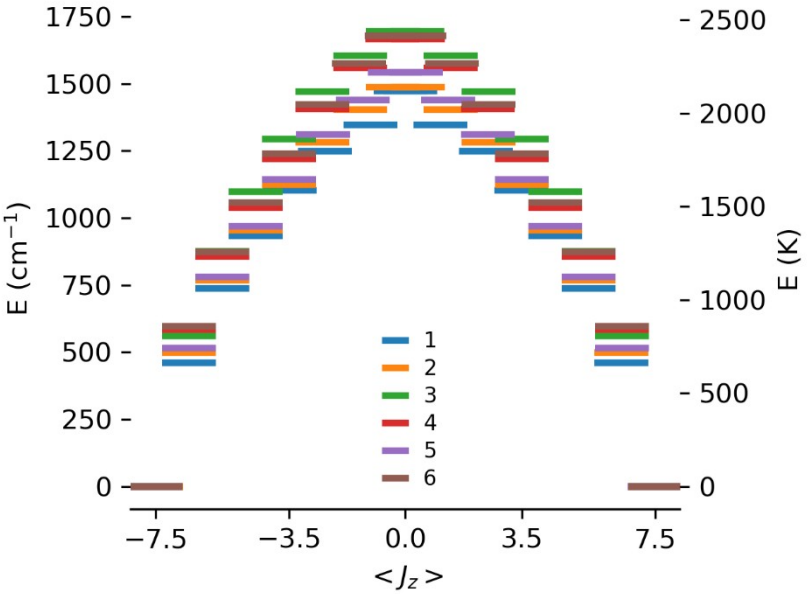

Figure S16. Comparison of the static electronic structure of compounds **1**-**6** calculated with the crystal field parameters obtained from "low" CASSCF-SO calculations, at the crystal geometries.

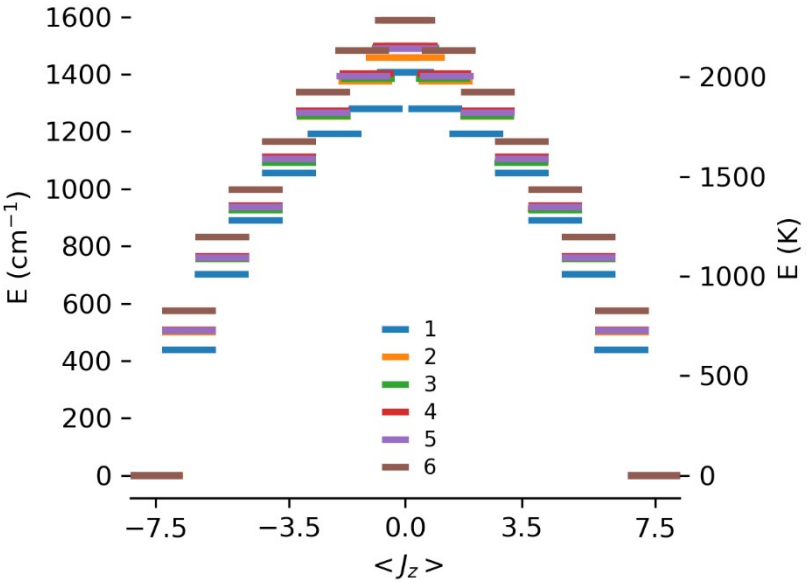

Figure S17. Comparison of the static electronic structure of compounds **1**-**6** calculated with the crystal field parameters obtained from "low" CASSCF-SO calculations, at the PBE0 optimised geometries.

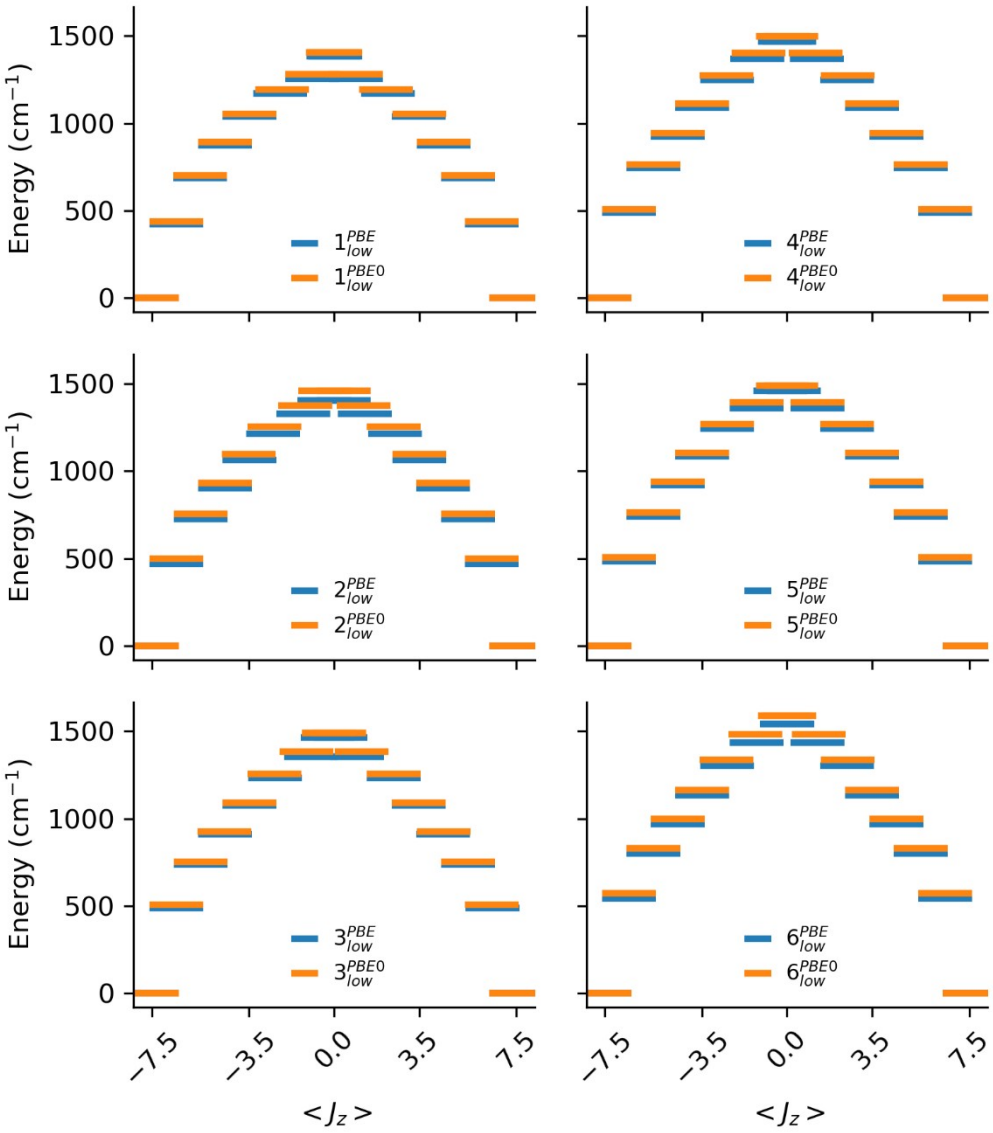

Figure S18. Comparison of the static electronic structure of compounds **1-6** calculated with the crystal field parameters obtained from "low" CASSCF-SO calculations, at the PBE and PBE0 optimised geometries.

S4. Spin-dynamics approach

We seek to reproduce, *ab initio*, the relaxation dynamics involved in the Orbach process, in which the electronic structure (crystal field) is coupled individually to each harmonic vibrational mode of the molecule. These couplings allow transitions between a set of equilibrium crystal field eigenstates resulting in a step wise relaxation process.

In order to describe such dynamics, we assume that *i)* the Born-Oppenheimer approximation for electronic-nuclear decoupling is valid i.e. that the spin-phonon coupling operates in the weak limit, *ii)* the time scale for spin-relaxation is orders of magnitude slower than the lifetimes of vibrational modes i.e. that the phononic bath of the lattice is always in equilibrium and at the temperature of the cryostat, and *iii)* the gas-phase vibrational modes within the harmonic approximation are valid. The change in population of each electronic state with time is then a stochastic process governed by the classical master equation[20,21]

$$\frac{d}{dt} p_i(t) = \sum_{f \neq i} [\gamma_{if} p_f(t) - \gamma_{fi} p_i(t)] \qquad \text{(S1)}$$

where $p_i(t)$ and $p_f(t)$ are the time dependent populations of states *i* and *f*, γ_{if} is the rate of the transition $f \rightarrow i$ between states *i* and *f*, which must fulfil the detailed balance criterion such that $\gamma_{fi} = \gamma_{if} e^{-|E_f - E_i|/k_B T}$ where E_i and E_f are the energies of states *i* and *f*, respectively. The solutions to this set of differential equations can be found by solving the eigenvalue equation for the matrix $\Gamma_{f,i} = (1-\delta_{f,i})\gamma_{f,i} - \delta_{f,i} \sum_{m \neq i} \gamma_{m,i}$, where the eigenvalues are the negative of the characteristic relaxation rates $\frac{-1}{\tau_k}$.**Error! Bookmark not defined.**

The crystal field splitting of the 2*J* + 1 states of the ground state multiplet $^{2S+1}L_J$ is described by the crystal field Hamiltonian

$$\hat{H}_{CF} = \sum_{k}^{2,4,6} \sum_{q=-k}^{k} \theta_k B_k^q(Q_{eq}) \hat{O}_k^q \qquad \text{(S2)}$$

where $B_k^q(Q_{eq})$ is a CF parameters (CFP) at the equilibrium geometry Q_{eq}, θ_k is an operator equivalent factor and $\hat{O}_k^q$ an extended Stevens operator.[22] The 2*J* + 1 eigenstates $\psi$of S2 are the reference eigenstates to which the as yet undefined spin-phonon perturbation $\hat{H}_{SP}$ is applied.

Assuming that the spin-phonon perturbation is much larger than the equilibrium CF, we can use Fermi's Golden Rule[Error! Bookmark not defined.,23,24] from first order time-dependent perturbation theory to define the transition rates γ_{if}

$$\gamma_{fi} = \frac{2\pi}{\hbar} \left| \langle f | \widehat{H}_{SP} | i \rangle \right|^2 \rho\left(\left|\Delta E_{fi}\right|\right) \tag{S3}$$

Where $\rho\left(\left|\Delta E_{fi}\right|\right)$ is the phonon density of states (DOS) at the transition energy ΔE_{fi}. To define the spin-phonon perturbation we can take one of two approaches. In the first, we use quench dynamics to define a oscillatory time-dependent spin-phonon perturbation $\widehat{H}_{SP\,j}(t)$ caused by displacement along the normal mode vector Q_j of mode j

$$\widehat{H}_{SP_j}(t) = Q_j \sum_{k=2,4,6} \sum_{q=-k}^{k} B_{kj}^q \left(\acute{Q}_j \sin\left[\omega_j t + \phi_j\right]\right) \theta_k \widehat{O}_k^q \tag{S4}$$

Where $B_{kj}^q\left(\acute{Q}_j \sin\left[\omega_j t + \phi_j\right]\right)$ is a time-dependent CFP, which oscillates with angular frequency ω_j, phase ϕ_j, and amplitude $\acute{Q}_j$ (thermally-averaged magnitude of displacement along Q_j (*vide infra*)). Matrix elements of S4 are of the form

$$\left\langle f \left| \widehat{H}_{SP_j}(t) \right| i \right\rangle = \left\langle f \left| Q_j \sum_{k=2,4,6} \sum_{q=-k}^{k} \theta_k B_{kj}^q \left(\acute{Q}_j \sin\left[\omega_j t + \phi_j\right]\right) \widehat{O}_k^q \right| i \right\rangle = \left\langle \psi_f \left| \sum_{k=2,4,6} \sum_{q=-k}^{k} \theta_k B_{kj}^q \left(\acute{Q}_j \sin\left[\right.\right.\right. \tag{S5}$$

Where the electronic and vibrational components have been separated. We follow the work of Orbach and Stevens,[25,26] and remove the explicit dependence on the vibrational basis (where n_j is the vibrational quantum number of mode j) and define the non-zero matrix elements

$$\left| \langle n_j + 1 | Q_j | n_j \rangle \right|^2 = \frac{1}{2} \left(1 - e^{\frac{-\hbar \omega_j}{k_B T}} \right)^{-1} \tag{S6}$$

$$\left| \langle n_j - 1 | Q_j | n_j \rangle \right|^2 = \frac{1}{2} \left(e^{\frac{\hbar \omega_j}{k_B T}} - 1 \right)^{-1} \tag{S7}$$

Which correspond to gain and loss of a vibrational quantum respectively, and are referred to here as occupation numbers as they arise from Bose-Einstein statistics. Boltzmann statistics can be used to make a similar substitution.

$$\left| \langle n_j + 1 | Q_j | n_j \rangle \right|^2 = \frac{1}{2} \tag{S8}$$

$$\left| \langle n_j - 1 | Q_j | n_j \rangle \right|^2 = \frac{1}{2} e^{-\hbar \omega_j / k_B T} \tag{S9}$$

In our work we see little difference between the two statistical approaches (Figure S19). We are then are able to define our transition rates purely within the basis of equilibrium CF eigenstates ψ, such that for $E_f > E_i$

$$\gamma_{fi}=\frac{2\pi}{\hbar}\sum_j \left|\left\langle \psi_f \middle| \widehat{H}_{SPj} \middle| \psi_i \right\rangle\right|^2 \left|\left\langle n_j-1 \middle| Q_j \middle| n_j \right\rangle\right|^2 \rho_j\left(\left|\Delta E_{fi}\right|\right) \tag{S10a}$$

$$\gamma_{if}=\frac{2\pi}{\hbar}\sum_j \left|\left\langle \psi_i \middle| \widehat{H}_{SPj} \middle| \psi_f \right\rangle\right|^2 \left|\left\langle n_j+1 \middle| Q_j \middle| n_j \right\rangle\right|^2 \rho_j\left(\left|\Delta E_{if}\right|\right) \tag{S10b}$$

where we have now removed the explicit time dependence of $\widehat{H}_{SP\,j}$ by replacing it with the average of its value at maximal positive and negative displacements choosing, arbitrarily, the phase of the matrix elements corresponding to positive displacement.

$$\left\langle \psi_f \middle| \widehat{H}_{SP} \middle| \psi_i \right\rangle = ¿¿ \tag{S11}$$

The matrix elements of $\widehat{H}_{SP\,j}{}^{\pm}$ can be computed either at the zero point displacement (*vide infra*) (per reference 28) or by using a temperature dependent displacement factor (per reference [27]).

In the second approach to defining $\widehat{H}_{SP}$ we expand the CFPs in a Taylor series in the jth normal mode displacement Q_j around the equilibrium structure $Q_{eq}=0$ [25]

$$B_k^q(Q_j)=B_k^q(Q_{eq})+\sum_j^{3N-6} Q_j\left(\frac{\partial B_k^q}{\partial Q_j}\right)_{eq}+\frac{1}{2}\sum_j^{3N-6}\sum_{j'}^{3N-6} Q_j Q_{j'}\left(\frac{\partial^2 B_k^q}{\partial Q_j \partial Q_{j'}}\right)_{eq}+\ldots \tag{S12}$$

The term independent of Q corresponds to the equilibrium CFPs and can be discarded, whereas those linear and quadratic in Q describe the spin one- and two-phonon interactions respectively. As we are interested in the Orbach process we need only to use the linear term to define the spin-phonon Hamiltonian

$$\widehat{H}_{SP_j}=Q_j\sum_{k=2,4,6}\sum_{q=-k}^{k}\theta_k\left(\frac{\partial B_k^q}{\partial Q_j}\right)_{eq}\widehat{O}_k^q \tag{S13}$$

Matrix elements of S13 are of the form

$$\left\langle f \middle| \widehat{H}_{SP_j} \middle| i \right\rangle=\left\langle f \middle| Q_j\sum_{k=2,4,6}\sum_{q=-k}^{k}\theta_k\left(\frac{\partial B_k^q}{\partial Q_j}\right)_{eq}\widehat{O}_k^q \middle| i \right\rangle=\left\langle \psi_f \middle| Q_j\sum_{k=2,4,6}\sum_{q=-k}^{k}\theta_k\left(\frac{\partial B_k^q}{\partial Q_j}\right)_{eq}\widehat{O}_k^q \middle| \psi_i \right\rangle\left\langle n_j' \middle| Q_j \middle| n \right. \tag{S14}$$

Where similarly to S5, the electronic and vibrational components have been separated. As before, we then use S6 and S7 (or S8 and S9) to remove the explicit treatment of the vibrational basis to give S10a and S10b, where $\widehat{H}_{SP_j}$ is defined in S13.

Crucially, for both methods we must define, quantitatively, the physical displacement along each vibrational mode. In our original work[28] we defined the zero-point displacement (ZPD) for each normal mode as $Q_{j,0}=a_0/\sqrt{\mu_j}$ (where μ_j is the effective reduced mass of mode j obtained with DFT and a_0 is the Bohr radius), which

leads to a wrong expression for the force constant. Thus, in our revised approach, we define the ZPD

$$Q_{j,0}=\sqrt{\frac{h\acute{\nu}_j c}{k_j}} \tag{S15}$$

where h, $\acute{\nu}_j$, c and k_j are the Planck constant, the wavenumber of mode j, the speed of light and the force constant of mode j, respectively. At some temperature T there will be a non-zero population of vibrationally excited states which have larger maximal displacements than the zero point energy level. To account for this we calculate a Boltzmann distribution across the harmonic energy levels of each vibrational mode and use this to define the thermally weighted maximal displacement for each mode

$$\acute{Q}_j(T)=\frac{Q_{j,0}}{Z_j}\sum_{n=0}^{\infty} e^{\frac{-\acute{\nu}_j n}{k_B T}}\sqrt{1+2n} \tag{S16}$$

Where Z_j is the corresponding partition function. We can express this quantity in terms of the ZPD by calculating the ratio

$$D_j=\acute{Q}_j(T)/Q_{j,0} \tag{S17}$$

In our work, we choose to set a minimum value of $D_j=1.5$ for all modes, though if $D_j>1.5$, we set it to 110% of its calculated value; this ensures that we are always in the interpolation regime for the temperature-dependent spin-phonon coupling matrix elements. To calculate either $B_{kj}^q\left(\acute{Q}_j \sin\left[\omega_j t+\phi_j\right]\right)$ or $\left(\frac{\partial B_k^q}{\partial Q_j}\right)_{eq}$ we distort the equilibrium molecular structure along each vibrational mode separately up to $D_j Q_{j,0}$ in a series of steps in positive and negative directions, recalculating the electronic structure and expressing it in terms of a set of CFPs at each step. We then fit changes in the CFPs (compared to those calculated at the equilibrium geometry) to cubic polynomials

$$B_k^q(Q_j)=a Q_j^3+b Q_j^2+c Q_j+B_k^q(Q_{eq}) \tag{S18}$$

Which can be used in their entirety to define $B_{kj}^q\left(\acute{Q}_j \sin\left[\omega_j t+\phi_j\right]\right)$, or simply the linear term $c Q_j$ can be used to define $\left(\frac{\partial B_k^q}{\partial Q_j}\right)_{eq}=c$.

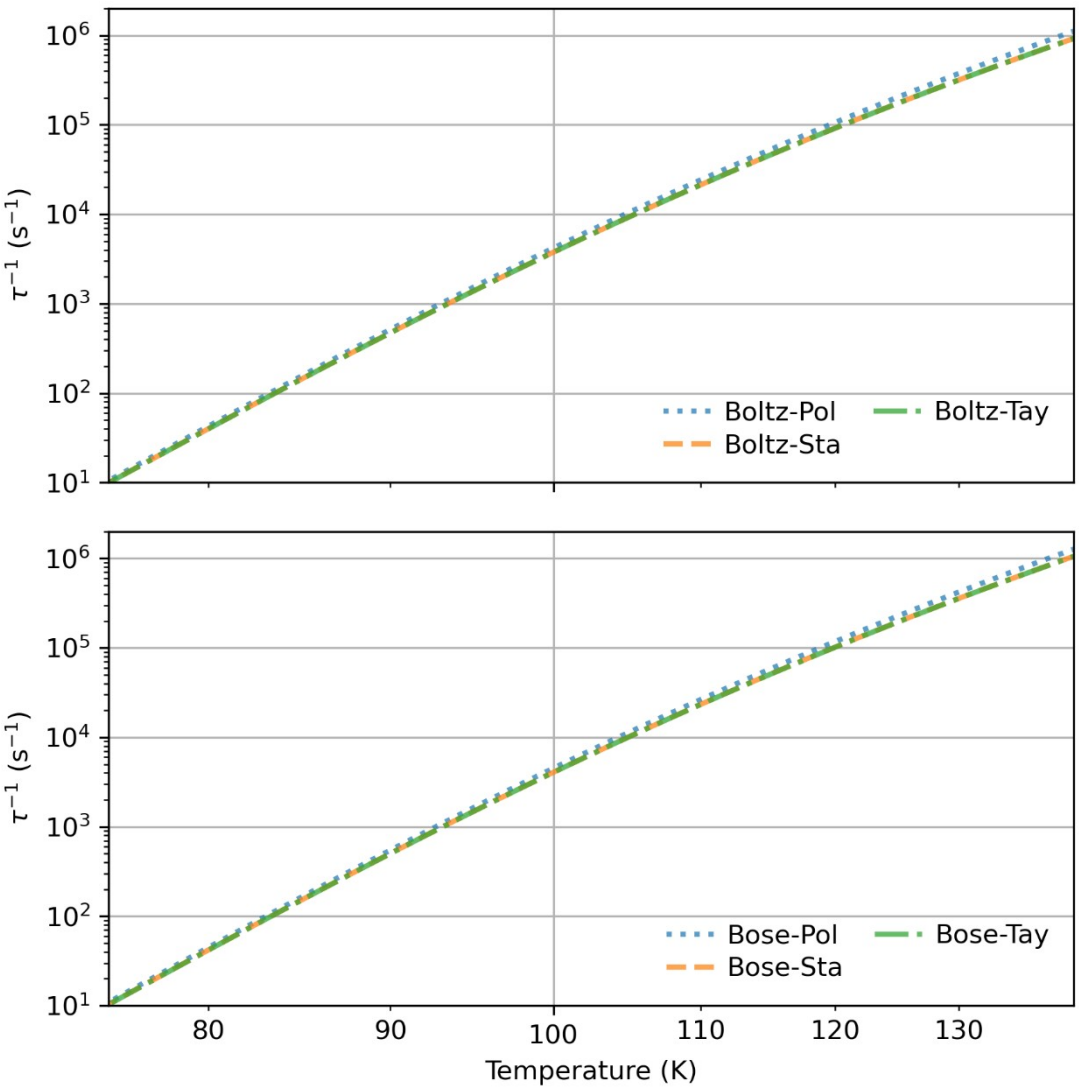

Figure S19. Comparison of predicted rates for **2** (using the PBE density-functional) calculated with Boltzmann (upper) and Bose-Einstein (lower) phonon statistics. For each case, we employ temperature-dependent CFPs ("Polynomial"), fixed ZPD CFPs ("Static") and first-derivative ("Taylor") definitions for $\langle f | \widehat{H}_{SP} | i \rangle$.

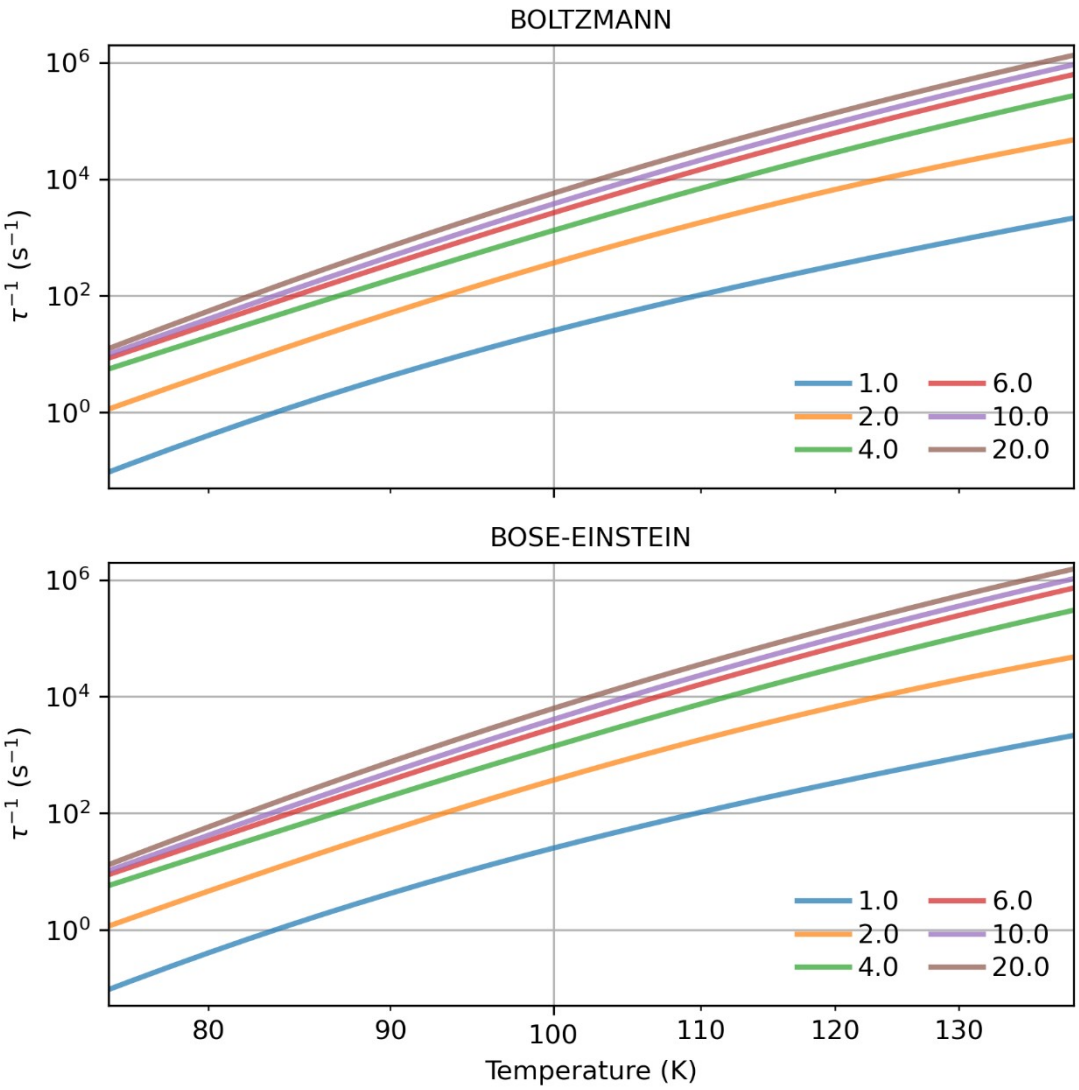

Figure S20. FWHM linewidth dependence of predicted rates for **2** (using the PBE density-functional) calculated with Boltzmann (upper) and Bose-Einstein (lower) phonon statistics.

S4.1. Effect of linewidth model

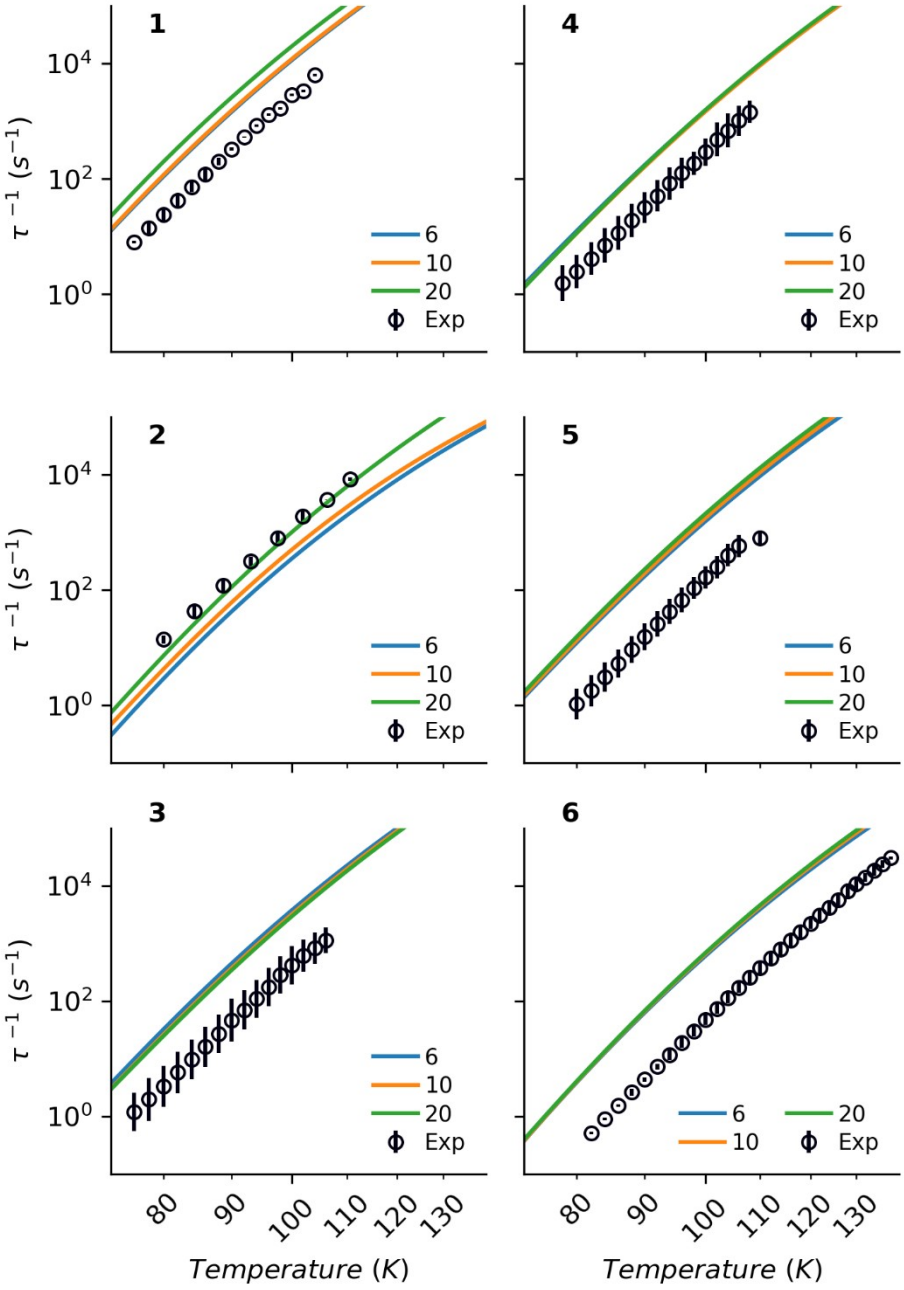

Figure S21. Comparison of experimental (circles) and PBE0 calculated (lines) rates for **1-6**. Solid lines are obtained without IR calibration, using "Taylor" for the spin-phonon coupling, Bose-Einstein phonon statistics and calculated with fixed full-width half-maxima of 6, 10 and 20 cm^{-1}. Experimental error bars are estimated standard deviations derived from the generalised Debye model.[1]

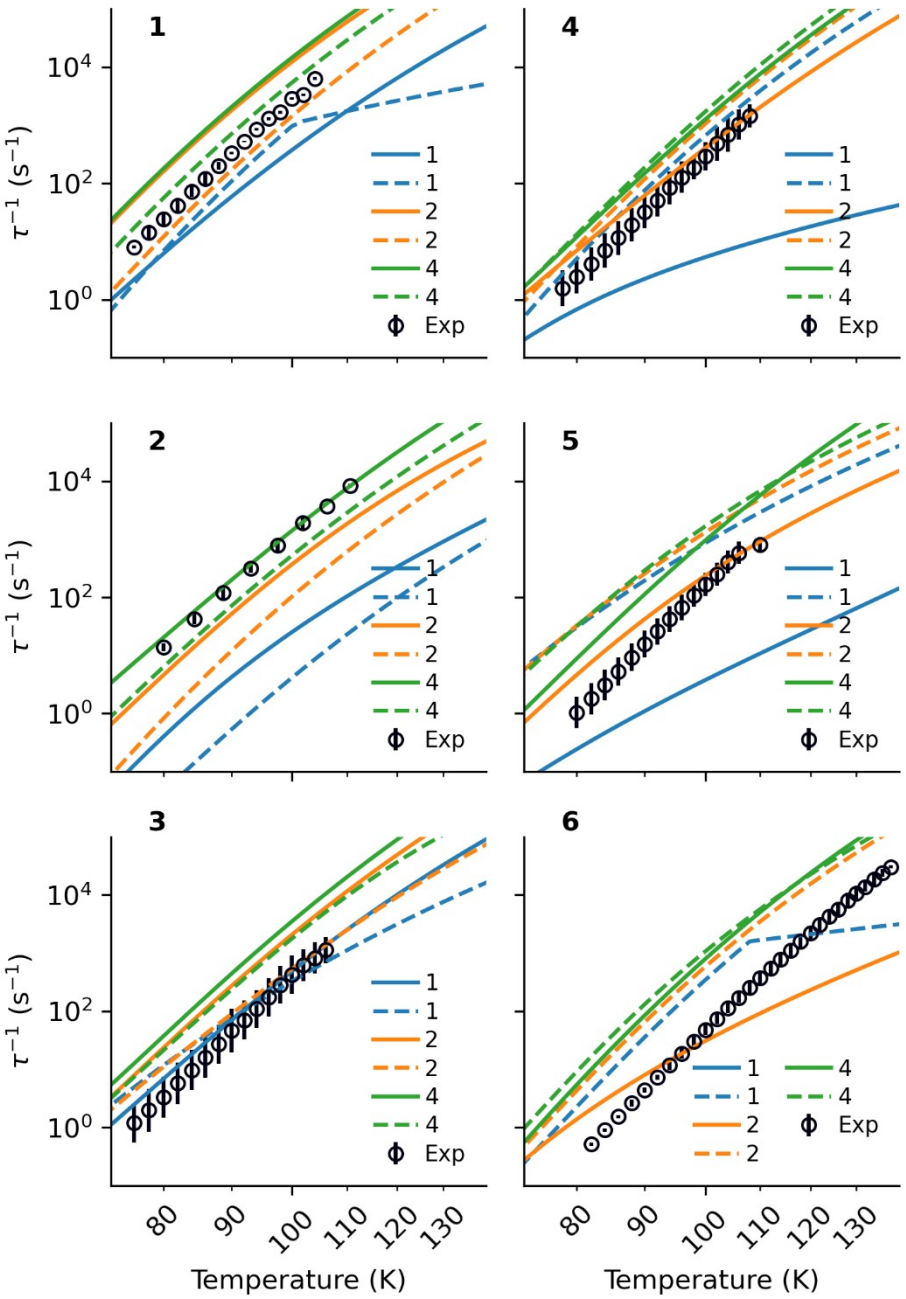

Figure S22. Comparison of experimental (circles) and PBE calculated (lines) rates for **1**-**6**. Solid and dashed lines are obtained without and with IR calibration, respectively, using "Taylor" for the spin-phonon coupling, Bose-Einstein phonon statistics and calculated with fixed full-width half-maxima of 1, 2 and 4 cm^{-1}. Experimental error bars are estimated standard deviations derived from the generalised Debye model.[1]

Within our approximation considering only gas-phase molecular vibrations, we include the temperature dependence of the transition rates by solving the master matrix (Eq. 1 in the main text) at different temperatures. In our original approach,[28] the spin-

phonon coupling matrix elements $\langle \psi_f | \hat{H}_{SP} | \psi_i \rangle$ were assumed to be temperature independent and the line-shape of the vibrational density of states for each mode was set to an area normalized Gaussian function with constant linewidth (σ), approximated by comparison with experimental vibrational spectra.

$$\rho_j(\Delta E) = \frac{1}{\sigma\sqrt{2\pi}} e^{\frac{-(\Delta E - \hbar\omega_j)^2}{2\sigma^2}} \quad \text{(S19)}$$

Therefore, as we used Boltzmann statistics, the only term with an explicit dependence on temperature was the phonon matrix element, defined as the probability of losing a vibrational quantum S9.

Considering a fixed value of σ for all normal modes is an oversimplification as it discards effects beyond the harmonic approximation, such as anharmonicity and phonon-lifetimes. To address this, we use the mode- and temperature-dependent linewidth of Lunghi et al.[29], based on the NVT canonical ensemble:

$$\sigma_j = (\hbar\omega_j)^2 e^{\frac{\hbar\omega_j}{k_B T}} / \left(e^{\frac{\hbar\omega_j}{k_B T}} - 1\right)^2 \quad \text{(S20)}$$

Comparing the calculated relaxation rates of **1** and **6** using the two different definitions of the phonon linewidth (Figure S23 and Figure S24). We find that the high temperature data appear similar to fixed linewidths of *ca.* FWHM ~ 2 cm^{-1}, however the rates differ drastically from our fixed linewidth calculations at lower temperatures. The precipitous fall in relaxation rates occurs due to a drastic narrowing of the linewidth at low temperatures. Because we have shown (see main text) that the experimental ordering of the rates for **1-6** is not obeyed when FWHM < 6 cm^{-1}, and that using the mode-energy- and temperature-dependent linewidth model behaves like FWHM ~ 2 cm^{-1}, we suggest that this approximation is not appropriate in this case.

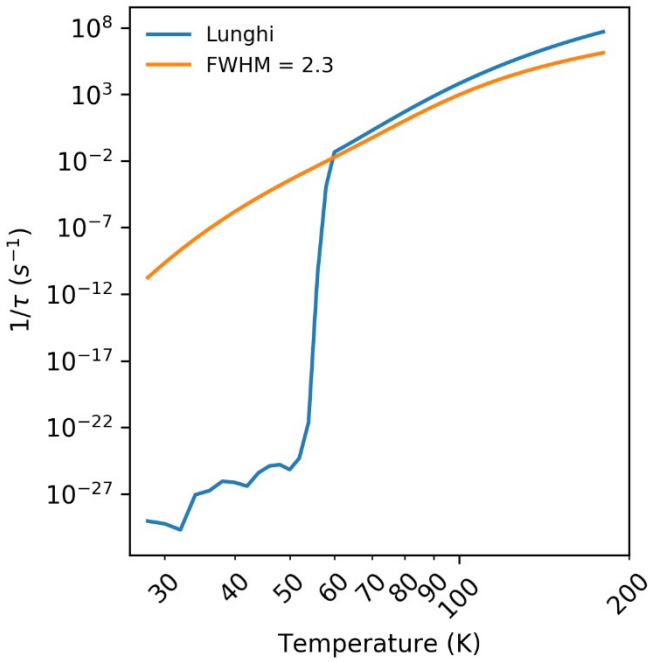

Figure S23. Comparison of calculated rates obtained with a fixed and a temperature dependent phonon linewidth for **1**.

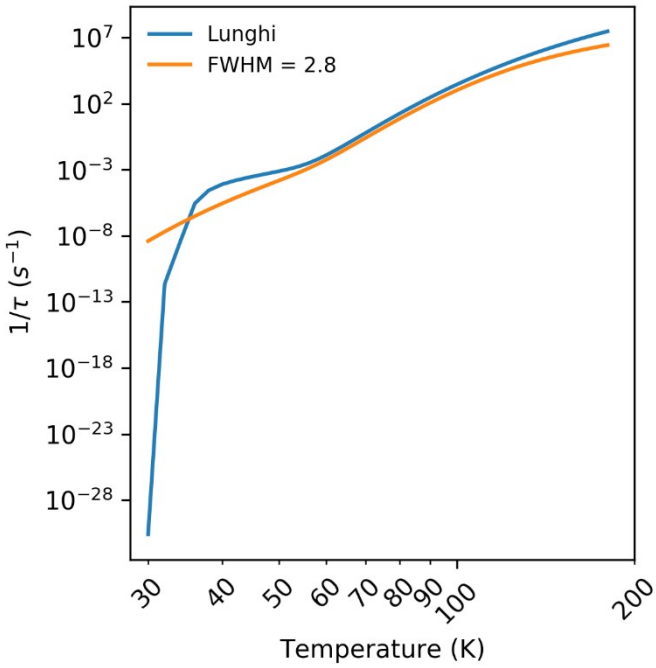

Figure S24. Comparison of calculated rates obtained with a fixed and a temperature dependent phonon linewidth for **6**.

S4.2. Understanding the origin of different relaxation rates

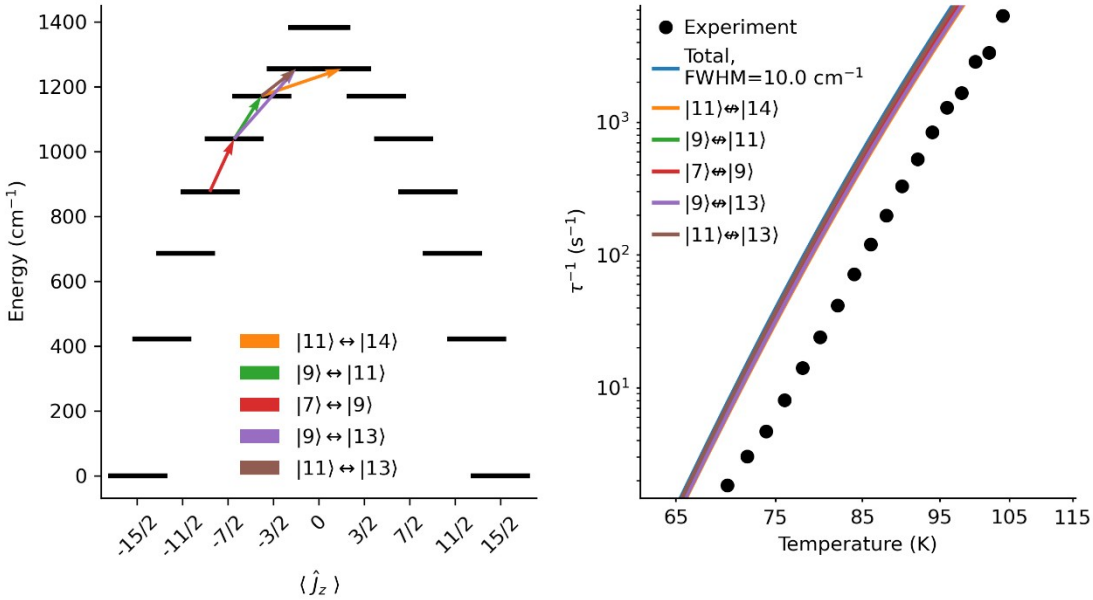

Figure S25. Most important transitions identified by the "knockout method" (left) and the effect of their sequential removal on the calculated rates (right) for **1**. Energy levels are based on the crystal field parameters calculated with CASSCF-SO. Rates obtained at the PBE geometry, without IR calibration and using a FWHM value of 10 cm^{-1}.

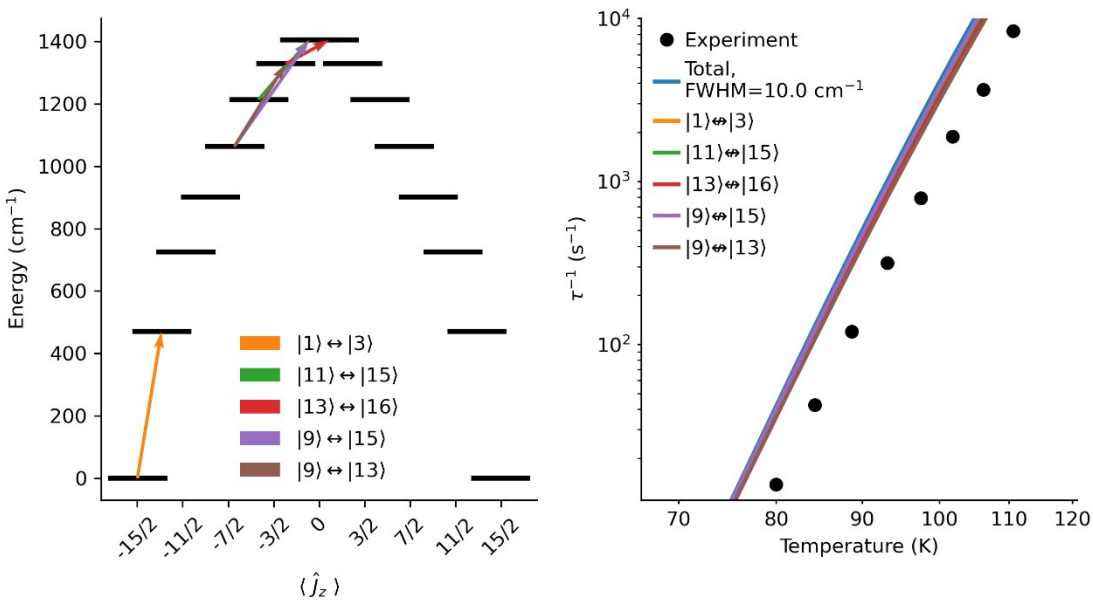

Figure S26. Most important transitions identified by the "knockout method" (left) and the effect of their sequential removal on the calculated rates (right) for **2**. Energy levels are based on the crystal field parameters calculated with CASSCF-SO. Rates obtained at the PBE geometry, without IR calibration and using a FWHM value of 10 cm^{-1}.

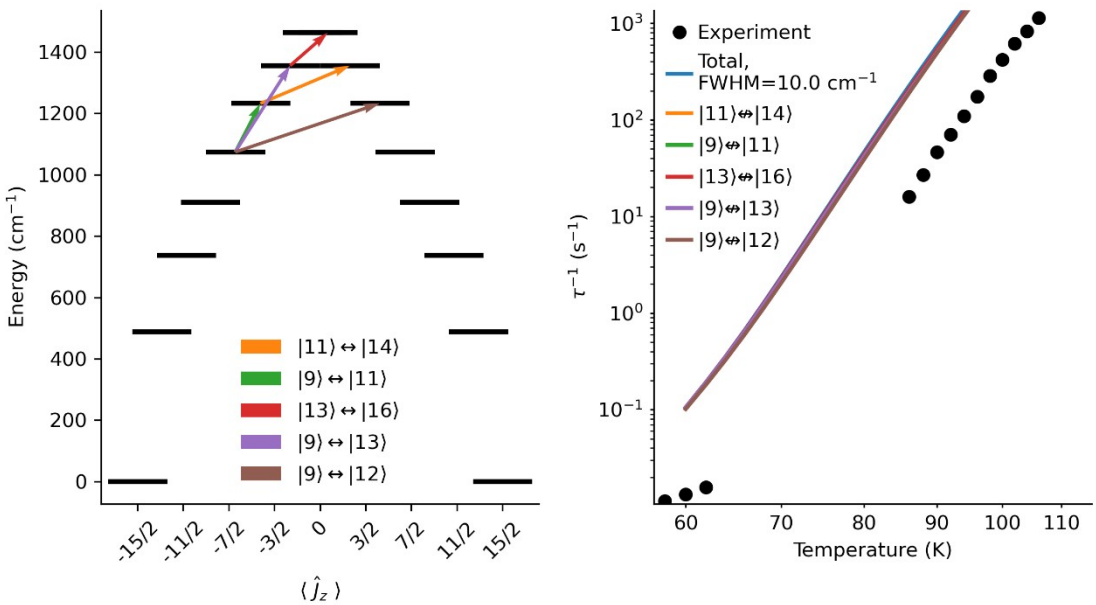

Figure S27. Most important transitions identified by the "knockout method" (left) and the effect of their sequential removal on the calculated rates (right) for **3**. Energy levels are based on the crystal field parameters calculated with CASSCF-SO. Rates obtained at the PBE geometry, without IR calibration and using a FWHM value of 10 cm^{-1}.

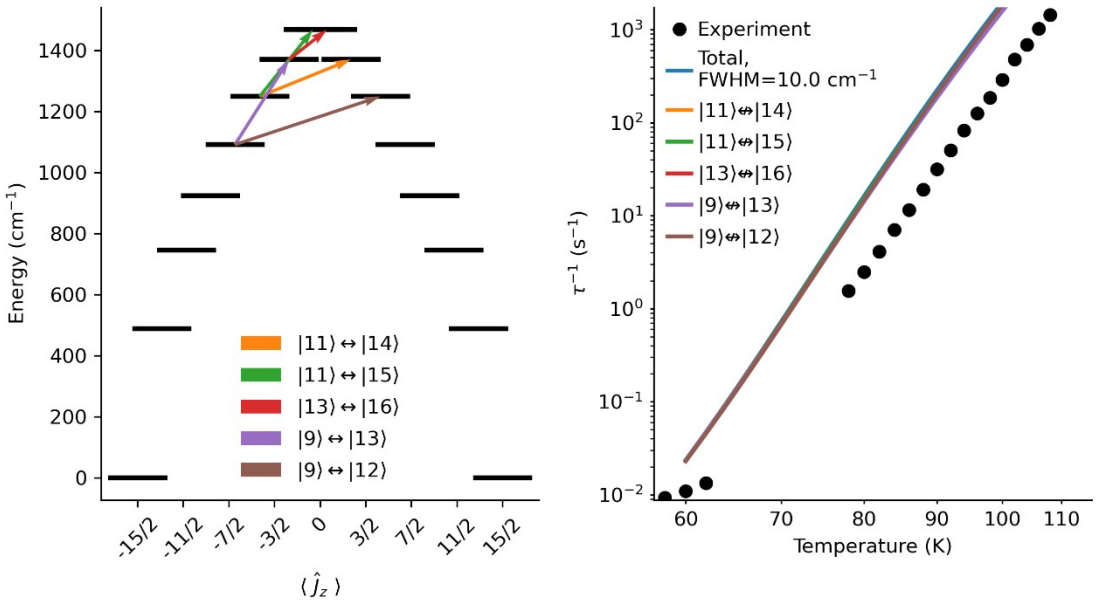

Figure S28. Most important transitions identified by the "knockout method" (left) and the effect of their sequential removal on the calculated rates (right) for **4**. Energy levels are based on the crystal field parameters calculated with CASSCF-SO. Rates obtained at the PBE geometry, without IR calibration and using a FWHM value of 10 cm^{-1}.

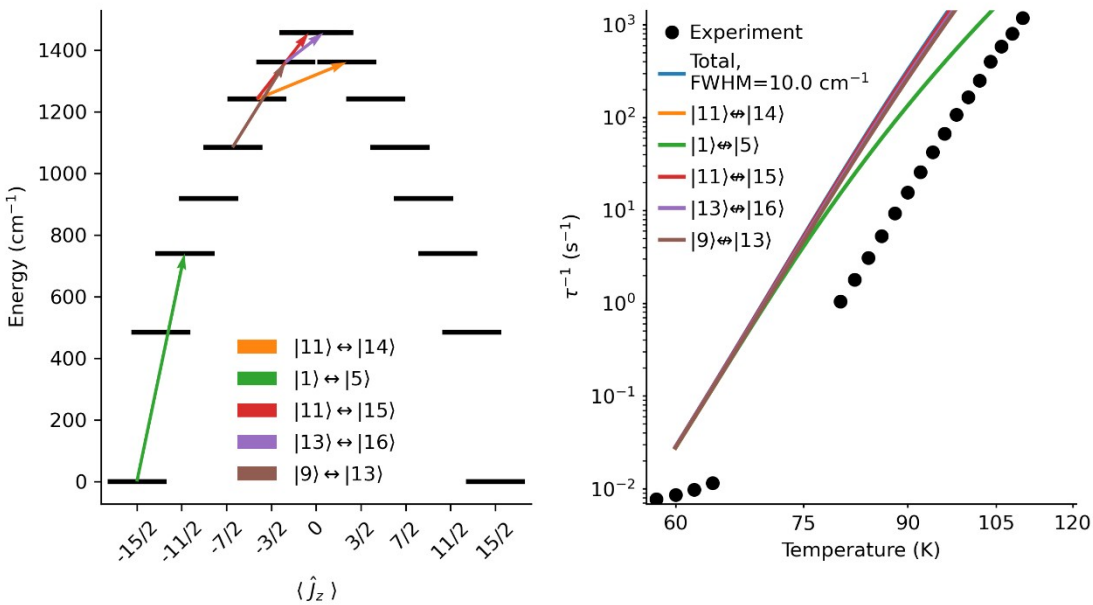

Figure S29. Most important transitions identified by the "knockout method" (left) and the effect of their sequential removal on the calculated rates (right) for **5**. Energy levels are based on the crystal field parameters calculated with CASSCF-SO. Rates obtained at the PBE geometry, without IR calibration and using a FWHM value of 10 cm^{-1}.

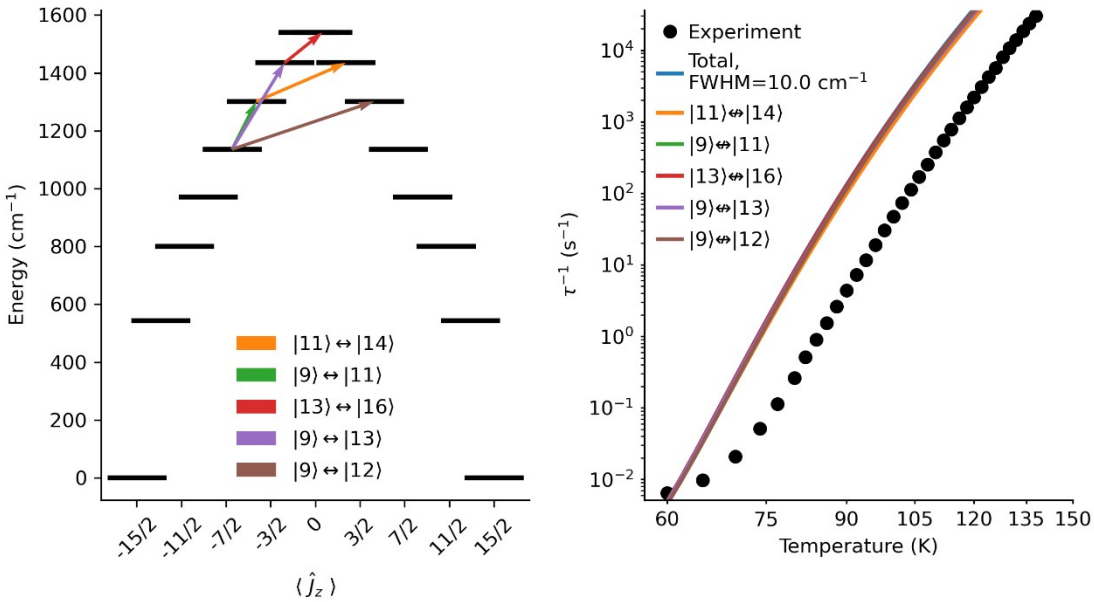

Figure S30. Most important transitions identified by the "knockout method" (left) and the effect of their sequential removal on the calculated rates (right) for **6**. Energy levels are based on the crystal field parameters calculated with CASSCF-SO. Rates obtained at the PBE geometry, without IR calibration and using a FWHM value of 10 cm^{-1}.

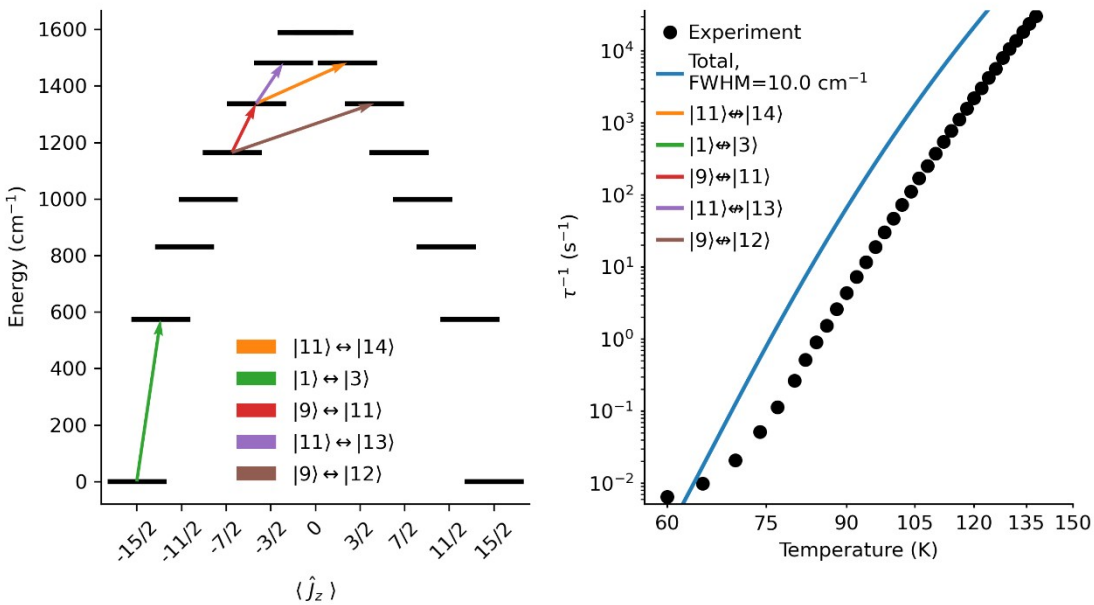

Figure S31. Most important transitions identified by the "knockout method" (left) and the effect of their sequential removal on the calculated rates (right) for **6**. Energy levels are based on the crystal field parameters calculated with CASSCF-SO. Rates obtained at the PBE0 geometry, without IR calibration and using a FWHM value of 10 cm^{-1}.

We define the overall spin-phonon coupling strength for each mode as S;[30] note here that B_q^k are CFPs in Wybourne notation and are linear combinations of the CFPs in Stevens notation B_k^q.[31]

$$S=\sqrt{\frac{1}{3}\sum_k \frac{1}{2k+1}\sum_{q=-k}^{k}\left|\left(\frac{\partial B_q^k}{\partial Q_j}\right)_{eq}\right|^2} \tag{S16}$$

In Figure S32-S38, the electronic states are labelled in increasing order such that the two states of the ground doublet are $|1\rangle$ and $|2\rangle$ and those of the most excited doublet $|15\rangle$ and $|16\rangle$.

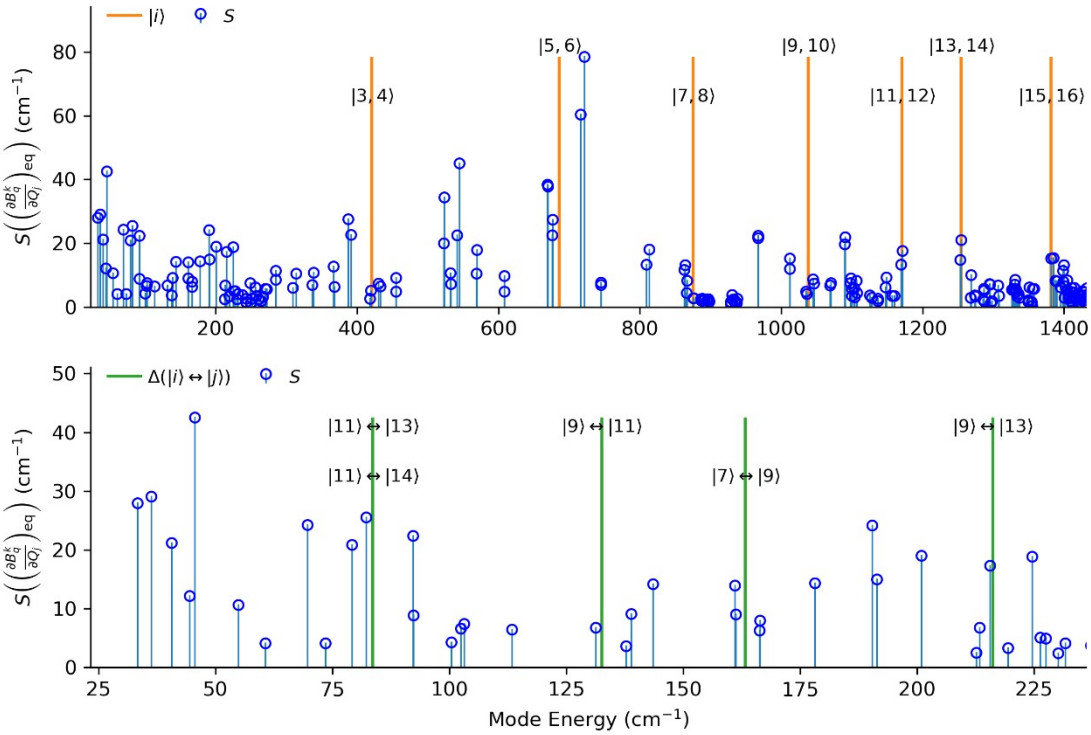

Figure S32. Strength of the crystal field distortions induced by each vibrational mode for PBE optimised **1**. Uncalibrated vibrational modes using "Taylor". Electronic states (orange) and the most important transitions (green, @ 100K FWHM = 10 cm^{-1}) are calculated from the crystal field parameters obtained with CASSCF-SO, using the knockout method.

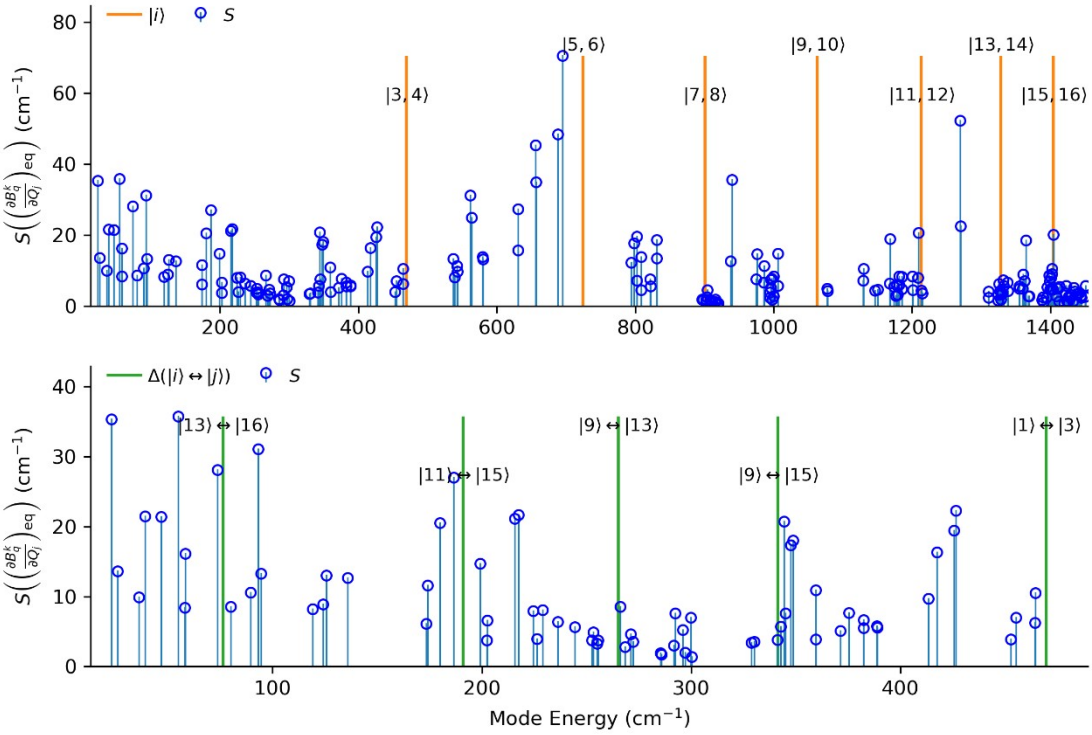

Figure S33. Strength of the crystal field distortions induced by each vibrational mode for PBE optimised **2**. Uncalibrated vibrational modes using "Taylor". Electronic states (orange) and the most important transitions (green, @ 100K FWHM = 10 cm^{-1}) are calculated from the crystal field parameters obtained with CASSCF-SO, using the knockout method.

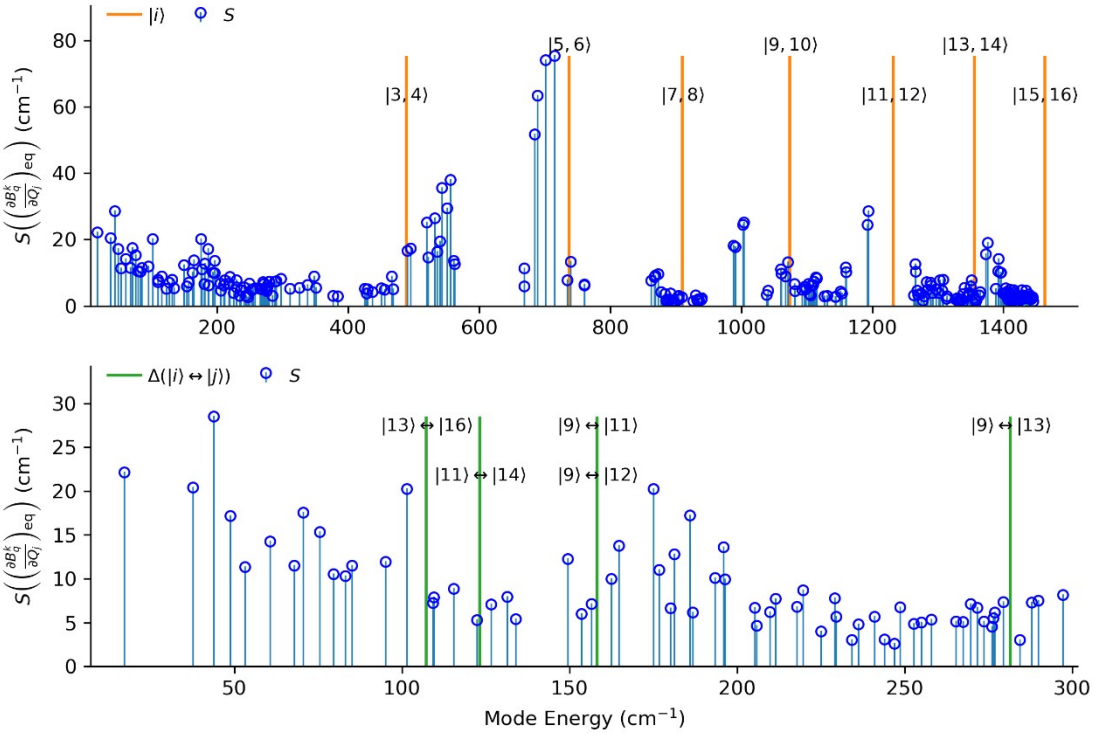

Figure S34. Strength of the crystal field distortions induced by each vibrational mode for PBE optimised **3**. Uncalibrated vibrational modes using "Taylor". Electronic states (orange) and the most important transitions (green, @ 100K FWHM = 10 cm^{-1}) are calculated from the crystal field parameters obtained with CASSCF-SO, using the knockout method.

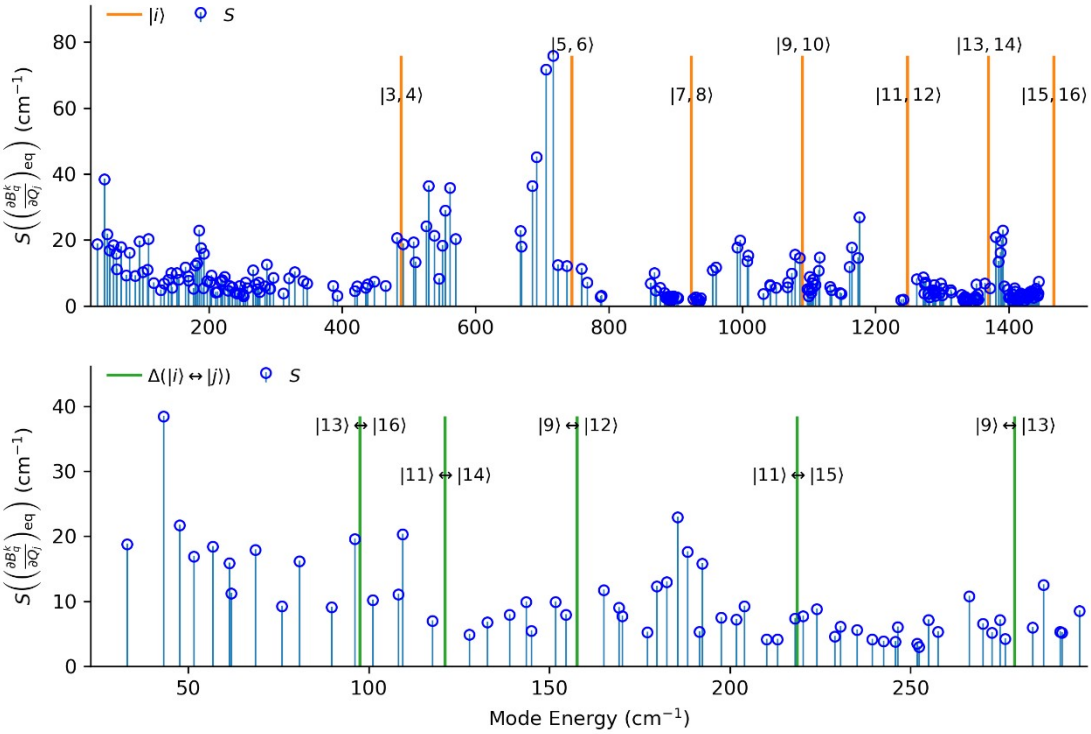

Figure S35. Strength of the crystal field distortions induced by each vibrational mode for PBE optimised **4**. Uncalibrated vibrational modes using "Taylor". Electronic states (orange) and the most important transitions (green, @ 100K FWHM = 10 cm^{-1}) are calculated from the crystal field parameters obtained with CASSCF-SO, using the knockout method.

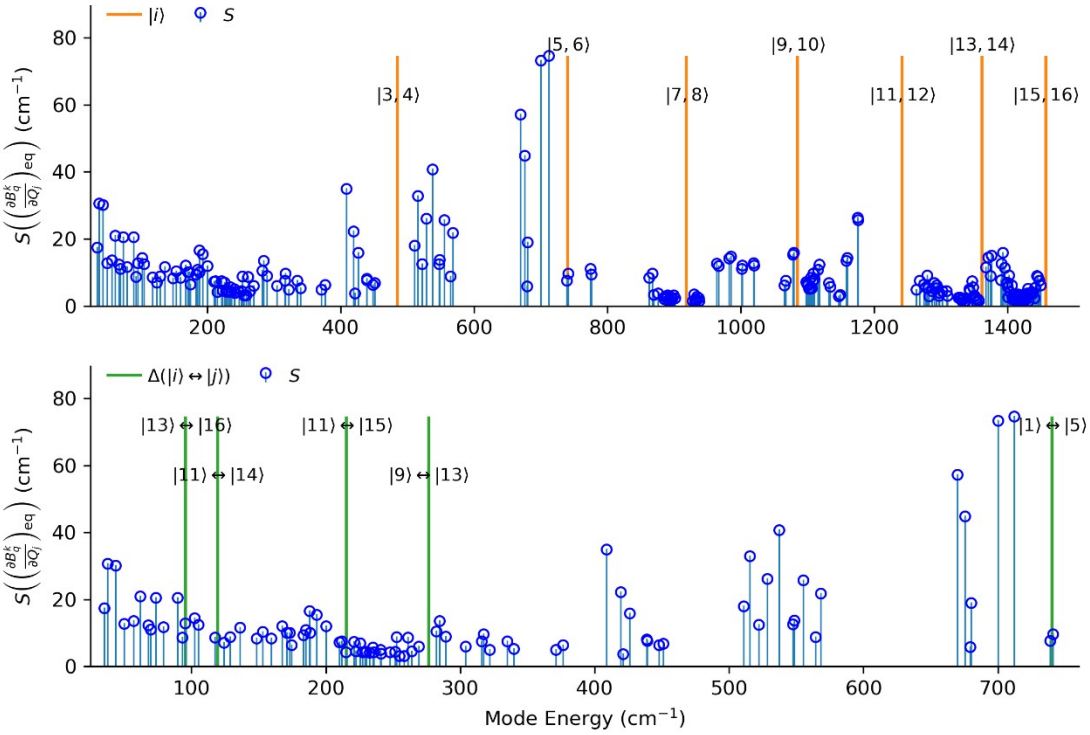

Figure S36. Strength of the crystal field distortions induced by each vibrational mode for PBE optimised **5**. Uncalibrated vibrational modes distorted to one unit of ZPD. Electronic states (orange) and the most important transitions (green, @ 100K FWHM = 10 cm^{-1}) are calculated from the crystal field parameters obtained with CASSCF-SO, using the knockout method.

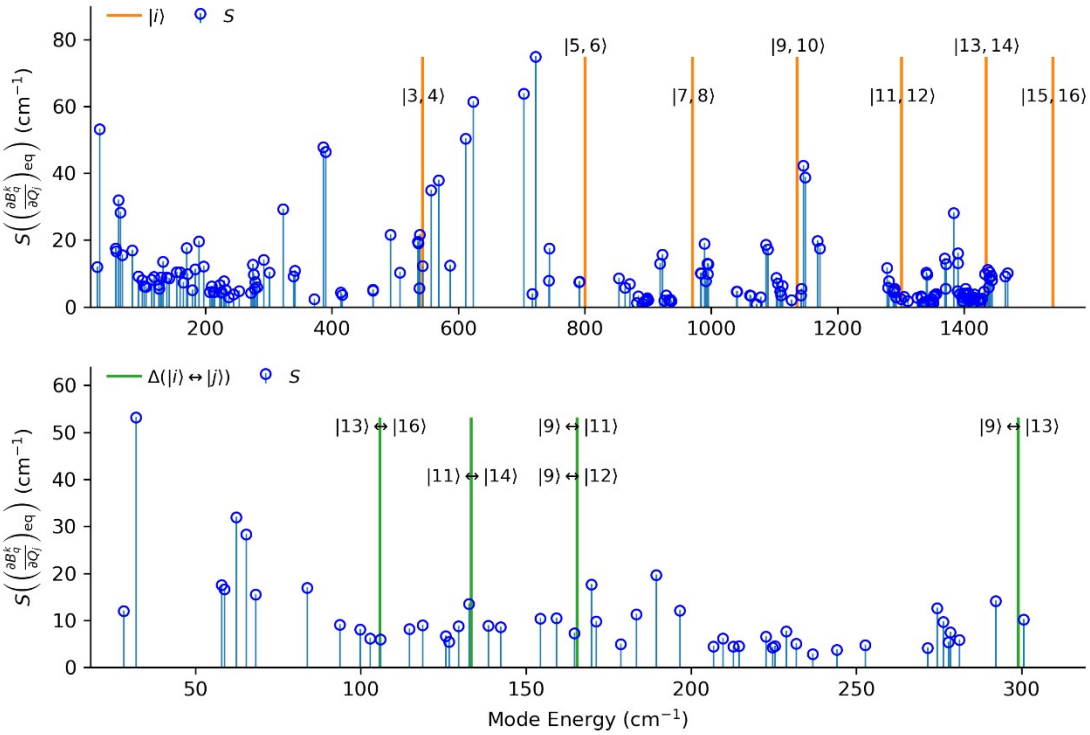

Figure S37. Strength of the crystal field distortions induced by each vibrational mode for PBE optimised **6**. Uncalibrated vibrational modes using "Taylor". Electronic states (orange) and the most important transitions (green, @ 100K FWHM = 10 cm^{-1}) are calculated from the crystal field parameters obtained with CASSCF-SO, using the knockout method.

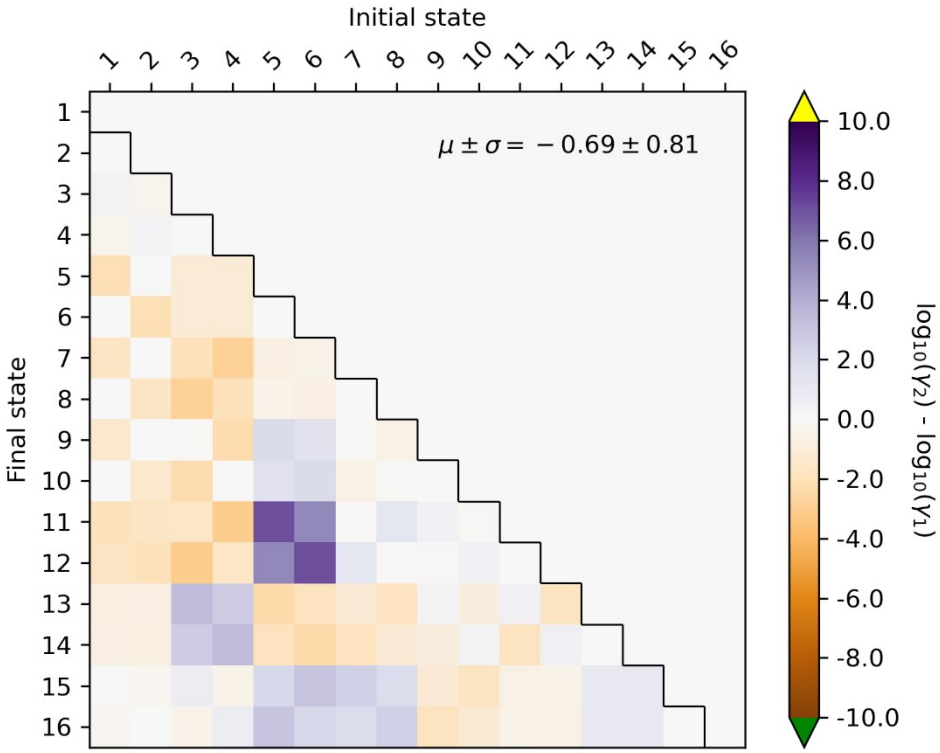

Figure S38. Comparison of gamma matrices between **1** and **6** calculated with PBE, 100 K, with a FWHM of 10 cm^{-1} and without IR calibration. We are only interested in the lower-triangle (phonon absorption) because the upper-triangle (phonon emission) carries the same information about spin-phonon coupling and phonon density-of-states (DOS) as the lower-triangle, but lacks dependence on the phonon occupation number (*i.e.* dependence on the energy splitting and hence occupation of the vibrational modes).

Table S11. Breakdown of relaxation rates between **2** and **6** *via* a mode-averaging procedure. Relaxation rates are calculated using the PBE density-functional, without calibration, at 100 K with FWHM = 10 cm^{-1}. Top portion corresponds to a base $\acute{\gamma}$ matrix of **2**, while bottom portion corresponds to a base matrix of **6**. Rows are ordered by increasing rate.

$\langle \acute{V} \rangle$	$\langle \acute{Q} \rangle$	$\langle \acute{\rho} \rangle$	$\langle \acute{n} \rangle$	τ^{-1}	τ^{-1}/τ^{-1}_{2}
2	**6**	**2**	**2**	7.79×10^{2}	0.19
6	**2**	**2**	**2**	3.26×10^{3}	0.80
2	**2**	**2**	**2**	4.05×10^{3}	1.00
2	**2**	**2**	**6**	4.31×10^{3}	1.06
2	**2**	**6**	**2**	6.18×10^{3}	1.53
$\langle \acute{V} \rangle$	$\langle \acute{Q} \rangle$	$\langle \acute{\rho} \rangle$	$\langle \acute{n} \rangle$	τ^{-1}	τ^{-1}/τ^{-1}_{6}
6	**6**	**6**	**2**	6.54×10^{2}	0.52
6	**6**	**2**	**6**	6.75×10^{2}	0.54
6	**6**	**6**	**6**	1.25×10^{3}	1.00
2	**6**	**6**	**6**	2.08×10^{3}	1.66

6	**2**	**6**	**6**	5.88×10^{3}	4.70

S5. Survey of hypothetical compounds

Table S12. Comparison of PBE optimised structural parameters for the hypothetical homoleptic compounds ordered by increasing CF splitting (Figure 5c). All angles and distances measured with respect to the ring (R) centroids. Compound 6 is shown for comparison.

	R^1-Dy (Å)	Dy-R^2 (Å)	R-Dy-R (degrees)	Calculated U_{eff} (K)	Calculated τ_0 (s)
$[DyFluorene\mathit{i}Pr_3]^+$	2.26	2.32	145.75	1095	1.14×10^{-12}
$[Dy(N_5)_2]^+$	2.24	2.24	145.27	1292	6.42×10^{-12}
$[Dy(C_5H_5)_2]^+$	2.28	2.43	170.12	1347	4.93×10^{-10}
$[Dy(C_5I_5)_2]^+$	2.31	2.31	148.39	1527	8.82×10^{-12}
$[Dy(C_4Me_4)_2]^-$	2.27	2.27	138.54	1833	8.03×10^{-13}
$[Dy(C_4{}^{i}Pr_4)_2]^-$	2.28	2.29	148.80	1939	6.83×10^{-13}
$[Dy(C_5Me_5)_2]^+$	2.26	2.26	144.38	1549	8.90×10^{-8}
$[Dy(C_4H_4)_2]^-$	2.29	2.29	141.82	2093	2.48×10^{-11}
$[Dy(C_4{}^{t}Bu_4)_2]^-$	2.32	2.34	161.83	2117	7.54×10^{-13}
6	2.31	2.29	160.0	2048	1.03×10^{-12}

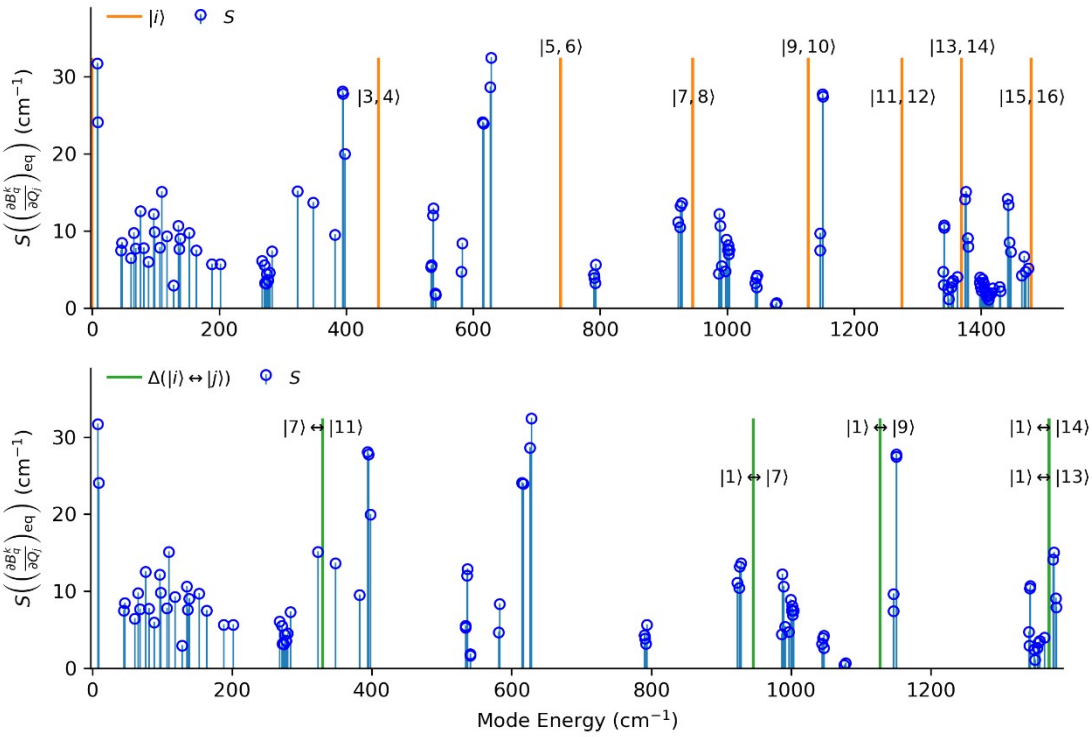

Figure S39. Strength of the crystal field distortions induced by each vibrational mode for PBE optimised $[DyC_5Me_5]_2^+$. Uncalibrated vibrational modes using "Taylor". Electronic states (orange) and the most important transitions (green, @ 100K FWHM = 10 cm^{-1}) are calculated from the crystal field parameters obtained with CASSCF-SO, using the knockout method.

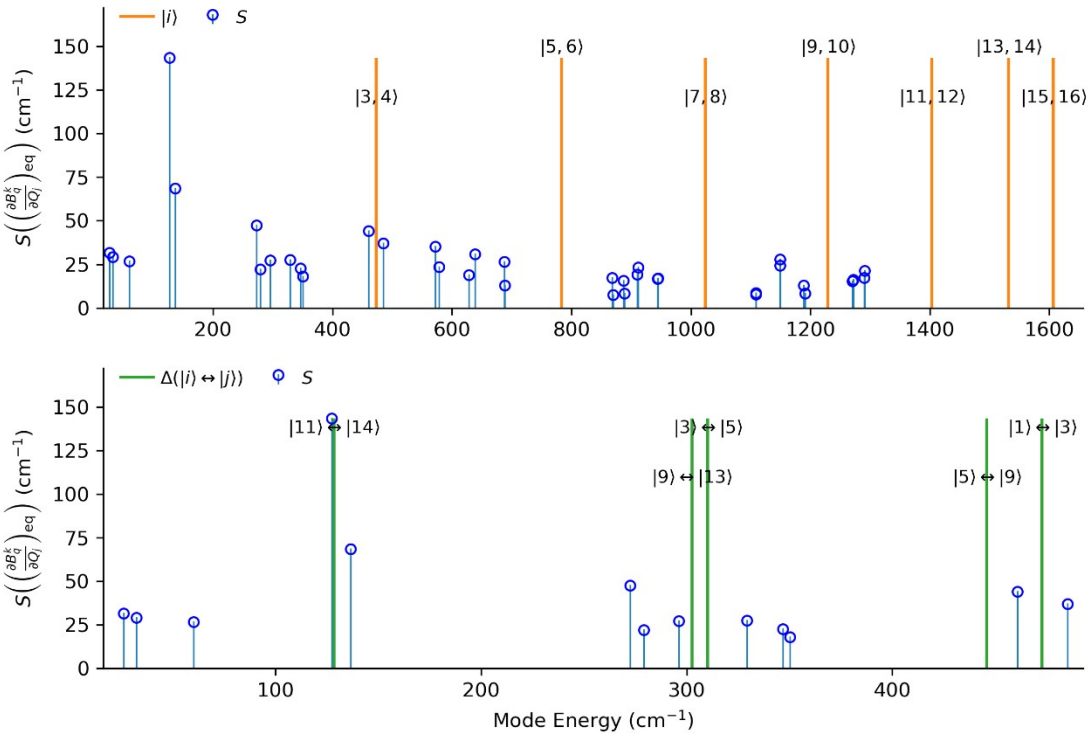

Figure S40. Strength of the crystal field distortions induced by each vibrational mode for PBE optimised $[DyC_4H_4]_2^-$. Uncalibrated vibrational modes using "Taylor". Electronic states (orange) and the most important transitions (green, @ 100K FWHM = 10 cm^{-1}) are calculated from the crystal field parameters obtained with CASSCF-SO, using the knockout method.

Table S13. Breakdown of relaxation rates between $[Dy(C_4H_4)_2]^-$ and **6** *via* a mode-weighting procedure. Relaxation rates are calculated using the PBE density-functional, without calibration, at 100 K with FWHM = 10 cm^{-1}. Top portion corresponds to a base $\acute{\gamma}$ matrix of $[Dy(C_4H_4)_2]^-$, while bottom portion corresponds to a base matrix of **6**. Rows are ordered by increasing rate.

$\langle \acute{H}_{SP} \rangle$	$\langle \acute{Q} \rangle$	$\langle \acute{\rho} \rangle$	$\langle \acute{n} \rangle$	τ^{-1}	$\tau^{-1}/\tau^{-1}_{[Dy(C_4H_4)_2]^-}$ ¿
6	$[Dy(C_4H_4)_2]^-$	$[Dy(C_4H_4)_2]^-$	$[Dy(C_4H_4)_2]^-$	2.16×10^1	0.67
$[Dy(C_4H_4)_2]^-$	$[Dy(C_4H_4)_2]^-$	$[Dy(C_4H_4)_2]^-$	$[Dy(C_4H_4)_2]^-$	3.23×10^1	1.00
$[Dy(C_4H_4)_2]^-$	$[Dy(C_4H_4)_2]^-$	$[Dy(C_4H_4)_2]^-$	**6**	4.10×10^1	1.27
$[Dy(C_4H_4)_2]^-$	**6**	$[Dy(C_4H_4)_2]^-$	$[Dy(C_4H_4)_2]^-$	1.27×10^2	3.93
$[Dy(C_4H_4)_2]^-$	$[Dy(C_4H_4)_2]^-$	**6**	$[Dy(C_4H_4)_2]^-$	1.03×10^3	31.89
$\langle \acute{H}_{SP} \rangle$	$\langle \acute{Q} \rangle$	$\langle \acute{\rho} \rangle$	$\langle \acute{n} \rangle$	τ^{-1}	τ^{-1}/τ^{-1}_{6}
6	**6**	$[Dy(C_4H_4)_2]^-$	**6**	9.83×10^1	0.08
6	$[Dy(C_4H_4)_2]^-$	**6**	**6**	3.29×10^2	0.26
6	**6**	**6**	$[Dy(C_4H_4)_2]^-$	6.16×10^2	0.49

6	**6**	**6**	**6**	1.25×10^{3}	1.00
$[Dy(C_4H_4)_2]^-$	**6**	**6**	**6**	1.88×10^{4}	15.04

S6. References

[1] D. Reta, N. F. Chilton, *Phys. Chem. Chem. Phys.*, 2019, **21**, 23567-23575.

[2] M. J. Frisch, et al. Gaussian 09, Revision D.01, Gaussian, Inc., Wallingford CT, 2016

[3] J. P. Perdew, K. Burke and M. Ernzerhof, *Phys. Rev. Lett.* 1996, **77** (18), 3865–3868.

[4] J. P. Perdew, K. Burke and M. Ernzerhof, *Phys. Rev. Lett.* 1997, **78** (7), 1396–1396.

[5] C. Adamo, V. Varone, J. Chem. Phys., 110 (1999) 6158-69.

[6] T. H. Dunning, *J. Chem. Phys.* 1989, **90** (2), 1007–1024.

[7] J. M. L. Martin and A. Sundermann, *J. Chem. Phys.* 2001, **114** (8), 3408–3420.

[8] S. Grimme, *J.* Comput. *Chem.* 2004, **25** (12), 1463–1473.

[11] W. Kabsch, IUCr, Acta Crystallogr. Sect. A 32 (1976) 922e923.

[12] W. Kabsch, IUCr, Acta Crystallogr. Sect. A 34 (1978) 827e828.

[13] J. C. Kroman, A. Bratholm, GitHub: Calculate RMSD for two XYZ structures. http://github.com/charnley/rmsd, 2016

[14] McClain, K. R.; Gould, C. A.; Chakarawet, K.; Teat, S. J.; Groshens, T. J.; Long, J. R.; Harvey, B. G. *Chem. Sci.* **2018**, *9*, 8492-8503.

[15] B. O. Roos, R. Lindh, P.-Å. Malmqvist,V. Veryazov and P.-O. Widmark, *J. Phys. Chem. A.* 2004, **108**, 2851–2858.

[16] B. O. Roos, R. Lindh, P.-Å. Malmqvist,V. Veryazov and P.-O. Widmark, *J. Phys. Chem. A.* 2005, **109**, 6575–6579.

[17] F. Aquilante, L. Gagliardi, T. B. Pedersen and R. Lindh, *J. Chem. Phys.*, 2009, **130**, 154107.

[18] L. Ungur and L. F. Chibotaru, *Chem. Eur. J.* 2017, **23**, 3708–3718.

[19] Guo, F.-S.; Day, B. M.; Chen, Y.-C.; Tong, M.-L.; Mansikkamäki, A. & Layfield, R. A. *Science*, **362**, 1400, (2018).

[20] D. Gatteschi, R. Sessoli and J. Villain, *Molecular Nanomagnets*; Oxford University Press, 2006.

[21] M. H. Alexander, G. E. Hall and P. J. Dagdigian, *J. Chem. Educ.* 2011, **88** (11), 1538–1543.

[22] N. F. Chilton, R. P. Anderson, L. D. Turner, A. Soncini and K. S. Murray, *J. Comput. Chem.* 2013, **34**, 1164–1175.

[23] R. Orbach, *Proc. Roy. Soc. A.* 1961, **264**, 458–484.

[24] Messiah, A. in *Quantum Mechanics*, Dover, New York, 2nd edition, 1995, vol. 2, ch. XVII, pp. 722-762.

[25] R. Orbach, *Proc. R. Soc. London. Ser. A. Math. Phys. Sci.*, 1961, **264**, 458–484.

[26] K. W. H. Stevens, *Reports Prog. Phys.*, 1967, 30, 189–226.

[27] Evans, P., Reta, D., Whitehead, G. F.S., Chilton, N. F. & Mills, D. P. *J. Am. Chem. Soc.*, **141**, 19935−19940 (2019).

[28] C. A. P. Goodwin, F. Ortu, D. Reta, N. F. Chilton and D. P. Mills, *Nature* 2017, **548** (7668), 439–442.

[29] A. Lunghi, F. Totti, R. *Sessoli* and S. Sanvito, *Nat. Commun.*, 2017, **8**, 14620.

[30] N. C. Chang, J. B. Gruber, R. P. Leavitt and C. A. Morrison, *J. Chem. Phys.*, 1982, 76, 3877–3889.

[31] J. Mulak and Z. Gajek, *The effective crystal field potential*, Elsevier, Oxford, 2000.